AN EXPERIMENTAL STUDY ON THERMAL BONDING EFFECTS OF PMMA BASED MICRO-DEVICES USING HOT EMBOSSING

by

VARUN SOOD

Presented to the Faculty of the Graduate School of

The University of Texas at Arlington in Partial Fulfillment

of the Requirements

for the Degree of

MASTER OF SCIENCE IN MECHANICAL ENGINEERING

THE UNIVERSITY OF TEXAS AT ARLINGTON

December 2007

ACKNOWLEDGEMENTS

I express my gratitude towards my supervising professor Dr. Panos Shiakolas for constantly motivating and encouraging me, and also for his invaluable advice, guidance and support throughout the course of my research work. I wish to thank Dr. Seiichi Nomura and Dr. Woo Ho Lee for their interest in my research and for taking time to serve in my thesis defense committee.

I reserve my special thanks to Mr. Tom Leeds, Mr. Mike Baker and Mr. Sam Williams of the Mechanical Engineering machine shop for their invaluable advice during this research especially during the fabrication of the tensile testing fixture. I am especially grateful to also thank Dr. Sunil Belligundu for his assistance with initial embossing experiments on the HEMM setup. I want to thank Mr. Nitin Uppal for helping me with the Regression Analysis. I would also thank Mr. Puneet Saggar and Mr. Viswaas Bedekar for their help with bond strength measurement experiments. Finally, I also appreciate the support of my colleagues in the MARS lab – Mr. Krishanu Saha and Mr. Mohsin Rizwan. I am grateful to all the teachers who taught me during the years I spent in school, first in India and finally in the United States.

Nov 23, 2007

ABSTRACT

AN EXPERIMENTAL STUDY ON THERMAL BONDING EFFECTS OF PMMA BASED MICRO-DEVICES USING HOT EMBOSSING

Varun Sood, MS.

The University of Texas at Arlington, 2007

Supervising Professor: Panayiotis S. Shiakolas

Basic configuration and functioning of various subsystems of a developed HEMM system for thermal bonding are discussed. The bond strength and micro channel geometry degradations dependence on controlled process parameters in thermal bonding using hot embossing has been investigated. The process parameters examined were bonding temperature, bonding or applied load and holding time. Polymeric substrates with different feature dimensions and thickness were embossed and bonded using hot embossing technology. The feature dimensions before and after bonding were examined to assess the geometry changes as functions of the bonding process. This assessment could provide guidance during the design phase of micro-fluidic devices considering the bonding step.

The results from the experiments show that high bond strength can be obtained at higher temperature and pressure and longer holding time. Also, to obtain minimum

degradation, the bonding temperature and pressure should be kept low with longer holding times. The experiments also suggest combination of input parameters to obtain good bond strength and minimum degradations. ANOVA analysis of the experimental data was performed to find the regression models to estimate the outputs knowing the controlled inputs and to find the sensitivity of controlled process parameters on bond strength and channel degradations. The models are linearized to estimate the input process to obtain the desired bond strength or channel geometry.

TABLE OF CONTENTS

LIST OF FIGURES

LIST OF TABLES

CHAPTER 1

INTRODUCTION

1.1 MicroElectroMechanical Systems

1.1.1 Introduction

"Micro-Electro-Mechanical Systems" (MEMS) is the integration of mechanical elements, sensors, actuators, and electronics on a common silicon substrate through micro-fabrication technology. These are the microscopic structures integrated onto silicon that combine mechanical, optical and fluidic elements with electronics. Typically no bigger than a grain of sand, these MEMS devices are complex machines that enable chips to become intelligent. These devices act as the most direct links between digital electronics and the physical world, allowing the integration of electronics and mechanical systems on a single chipset [1].

First developed in the 1970s and then commercialized in the 1990s [2], MEMS make it possible for systems of all kinds to be smaller, faster, more energy-efficient and less expensive. Microelectronic integrated circuits can be thought of as the "brains" of a system and MEMS augments this decision-making capability with "eyes" and "arms", to allow microsystems to sense and control the environment. Sensors gather information from the environment through measuring mechanical, thermal, biological, chemical, optical, and magnetic phenomena. The electronics then process the information derived from the sensors and through some decision making capability direct the actuators to

respond by moving, positioning, regulating, pumping, and filtering, thereby controlling the environment for some desired outcome or purpose [1]. A micro device is a device consisting of components with dimensions less than one millimeter. Due to advancements in micro engineering and microfabrication, these micro devices are used for a variety of applications such as in the automotive, aerospace, telecommunications and biomedical industry.

Some main applications of microdevices include

- **Genomic and Proteomics [3] -** DNA fingerprinting, gene assays.
- **Chemical/biological warfare –** Detection and identification of pathogens.
- **Accelerometers [4]** in modern cars for a large number of purposes including airbag deployment in collisions.
- **MEMS gyroscopes [5]** used in modern cars and other applications to detect yaw; e.g. to deploy a roll over bar or trigger dynamic stability control.
- **Clinical Analysis [6] –** Rapid analysis of blood and bodily fluids.
- **Pressure sensors** e.g. car tire pressure sensors, and disposable blood pressure sensors.
- **Optical switching technology [7]** which is used for switching technology for data communications, and is part of the emerging technology of smart dust.
- **Biomedical devices [8], [9]** implantable devices – drug delivery.
- **Displays [10]** e.g. the Digital Micro mirror Device (DMD) chip in a projector based on DLP technology has on its surface several hundred thousand micro mirrors.

A Micro fluidic device is one that has one or more channels with at least one dimension less than 1 mm [11]. Because of the increase in micromachining technology, hundreds of microfluidic devices can be made from a single 8 inch wafer of silicon. The size of microdevices in comparison to a dime is shown in figure 1.1 [12].

Figure 1.1. Size of a MEMS fabricated chip compared to a dime [12].

Microfluidic devices have lots of advantages as compared to macro systems being extremely light and small in size, enhanced performance, low power consumption, unprecedented level of functionality, reliability and sophistication on a small chip, non-cumbersome moving electrical parts. Also there is considerable price reduction for products that incorporate this technology [13], [14].

1.1.2 Use of Polymers

Currently there are a number of MEMS processing materials that are available. Some of the most commonly used are silicon, quartz, glass, polymers like PMMA, PLLA and metals like gold, nickel, aluminum, chromium, tungsten, titanium, platinum and silver. Polymers are mostly used in MEMS processing because they are bio-compatible, easy to manufacture, have low cost for high volume production, low conductivity, lower bonding temperatures, possess wide range of optical and elastic properties and have high bond strength. All these properties make them suitable for micro and even nano applications.

1.1.3 PMMA – A Polymer

"In this research, PMMA is used. "PolyMethylMethAcrylate (**PMMA**) or poly (methyl 2-methylpropenoate) is the synthetic polymer of methyl methacrylate. This thermoplastic and transparent plastic is sold by the tradenames Plexiglas, R-Cast, Perspex, Plazcryl, Acrylite, Acrylplast, Altuglas, Polycast and Lucite and is commonly called acrylic glass or simply acrylic. The PMMA structure is basically a long polymer chain of methyl methacrylate (a monomer)" [15]. OPENING QUOTES?????????????

PMMA is generally preferred over other polymers [16] such as PDMS, Polyesters, Polysulphone, Polycarbonates, polyamides etc. and even glass because of the following properties:

- PMMA is less dense; its density can range from 1150-1190 kg/m^3.
- PMMA has higher impact strength and does not shatter but instead breaks into large dull pieces.

- PMMA does not filter ultraviolet (UV) light. PMMA transmits UV light down to 300 nm. This is overcome by adding a coating to PMMA sheets to make them absorb UV light. PMMA molecules have great UV stability.
- PMMA allows infrared light (IR) of up to 2800 nm wavelength to pass through. IR of longer wavelengths, up to 25,000 nm, is essentially blocked. Special formulations of colored PMMA exist to allow specific IR wavelengths to pass while blocking visible light.
- PMMA has a glass transition temperature of 106 ^{0}C. This is the temperature above which the PMMA behaves as a viscous substance. The reason for this viscosity in PMMA is because at higher temperatures the longer polymer chain becomes thinner and smoother, and hence, can more easily slide past each other.

1.2 Different Polymer Bonding Techniques

Having these advantages over numerous other polymer MEMS materials, PMMA is mainly used in the micro fabrication industry. A polymer micro fluidic device is typically produced by fabricating features such as channels and reservoirs on the first substrate and subsequently bonding the second substrate/cover on the first to seal these features. In some cases, more than two substrates are bonded, with more than one substrate having features on them. Bonding should have adequate strength to withstand fluid pressures, permit leak free operation, and should cause minimum damage to the fabricated features during this process. Various polymer bonding techniques are described below.

1.2.1 Adhesive Bonding

The easiest way for bonding is by the use of adhesives [17], [18]. For this purpose, a number of options exist, i.e. isotropic conductive adhesives, anisotropic systems and epoxy.

Isotropic conductive adhesives have a curing time of 3 to 10 min at 120 to150 ^{0}C. They possess some elastic properties. Most commonly used adhesives in this category are acrylic and polyamide type adhesives.

Anisotropic adhesives have faster curing time and lower temperatures. They possess interconnections and flip-chip bonding, hence, has high bond strength. Most commonly used adhesives in this category are Ag-filled UV-acrylate, solder (SnBi) filled systems and Au coated plastics. The use of epoxy to glue materials is well known. A diluted solution is made using n-methylpyrrolidon (NMP) and toluene to obtain the necessary epoxy layer. They have very high bond strength [19].

Adhesive bonding is a continuous process, so there is more uniform distribution of stresses over the bonded area. As a result the local concentration of stresses (present in spot welds, thermally or mechanically fastened joints) is avoided. Also it helps to produce a stiffer structure [20], [21].

On the other hand, as these adhesives are drawn from synthetic resins, they are not as strong as metals and with increase in temperature, the bond strength decreases even further because the properties of the adhesive moves from elastic to plastic. Also with most adhesives maximum bond strength is not produced instantly as it is with mechanical fastening or with welding. The assembled joint must be supported for at least part of the time during which the strength of the bond is building up.

1.2.2 Induction Heating

One of the bonding techniques in polymers is Induction Heating [22]. It is a non-contact electromagnetic process. A specially designed coil is used for localized heating of polymers. Induction heating of a material occurs when an induction coil, which generates a magnetic field, is placed near the material and heats a susceptor such as metal screen or powder. Generally, the process is suitable for welding long/thin parts.

Induction heating has the ability to make continuous joints by moving the coil along the joint without disturbing individual metallurgical characteristics. It is highly directional, reliable, repeatable, non-contact and energy efficient i.e. heating in a minimum amount of time.

1.2.3 Laser Heating

Temperature at a joint surface can be raised to or above the melting temperature using high intensity laser beams [22]. This can be done by selecting a transparent upper layer that allows the laser beam to penetrate through and thus focus on the lower material which is highly absorbing. Thus raise the temperature at the joint and results in a bond. This is used mainly for thermoplastic materials. Bonding using Laser Heating is shown in Figure 1.2.

Laser heating is continuous and highly localized. Laser beams can also be focused to small spots (typically a few tens to hundreds of microns in diameter). But since, the spot size of the laser tends to be in the order of tens of microns, thousands of spots need to be used to bond the polymer having enough strength to sustain fluidic pressures and provide proper sealing. Also rapid cooling rates may cause cracking in certain polymers. Also laser heating associate high capital and maintenance cost.

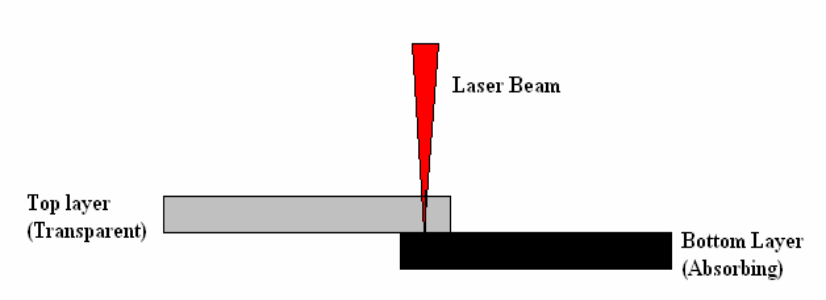

Figure 1.2. Laser Heating [23].

1.2.4 UV Nonimprint Lithograph (UV-NIL)

In this technique UV curable resists (generally acrylate monomers and photo initiators) imprinted with transparent stamps are cured by light in the near UV range. This process is performed at room temperature. To press the stamp in the substrate, a significantly low force is applied. Cooling is done by subsequent UV-light exposure and cross-linking. Structures in the sub 100 nm range on wafer sizes up to 150 nm have been replicated using this technique [23], [24].

As UV-NIL is performed at room temperature; stresses are minimized in the imprinted layers and the substrate. Also the overlay alignment is highly accurate. The UV-NIL process is schematically shown in Figure 1.3.

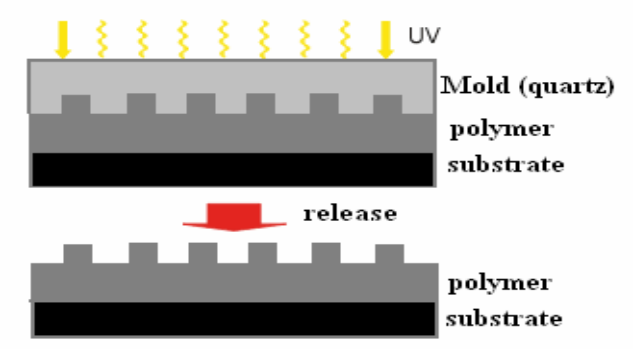

Figure 1.3. UV-NIL [25].

1.2.5 Microwave Bonding

PMMA is relatively transparent to microwave energy near the 2.4 GHz frequency band. This makes PMMA an excellent material for microwave bonding [26]. PMMA to silicon and PMMA to PMMA substrates can be bonded together using selected microwave frequencies to locally melt the interface metallic thin film between the substrates.

i) PMMA to Silicon bonding

Silicon to PMMA bonding is achieved by using 63 % Sn and 37 % Pb solder pre-forms which is 50 μm thick and melts at 183 ^{0}C. 50 nm Cr adhesion layer and 50 nm Au bonding layer were e-beam deposited onto both surfaces. Bonding is done at approximately 30W of applied power for 180 seconds [26].

ii) PMMA to PMMA bonding

Embossed PMMA and PMMA bonding is possible via thin film Au already deposited on the surface. 50 nm Cr adhesion layer and 50 nm Au bonding layer were e-beam deposited onto both embossed and bare PMMA surface. Two substrates are bonded at 10 W for approximately 120 seconds [26].

Microwave bonding being highly localized, results in high bond strength and higher device reliability. This is a low cost process because the heating takes place simultaneously and quick. Also, as this is a globally low temperature process, so polymers with low melting temperatures can be used as substrates. Also, adverse thermal coefficient of expansion mismatches is minimized [27].

1.2.6 UV irradiation and subsequent welding at low temperature

Many polymers undergo changes in their chemical and morphological structure, when they are exposed to ultra-violet (UV) radiations [28], [29]. Different polymers have

different range of UV wavelength at which photo degradation occurs which generates a thin surface layer with a low softening point on the polymer. Then welding or sealing of the microstructure is possible at low temperature. Thus, there is no loss in structure quality, and the fluidic and optical microstructures are not affected by this process. Using this technique, microchannels for capillary electrophoresis were also successfully sealed [29].

1.2.7 Flip-Chip Bonding Technique

Some thermoplastic conductive polymers possess the property of melting or re-wetting when heated to a specific temperature. First the substrate is pre-heated to approximately 20 ^{0}C above the melting temperature of thermoplastic polymer. Then a diced flip-chip is flipped, aligned and contacted onto it. The thermoplastic bump melts onto the conductor pads of the substrate. A small amount of pressure is applied by applying some load on the chip. Then the substrate is cooled below the melting temperature, and a bond is established [30], [31]. Figure 1.4 shows the arrangement in flip-chip bonding.

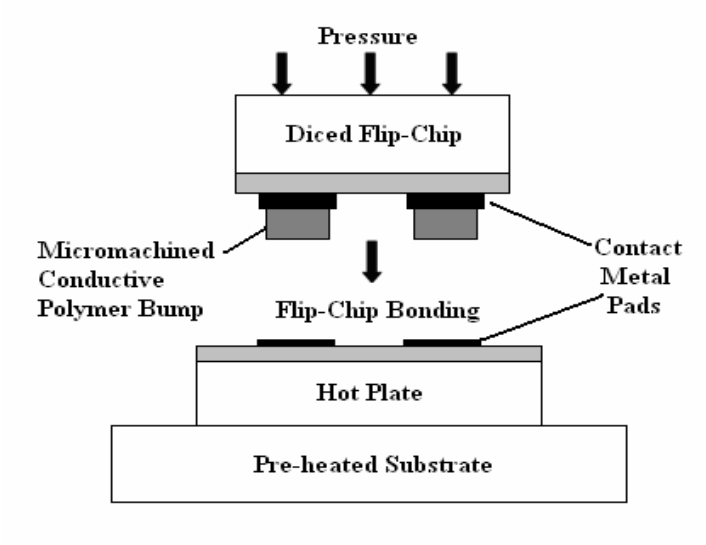

Figure 1.4. Flip-Chip bonding [32].

1.2.8 Hot Embossing Technique (HE)

This technique is used for the embossing and bonding of thermoplastic polymers [24], [32], [33], [34]. The polymer is heated above its glass transition temperature. Then, high contact forces are applied to make the heated polymer flow in the cavities of the mold. Then, the polymer is cooled below the glass transition temperature (keeping the pressure still on), and finally the polymer is separated from the mold. Finally the negative structures are replicated on the polymer surface. Structures ranging form 70 nm to 100 μm are imprinted using Hot Embossing. This is also a very efficient process in polymer bonding which is discussed in the later chapters. Hot embossing technique is shown in figure 1.5.

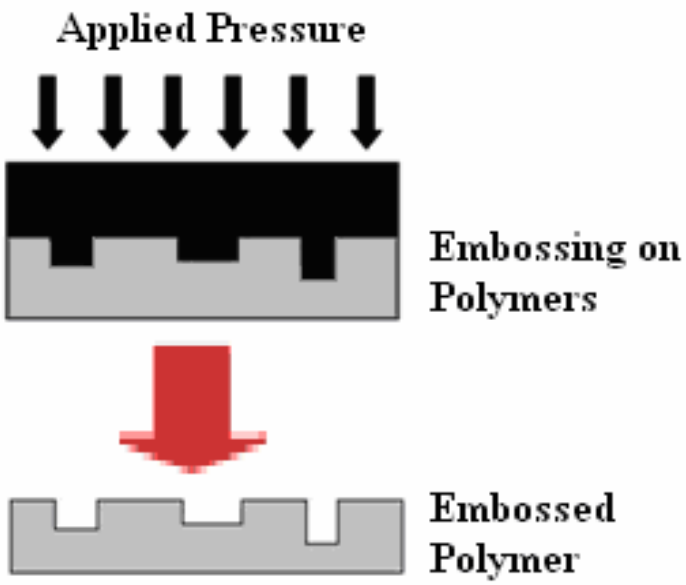

Figure 1.5. Hot Embossing [35]

Hot Embossing is widely used these days for bonding and embossing purposes because of its low cost, high resolution, time efficiency due to low process cycle times, high degree of reproducibility and rapid prototyping for high volume production of fully patterned substrates for a wide range of materials.

High temperature embossing, however, has its disadvantages [36] such as non-localized heating, difficulty in demolding and significant residual thermal stresses due to the different coefficients of thermal expansion between the mold and the polymer.

1.2.9 Deep X-ray Irradiation

Deep X-ray irradiation [37] causes decrease in the molecular weight of polymers, which in turn decreases the T_g of the polymer. Lowered T_g on the surface of two polymer sheets makes bonding possible at low temperature. X-ray irradiation is applied at specific locations on the sheet which decreases the surface T_g to as low as 80 °C. Bonding experiments are performed using this method at pressures of 3 to 4 MPa with bond strength of about 0.96 MPa at a bond temperature of 92 °C.

1.2.10 Lamination

Lamination [38] is primarily used in macro-fabrication processes. In this process, a PET (polyethylene terephthalate) foil coated with an adhesive is rolled onto a polymer substrate where the adhesive melts and bonds the foil with the substrate. When the features sizes are in the order of microns, problem of the adhesive clogging the features exists.

1.3 Review of Thermal Bonding

Thermal bonding has been performed extensively in micro fluidic fabrication. The basic principle of thermal bonding is to heat the two polymer substrates near the glass transition temperature, then apply the desired amount of pressure and hold for a specific period of time. The process should be performed at a consistent temperature so as to avoid thermal and residual stresses and distortions. Comparable bonding strengths can be

obtained by subjecting the substrates to lower pressure for a longer period of time or higher pressures for a shorter period of time.

An air plasma surface modified PMMA [39], [40], [41] substrate was bonded with another PMMA cover plate at 85 °C, and a force of 5000 N was applied for 30 min [42]. Following bonding, the tool and substrate were cooled to 45 °C and the chamber was brought to atmospheric pressure and subsequently opened for removal of the bonded chip.

For solvent assisted bonding [39] on PMMA Chips, four drops of a solvent mixture (47.5 % DMSO, 47.5 % water, 5 % methanol ACS grade were evenly spread over the stamped polymer substrate, the cover plate (surface modified or unmodified PMMA) was placed in conformal contact and aligned, the two were then placed on the plates of the hot embosser and brought to 85 °C with a pressure of 4.7 MPa applied for 30 min. Following bonding, the tool and substrate were cooled to 45 °C, the chamber was opened and the bonded chip was removed.

Two cyclic olefin copolymer (COC) substrates (layers) after plasma activation in presence of various gases such N_2, O_2, 10 % H_2/Ar, power of 100 to 300 W are heated to about 70 °C (this is half of the glass temperature of the material) and a holding time of 30 to 120 seconds. This method is useful to fabricate micro-channel devices for single-molecule level optical based bio-detection systems that require less residual stress and deformation after bonding [43].

In laser assisted bonding process [44], plastic chips are held in close contact under the applied pressure of 0.5 to 10 MPa. The laser energy from the radiations are absorbed by

the plastic biochips and transformed into thermal energy, thus forming a bond. Bond strength of 13.7 MPa to 32 MPa is obtained.

Low pressure, high temperature thermal bonding [45] was performed as follows: The PMMA sheets were heated to 165 °C in 10 min, and then they were bonded at 165 °C for 30 min. Next, the bonded stack was cooled down to 80 °C in 20 min and annealed at this temperature for another 30 min to relieve stress. Finally, the bonded device was cooled to room temperature. High bond strength of 2.15 MPa was achieved.

A bonding technique using spin coated PDMS [46], [47], [48] in between PMMA substrate using a two stage process, shows a low bonding temperature (95 °C) and bonding strength of 0.015 MPa in the PMMA-PDMS-PMMA interface. Microfluidic channels with dimensions of 300 μm * 1600 μm * 100 μm were successfully bonded using this novel bonding method.

Embossed PC sheet [49] and membrane foils are bonded together using the same aluminum pressurized heater as used for hot embossing. The bonding was performed at 135 °C and 2000 lbs (0.4 MPa) for 1 hour. PMMA devices were bonded at 100 °C for at least 8 min [50]. The bonding strength of the chips was estimated to be about 1 MPa.

1.4 Scope of this Research

This research concentrates on thermal bonding of polymer using hot embossing. polymeric substrates with different feature dimensions and thickness were embossed and bonded using hot embossing technology. The process parameters were the bonding temperature, bonding or applied load and holding time. The feature dimensions before and after bonding were examined to assess the geometry changes as functions of the

bonding process. This assessment would provide guidance during the design phase of micro fluidic devices considering the bonding step.

The polymers with varying dimensions and thickness were used and bonded using different parameters like bonding temperature, applied load and holding time. Also polymers with channels of variable dimensions running through the length are used.

Finally a bonding rule is developed for bonding featured polymers used as micro-fluidic devices.

1.5 Report Layout

Chapter 2 introduces the hot embossing process and characterization of polymers during hot embossing and modifications of current system used for the experiments. Chapter 3 addresses microchannel measurement and development of tensile testing fixture. Chapter 4 discusses polymer bonding experiments using the hot embossing machine for featured and non-featured substrates. Chapter 5 discusses the testing results, regression analysis and verification. Finally, Chapter 6 concludes along with recommendations for future work.

CHAPTER 2

HOT EMBOSSING SYSTEM FOR THERMAL BONDING

2.1 Introduction

Hot Embossing [32], [33], [34], [51], [52] is a micro fabrication technique employed for replicating structures on a polymer surface. Structures in the order of microns and in nano scale, as well as a high aspect ratio features have been successfully replicated using this process.

2.2 Basic Configuration and Subsystems of HEMM System

The hot embossing system consists of a heating subsystem, a force application subsystem, a cooling subsystem and a vacuum chamber. A schematic of a Hot Embossing Micro-replication Micro-fabrication (HEMM) system developed in the Mechanical Engineering department at The University of Texas at Arlington, UTA, is shown in figure 2.1. The figure also shows the arrangement of the various subsystems in the main HEMM system.

The various subsystems constitute of a heating subsystem that is controlled by means of number of heating cartridges running through the holes in the two aluminum blocks. These heating cartridges are switched ON and OFF using solid state relays. The cooling subsystem consists of oil pipes running through the entire length of another two aluminum blocks. This is for rapid and uniform cooling of the embossing mold and

polymer assembly during bonding. The cooling of oil is governed by means of chiller and solenoids.

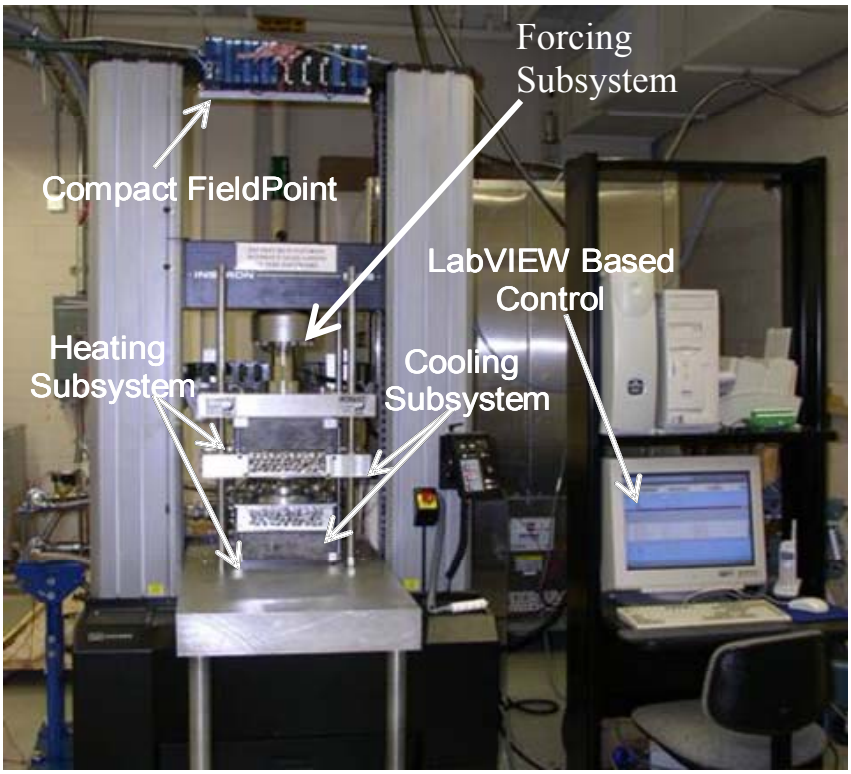

Figure 2.1. Picture of a hot embossing micro replication system.

The required embossing pressure through the mold on the heated polymer is provided and monitored by the forcing subsystem. The force is managed by the controller attached to it and is monitored by means of Instron 5800 console. The control subsystem uses Compact Field Point (CFP) system and LabVIEW by National Instruments for data acquisition and as a user interface to control the main system and individual sub systems. Also there is a vacuum subsystem (not shown in figure 2.1) to provide a clean and moisture free environment during embossing.

2.3 Process

The hot embossing process is similar to the injection molding process in that the negative features contained on a mold are transferred onto a polymer while in a plastic state.

The hot embossing process consists of the following steps:

1. The polymer is heated above T_g (glass transition temperature) to make it impressionable. The master (or mold) is also heated to the same temperature to prevent thermal shock.
2. The master is forced into the polymer by applying a predefined load with the help of load frame.
3. The master and the substrate are held together for a fixed length of time at a constant temperature and load.

The master and the substrate are cooled to below the T_g of the polymer so that it re-solidifies, and then the load is released and mold and the substrate are separated. A step by-step procedure is detailed by Figure 2.2 [51].

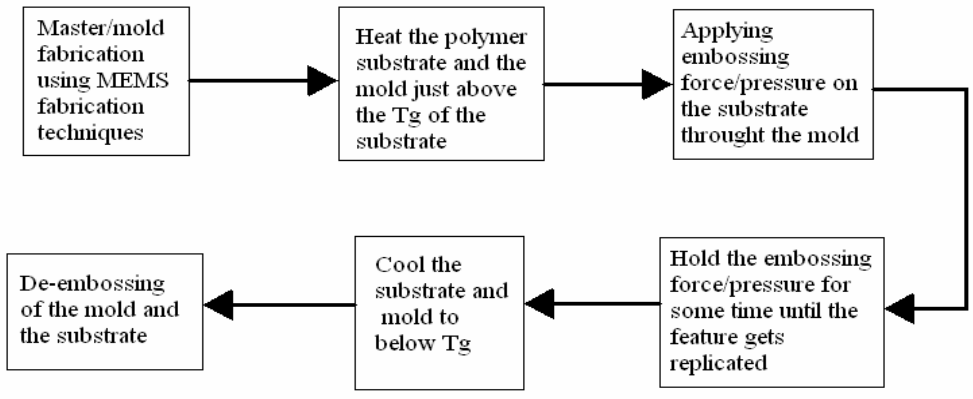

Figure 2.2. Steps for hot-embossing micro-replication process [51].

2.4 Current state of HEMM system

The HEMM system consists of 2 aluminum blocks which are heated and cooled separately using the heating and cooling subsystems. The temperature at the surface of the blocks is estimated by monitoring the temperature on some of the heating cartridges and on thermocouples located at 0.5 inch below the surface.

The software system used for data acquisition and real time control is LabVIEW by National Instruments. A VI (Virtual Instrument) is created in LabVIEW which allows controlling, monitoring and collecting data for the HEMM system. Temperatures at selected locations (on the heating cartridges and 0.5 inch below the surface on the aluminum block) are monitored using this interface and used to emboss and bond the various polymer substrates for micro fluidic devices.

2.4.1 Current System

The HEMM system in our laboratory uses an experimentally derived simple feed forward control loop system for controlling the behavior of the heating system.

The purpose of heating is two fold; to raise the temperature of the mold and substrate to a desired value (embossing temperature) such that both reach it simultaneously, and to maintain this temperature for the duration of embossing process. It was experimentally verified that the temperature remains within the desired error band of ($\pm$ 1 ^{0}C) for approximately 3 min. The tuning of the existing "open loop" type controller was performed based on experimental data. A series of experiments was performed and the results were analyzed to be used for control purpose. The data recorded were the initial, maximum and operating temperatures of the heating surface, and the time at which the heating elements are on, the time at which the maximum and operating

temperature is within a desired error band. A representative temperature profile showing various parameters measured is shown in Figure 2.3.

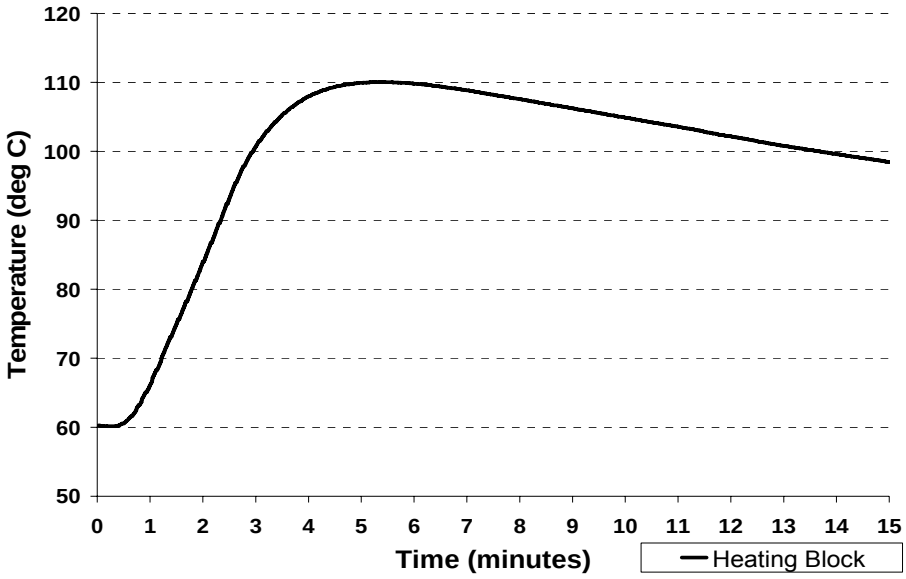

Figure 2.3. Representative temperature profile

2.4.2 Behavior

The behavior of the current system was analyzed by heating and raising the surface temperature within the embossing temperature range. The embossing temperature ($T_{embossing}$) ranges from 110 ^{0}C to 130 ^{0}C. Three values were selected as 110 ^{0}C, 120 ^{0}C and 130 ^{0}C from this range. Similarly, the starting temperature (T_{start}) range was from 60 to 80 ^{0}C, so the three values selected were 60 ^{0}C, 70 ^{0}C and 80 ^{0}C. A series of experiments was performed for different combinations of embossing and starting temperatures.

The temperature of the surface is raised 2 to 5 ^{0}C above the starting temperature and then allowed to cool down to T_{start} before actual experiments. Once the T_{start} is reached, then the heating cartridges are turned ON until the surface reaches $T_{embossing}$.

After that the system is allowed to cool down till the surface starts loosing heat at a constant rate. The temperature at the cartridges and 0.5 inch below the surface are monitored using thermocouples. The system behavior for two different cases of desired and initial temperatures is shown in Figure 2.4 and 2.5.

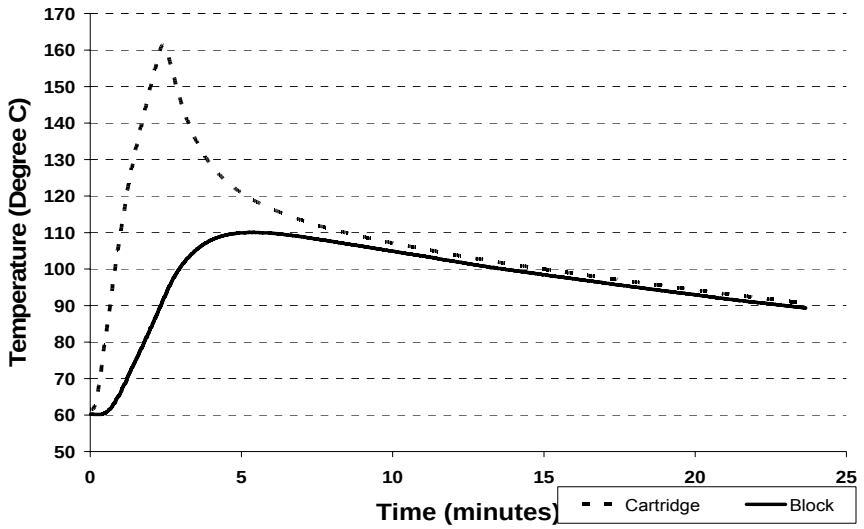

Figure 2.4. Plot of temperature profile with T_{start} = 60 ^{0}C and T_{stop} = 110 ^{0}C

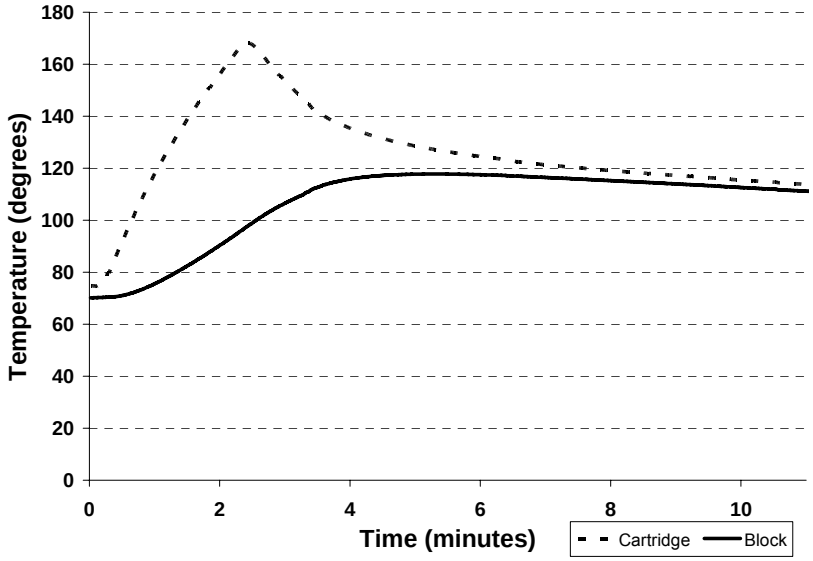

Figure 2.5. Plot of temperature profile with T_{start} = 70 ^{0}C and T_{stop} = 120 ^{0}C

After the first few seconds on commencing the experiment, an exponential rise in surface is observed. The heating cartridges behave in a similar way. It is important to note that though the rise rate of the cartridges and the surface looks the same; the cartridges are at a higher rise rate. This rise in temperature continues until the point the heating cartridges are turned OFF. Note that the temperature of the block keeps increasing for a short time; it does not stop at the same time when the heating cartridges are turned OFF. This is due to the result of heat flow due to conduction from the cartridges to the block.

Subsequent to turning OFF the cartridges, the cartridge temperature settles down for a short period of time, and then starts falling at a high rate. This is due to the fact that the cartridges, at a higher temperature than the block, start loosing heat to the block until they come to thermal equilibrium with it. The surface temperature of the block still continues to rise for another 7 to 9 ^{0}C, then stabilizes for a period of 2 to 3 min in the required error band of $\pm$1 ^{0}C, and then starts falling. The fall rate is higher in the beginning, but it slows down to a slower rate with time because the block surface slowly comes in equilibrium with the surroundings, and the rate of fall of temperature is directly proportional to the temperature difference between the blocks and the ambient air.

2.4.3 Limitations

As described, the basic procedure to start embossing requires heating the master and the substrate to the desired embossing temperature and then maintaining the temperature for the entire embossing process which could be up to 5 min depending on material, feature size and applied pressure. The limitation of the current HEMM system is that the desired temperature is maintained in the error band of $\pm$1 ^{0}C for no more than 2 to 3 min. This time period is not enough for embossing and if the embossing is delayed for some reason

then the entire run has to be repeated. Also, the final temperature that could be reached could vary by $\pm 2\ ^{0}C$. If any differences exist, then embossing may not take place at all.

Another limitation of the system is that both heating of the master and substrate blocks could start at different temperatures at the beginning of each experiment. However, they need to reach the same embossing temperature simultaneously. This may result in delays or even require repeating the procedure.

Thus, these issues motivate us to develop a detailed control strategy for the heating system.

2.5 Modifications to the Current System

The study of the temperature profile of the existing system indicates that the desired temperature can not be maintained for the entire process time (that could be approximately 5 min). Therefore, in order to overcome this limitation and maintain the desired process temperature for an extended time period, a controller strategy based on cycling power to the heating cartridges is developed. Once the desired process temperature is reached an intermittent ON and OFF cycle of the heating cartridges is performed.

A series of experiments was performed to characterize the effects of the ON and OFF state of the heating cartridges to maintain a constant temperature throughout the process cycle. The temperature profiles for process temperatures of $120\ ^{0}C$ and $100\ ^{0}C$ are shown in Figures 2.6 and 2.7 respectively by manually changing the heating cartridge state.

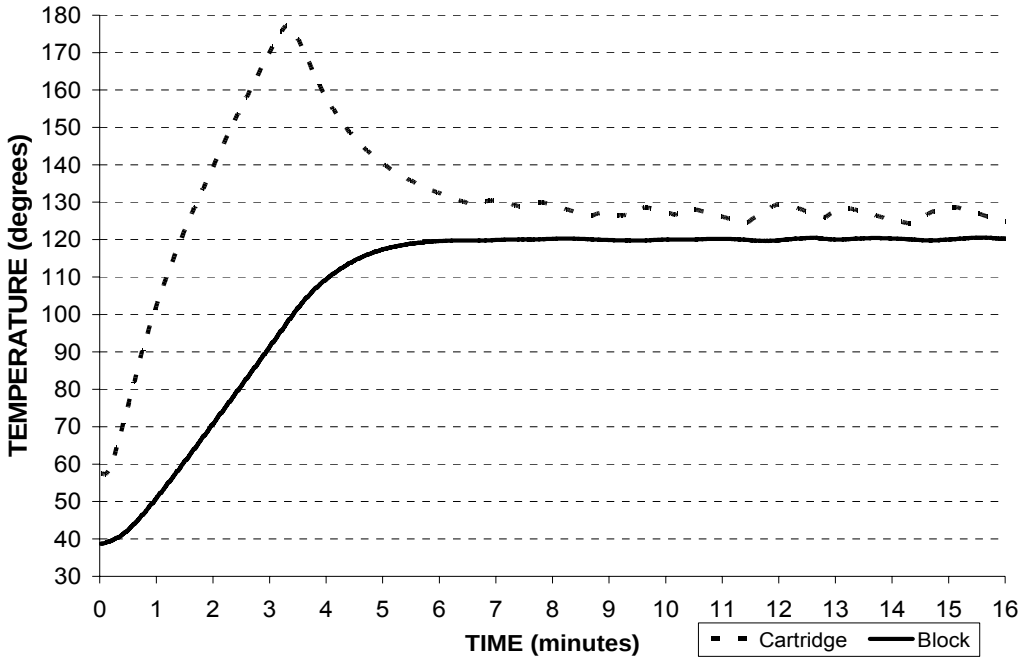

Figure 2.6. Plot of temperature profile for process temperature of 120 ^{0}C.

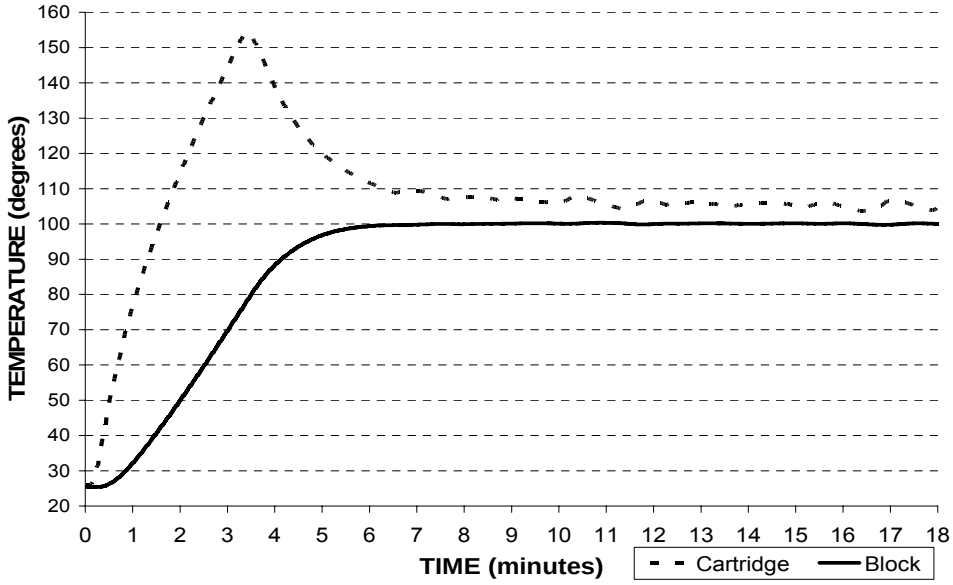

Figure 2.7. Plot of temperature profile for process temperature of 100 ^{0}C.

These experiments were performed by manually switching ON and switching OFF the heating cartridges from within LabVIEW (the monitor and control software used). A trend for the ON/OFF pulse was developed that can be used to maintain the desired process temperature for extended time periods at all values of embossing temperatures.

2.5.1 ON/OFF Pulse profile

The pulsing profile for the ON/OFF cycle is not constant or the same for all process temperatures. The cartridges are heated to a certain temperature and then turned off to allow the surface temperature to reach the desired embossing temperature (also called the process temperature). The temperature at which heating is stopped exhibits a linear relation to the desired temperature reached as is shown in table 2.1 and figure 2.8. After heating is stopped, the temperature is still rising and then it stabilizes to the desired process temperature after which the main process starts during which the ON/OFF pulsing starts.

Table 2.1. Relation between process temperature and stopping temperature for both upper and lower block.

Embossing Temperature required (^{0}C)	Temperature at which heating stopped (^{0}C)	
	Bottom Block	Top Block
80	67	68.6
85	72	73.5
90	77	78.5
95	81.8	83.4
100	86.5	88.6
105	91.6	94.3
110	96.4	99.5
115	101.2	102.3

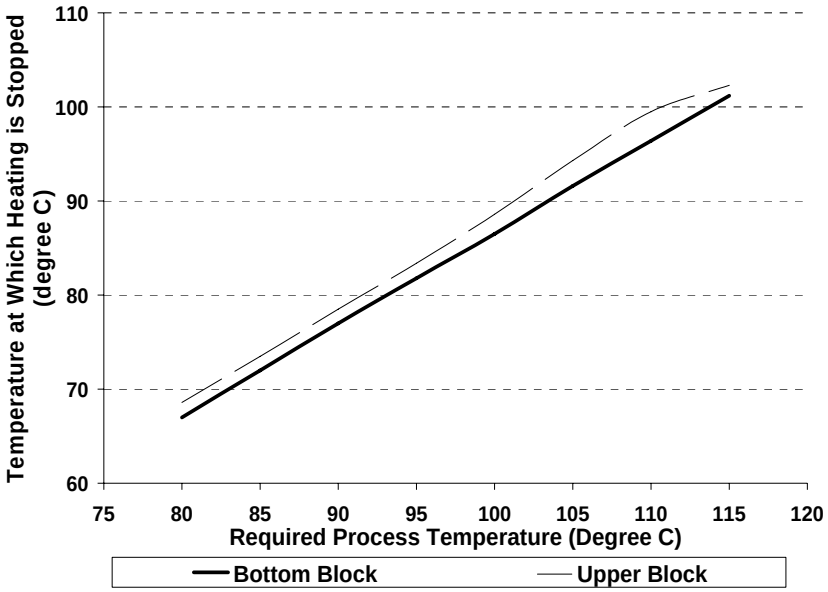

Figure 2.8. Plot relating required process temperature and temperature at which heating is stopped for upper and lower block.

Using this ON/OFF pulsing cycle, the process temperature of 100 ^{0}C was maintained for an unlimited amount of time. The temperature profile from the time when the process temperature is reached for the first time until the 18th minute is shown in Figure 2.9. The bonding and embossing processes require a minimum of 2-3 min. However, using the proposed control strategy, the process time can be extended desired by the process.

The success of controlling the 100 ^{0}C process temperature using the proposed approach, lead us to perform additional experiments for other process temperatures in order to identify the ON/OFF pulse timings. The ON/OFF cycle time for 5 different various process temperatures experimentally identified and verified and is shown in Table 2.2.

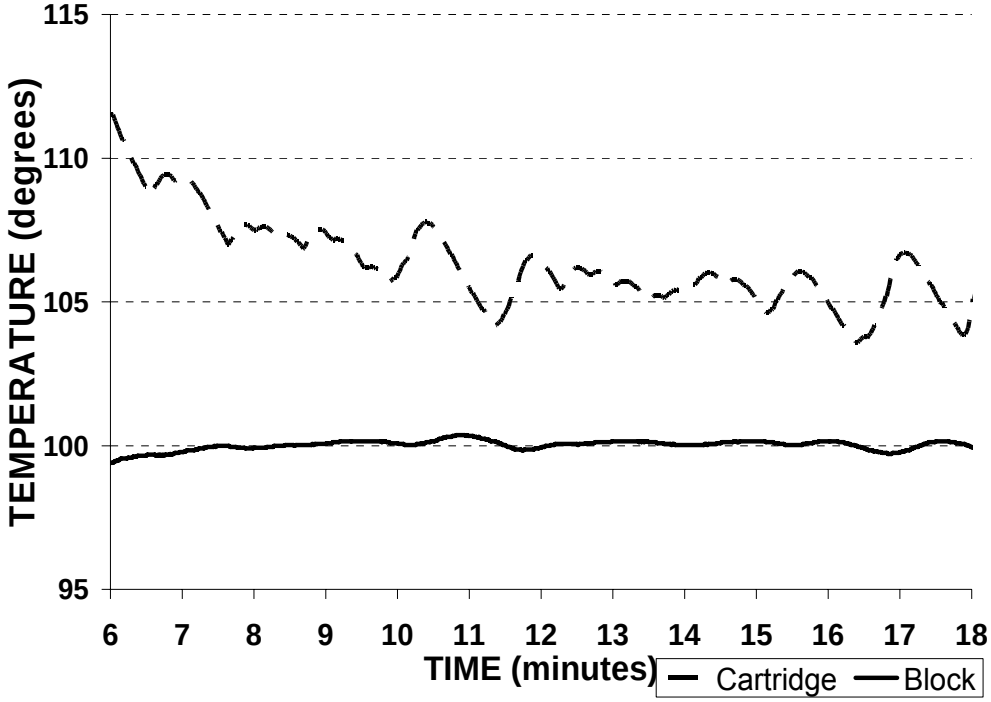

Figure 2.9. Plot for maintaining constant process temperature of 100 ^{0}C using ON/OFF pulsing of heating cartridges.

Table 2.2. Average ON and OFF time required to maintain the required Process Temperature.

Process Temperature (^{0}C)	Average ON Time (sec)	Average OFF time (sec)
95	7.67	16.36
100	12.84	22.84
105	16.8	27.94
110	19.55	31.67
120	21.44	35.00

Equations 1 and 2 give a trend for the ON and OFF time respectively. Using the proposed equations, one could identify the ON/OFF times for other temperatures within the range of the examined process temperatures and control the process temperature for an extended time period within the desired process error of $\pm 1\ ^{0}C$.

$$y = -0.0241x^2 + 5.7398x - 319.79 \quad (1)$$

$$y = -0.0275x^2 + 6.6584x - 367.99 \quad (2)$$

Further analysis of the ON/OFF times for the 5 process temperatures analyzed, allows one to identify the ON/OFF times for other temperatures a shown in Figure 2.10.

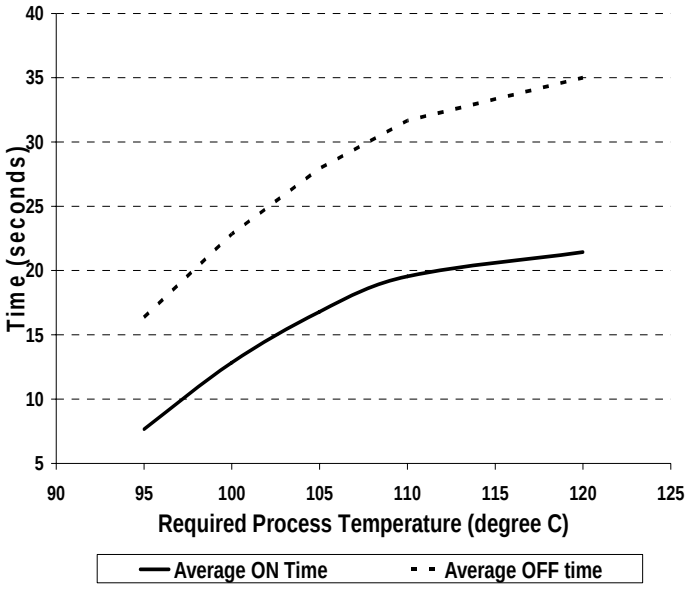

Figure 2.10. Plot for ON/OFF times for maintaining required process temperature.

2.5.2 Combining Force Control and Temperature Monitoring VIs

The next step in the improvement and modification for the HEMM systems was to combine the bonding and temperature VI with the force control VI into a single VI. This will fully automate the process, improve efficiency and ease of use and avoid the need for the user to execute two Vis for embossing leading to possible problems with controlling the times at which certain process actions take place. The force control VI is used to control the applied force and position of the INSTRON load frame.

The VI was modified in a way that when the process temperature is reached, the required force is applied for embossing. The applied load is held for the defined time period, after which the cooling system is energized to cool the system down to the pre-determined separation temperature. Then, the blocks separate and the polymer can be removed from the HEMM system for further secondary operations such as analysis and characterization.

2.5.3 Modification of Temperature Monitoring VI

The completion of the modifications to the existing HEMM control was verified with a series of experiments. During the verification procedure, the lower cooling block was accidentally damage due to overheating and overloading.

The block was repaired but in order to prevent further accidental damage, an additional aluminum plate (9”*9”*1/4”) with proper surface finish and parallelism was used. The addition of this plate, though, required the re-characterization of the temperature profile at the embossing temperature as a function of the thermocouple temperatures in the cooling block and the temperature of a set of heating cartridges that have their own thermocouples.

This relationship was experimentally identified by using a set of 4 thermocouples to measure the surface temperature. The temperature measurements for both the surface and the block were analyzed using the Minimum Least Square Method to identify the relationship. A linear relationship was defined as shown in equation 3.

$$T_{estimate} = a * T_{block} + b * T_{cartridge} + c \tag{3}$$

A series of experiments was performed in which the heating was stopped at various block thermocouple temperature values and a track record was maintained for the thermocouple values at the surface and the cartridges. Using the temperature values at the surface, at the block, and at the cartridge level, the software package MATLAB was used for data analysis that would allow for the estimation of the surface temperature. The values of the three coefficients (a, b and c) were identified for different process temperatures. These values were very close to each other leading to the following equation for estimating the surface temperature.

$$T_{estimate} = 1.1425 * T_{block} + 0.24 * T_{cartridge} - 0.001 \tag{4}$$

This formula was incorporated in the combined VI to account for the temperature on the additional plate surface, which would represent the new process temperature at the lower block. Further experiments were conducted to verify this control approach and results are shown in Figures 2.11 and 2.12 for two surface temperatures of 105 ^{0}C and 95 ^{0}C. The experiments indicate that the estimate equation was properly identified and was in good agreement with the actual surface temperature. Also, these experiments indicate that the

ON/OFF control strategy implemented successfully maintained the temperature at the desired level for the new process. Albeit, the time for reaching the desired temperature increased due to the addition of the extra plate as expected.

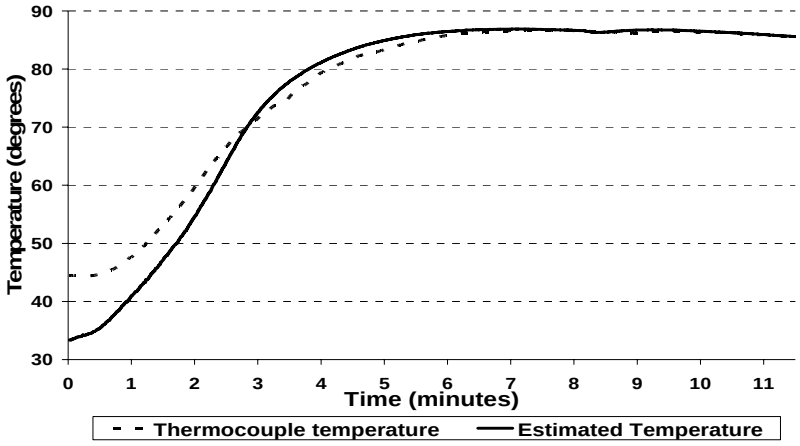

Figure 2.11. Plot for estimated surface temperature vs. thermocouple temperature measured at the surface (1).

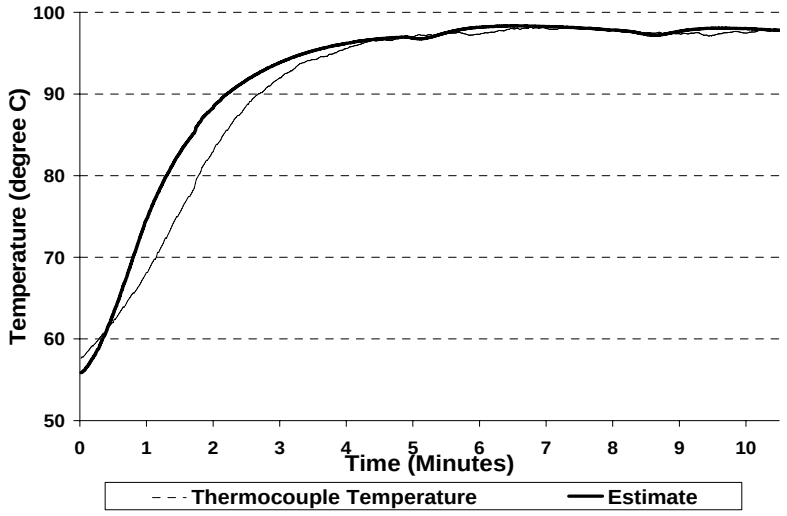

Figure 2.12. Plot for estimated surface temperature vs. thermocouple temperature measured at the surface (2).

2.6 Testing System

There are important embossing/bonding process parameters that are to be discussed and studied at various stages of this research; holding time applied pressure and temperature. A literature survey revealed two combinations of pressure and holding times; low pressure - high holding times, and high pressure - low holding times. The bonding temperature varied as per the bond requirements, either maximum bond strength or minimum degradations of microchannels. The effects of these parameters and their relative magnitudes on the bonding process and bonded features (microchannels) are the focus of this research.

2.6.1 Process Temperature

Process temperature is the temperature at which the main process (embossing or bonding) takes place. The embossing temperature for PMMA is slightly above the glass transition temperature of 105 ^{0}C in order to change the state of the polymer from solid to viscous to facilitate the imprinting of the mold on the polymer. In general, polymer surfaces with no features are bonded using process temperatures higher than the glass transition temperature to ensure good bond strength. However, for polymers with features, the bonding temperature should remain below the glass transition temperature (95 ^{0}C) to prevent the polymer from reaching a viscous state and prevent excessive degradation of the features.

2.6.2 Applied Pressure

The applied pressure depends on the process temperature as well. For high temperatures when the polymer is in viscous state, a low pressure can provide good bonding and embossing for non-featured polymers. On the other hand, for lower temperature an

increased holding time could be used while using low pressure (1 to 3 MPa) to avoid severe degradation of the already embossed.

2.6.3 Holding Time

The last process parameter to be considered for the embossing process is the holding time. Generally, if the process temperature is higher (in the range of glass transition temperature) the holding time should be small (2 min), however, if the process temperature is less than the glass transition temperature, the holding time is generally increased (10-30 min) to ensure efficient bonding or embossing.

CHAPTER 3

DEVELOPMENT OF TESTING FIXTURE

The main aim of bonding experiments with varying process parameters was to measure any change in the polymer thickness along with the degradation of channels and also focus on the bond strength. A variety of devices were used for the measurement of polymers, features and strength as discussed below.

3.1 Measuring Polymer Dimensions

The thickness of the polymers was analyzed using an outside micrometer having a least count of 0.0001 inch. An outside micrometer is typically used to measure wires, spheres, shafts and blocks. The precision of a micrometer is achieved by a using a fine pitch screw mechanism.

An additional feature of micrometers is the inclusion of a spring-loaded ratchet thimble. Normally, one could use the mechanical advantage of the screw to force the micrometer to squeeze the material, giving an inaccurate measurement. However, by attaching a thimble that will ratchet or friction slip at a certain torque, the micrometer will not continue to advance once sufficient resistance is encountered.

In addition to the thickness one other major concern was the polymer width and length, so that we could calculate the surface area and hence the pressure to be applied. This was facilitated by means of a digital vernier scale that could give measurements in

inches (least count as 0.0001) and millimeters (least count as 0.001). Knowing the surface area of the polymer, we could easily figure out the pressure by the applied load.

3.2 Measurement of Channels

To analyze in depth the micro-devices, bonding was performed with some polymers having channels on them. The larger channels (>500 μm) were made using the end milling cutter on a milling machine, whereas smaller channels were embossed on the polymers using a brass mold. The brass mold was made using the CNC Milling Machine. Once the mold was made, the embossing process was carried out at high temperature (115 ^{0}C) and at a low pressure (3 MPa) held for 2 min. At these process parameters, the channels were fully embossed on the polymers.

A Nikon Eclipse ME600 optical microscope with CCD camera for image analysis is used to perform feature measurements. Smaller channels were viewed and analyzed under a lens with 20X magnification, whereas larger channels were viewed and analyzed under lens with magnification of 10X.

The feature width is measured over three different points across the channel length, and an average value was considered for the results. The feature depth is measured by focusing at the top surface of the feature and then focusing at the bottom. The difference in the micrometer reading between the top and bottom gives the depth of the feature. The optical microscope has been used for measuring the channel dimensions both before and after bonding. The measurement error of the optical microscope is 5 μm. So, the degradations in the channels (both in depth and width) can be easily evaluated. Figures 3.1 and 3.2 show some pictures taken from the CCD camera attached to the optical microscope while measuring the channel dimensions.

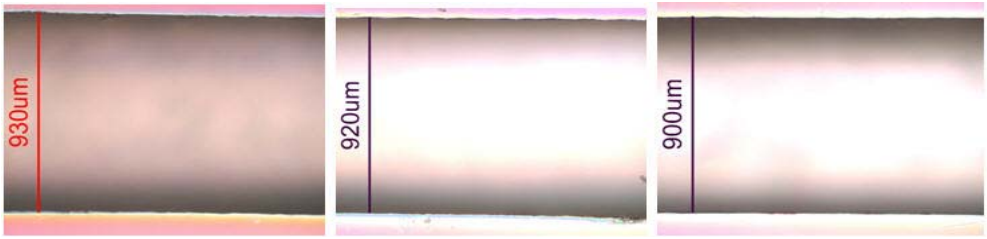

Figure 3.1. Photos from CCD camera fixed to the optical microscope showing width at the top of micro-channels.

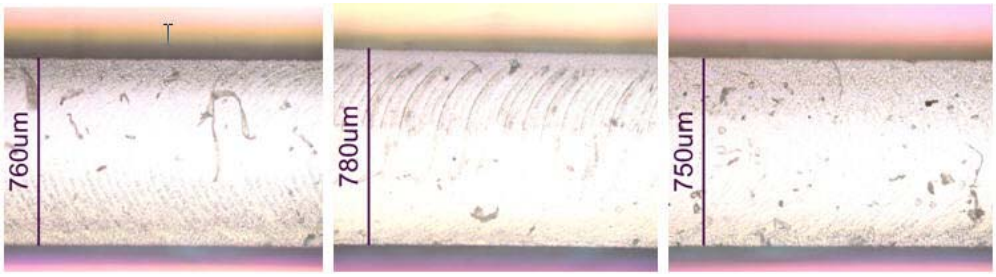

Figure 3.2. Photos from CCD camera fixed to the optical microscope showing width at the bottom of micro-channels.

3.3 Design of Fixtures to Examine the Bond Strength

Once the bonding of PMMA (with or without channels) has been accomplished, the next step was to analyze the bond strength. This is of great importance because the micro-fluidic channels that are formed by bonding the PMMA substrates are used in a variety of applications such as drug delivery and DNA replication and many more processes that require sending small volumes (micro or even nano scale) through these micro channels at certain pressure. So the bonding of the two PMMA substrates should be such that it can withstand that pressure.

To calculate the bond strength, tensile testing was performed on the MTS machine at the Material Science Department of The University of Texas at Arlington. The load cell of 150 kN capacity was used and the strain rate was defined to 0.02

inch/min. The design of the tensile testing fixture and its working is discussed in the following section.

3.3.1 Tensile Testing

The main mode of measuring the bond strength was to do tensile testing on the MTS machine. Tensile strength measures the force required to pull something such as rope, wire, or a structural beam to the point where it breaks. So, in the tensile testing for bond strength of PMMA substrates, each of the bonded PMMA substrates was pulled apart till the point where the bond between them breaks. The principle of tensile testing is shown in Figure 3.3.

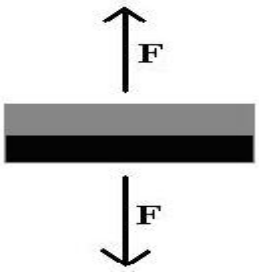

Figure 3.3. Principle of tensile testing.

To facilitate this process, the MTS machine is first calibrated with no load and no fixture attached to the vice. Two aluminum plates were designed (each ¼ inch thickness, and 2*2 $inch^2$ in dimensions) having a ¼ inch threaded circular hole at the centre. The bonded PMMA substrates is glued (with commercially available glue, Gorilla Glue) onto two aluminum plates and allowed to cure under a mild load at room temperature for a minimum of 24 hours. Two screws (each 3 inch long) are put into the threaded holes in the Aluminum plates and are then held on to the holders of the testing system. The speed of motion of the crosshead of the testing system was 0.02 inch/min. It was noticed that the break elongation of the samples equals yield elongation. This means that the sample

retains its original shape when the load is removed before the bond breaks. The bonded test sample mounted on the MTS machine for tensile testing is shown in Figure 3.4.

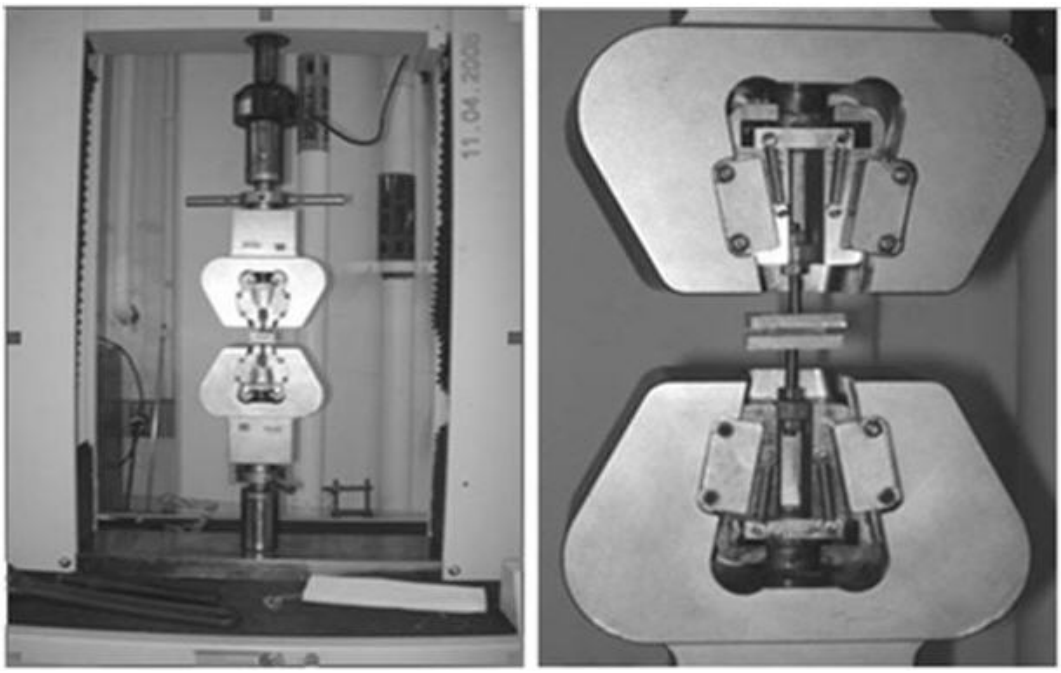

Figure 3.4. Bonded test samples mounted on the MTS machine.

A sample plot of the applied tensile force vs. elongation is shown in Figure 3.5. The breaking force is 284.476 lbs that translates into 1.96 MPa.

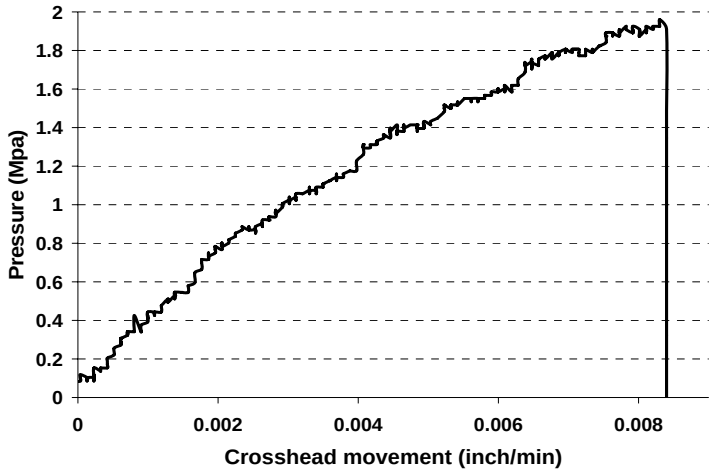

Figure 3.5. Tensile pressure applied (MPa) vs. crosshead movement (inch/min).

The irregularity of the load vs. crosshead extension plot is due to oscillations/vibrations in the crosshead movement accounting for deviation in the measured value (maximum deviation being 5 %). The results for the tensile testing experiments performed to account for the bond strength are discussed in the following chapters in details.

As the bonding parameters varied for different bonded substrates, so the results of the tensile experiments also gave us a range of data. The best bond strength for the PMMA substrates with channels with a reasonable amount of channels left for fluid flow was for 95 ^{0}C as the bond temperature, 2 MPa Bond pressure and 16 min of holding time. A load of 283.495 lbs (translated to 1.96 MPa) is required to break the bond formed under these process parameters. Also for the non-featured substrates, the bonding is effective at a temperature higher than 90 ^{0}C. Below this temperature there is no bonding unless the holding time is high (around 2 hours). The flattening of the substrates is higher as the temperature increases from this value. These effects of various process parameters on the bond strength and the microchannel degradations are discussed in details in chapters 4 and 5.

CHAPTER 4

POLYMER BONDING EXPERIMENTS

There are three bonding process parameters: Bonding temperature, applied pressure and holding time. The bonding process requires two polymeric pieces preferably of the same polymer. The bonding parameters were used for bonding of polymeric pieces, mainly PMMA. In this research, two major sets of experiments were performed. The first set was performed using flat and non-featured PMMA pieces to better understand the effects of the process parameters on the bonding strength and the changes on the PMMA shape. The second set was performed using one flat piece where the second piece was pre-embossed and had features on it such as channels. This second set would allow for the better understanding of the process parameters not only on the bonding strength but also their effect on the feature geometry. The goal of this research work was to experimentally identify the bonding process parameters for acceptable bonding while the embossed features undergo minimum degradation or deformation. This understanding will provide the means towards the development of feature design rules considering the bonding process. This chapter studies and analyzes the step by step bonding processes in order to identify the "optimum" combination of process parameters for acceptable bonding.

4.1 Flat PMMA to PMMA Bonding (Non-featured)

Flat pieces of PMMA with 0.059 inch thickness and surface area of 0.99 $inch^2$ were prepared. These flat pieces were used in the primary thermal bonding process using the Hot Embossing Microreplication Microfabrication (HEMM) system in the Bio-MEMS

laboratory at UTA [51]. The two PMMA pieces were placed one over the other and were sandwiched between two silicon wafers to prevent any contact of PMMA with the aluminum blocks. Then, the bonding process was performed with the desired set of process parameters and then cooling to room temperature and the changes in their dimensions were analyzed using micrometer and vernier caliper.

The bonding of flat PMMA to PMMA is at a temperature near the glass transition temperature. The reason for this is near the glass transition temperature the PMMA is in a viscous state, thus application of a little amount of pressure could lead to a good bond between the two PMMA pieces. The process temperatures examined were 100 ^{0}C and 105 ^{0}C for different pressures. The applied pressure varied between 2 MPa to 10 MPa. The holding time was kept constant at 300 sec. It was observed that the thickness decreases where the area of the PMMA increases due to flattening (as the overall volume of material remains the same). The process parameters, the initial and final pressure, and the initial and final area and thickness along with the corresponding percentage change are presented in table 4.1 for a temperature of 100 ^{0}C and in table 4.2 for a temperature of 105 ^{0}C.

The results presented in tables 4.1 and 4.2 indicate that as the bonding temperature increases and approaches the polymer glass transition temperature, the polymer pieces exhibit a larger deformation in the thickness and an increase in the area. The applied force (pressure) causes an increase in the thickness reduction and an increase in the area.

The process parameters of temperature and force must be monitored and controlled during the bonding process. The temperature profile during the whole bonding

process for a 100 ^{0}C bonding temperature is shown in figure 4.1. The temperatures for the cartridges (TC) and the average lower (LB) and upper (UB) blocks are shown as a function of process time. The collected data indicate that both upper and lower block temperatures reach the desired process temperature simultaneously and also verify that the developed controller maintains the desired process temperature for the defined process time. The applied force profile as recorded by the load cell on the HEMM system is shown in figure 4.2.

Table 4.1. Process parameters and geometry changes for bond temperature of 100 ^{0}C and holding time of 300 sec

Bonding Temperature (^{0}C)	Plate Seperation temperature (^{0}C)	Holding Time (sec)	Force(KN)	Pressure (Mpa)		Area (sq. Inch)		Thickness (inch)		Percentage Change in	
				Initial	Final	Initial	Final	Initial	Final	Thickness	Area
100	60	300	2.00	3.13	3.01	0.99	1.03	0.12	0.12	0.86	3.74
100	60	300	2.50	3.91	3.81	0.99	1.02	0.12	0.12	0.86	2.68
100	60	300	3.00	4.70	4.52	0.99	1.03	0.12	0.11	1.72	3.73
100	60	300	3.50	5.48	5.22	0.99	1.04	0.12	0.11	1.72	4.67
100	60	300	4.00	6.26	6.14	0.99	1.01	0.12	0.11	1.72	2.00
100	60	300	4.50	6.98	6.69	0.99	1.03	0.12	0.11	2.59	4.10
100	60	300	5.00	7.83	7.35	0.99	1.05	0.12	0.11	2.59	6.15
100	60	300	5.50	8.61	7.71	0.99	1.11	0.12	0.11	6.03	10.47
100	60	300	6.00	9.39	8.51	0.99	1.09	0.12	0.11	6.90	9.42

Table 4.2. Process parameters and geometry changes for bond temperature of 105 ^{0}C and holding time of 300 sec

Bonding Temperature (^{0}C)	Plate Seperation temperature (^{0}C)	Holding Time (sec)	Force(KN)	Pressure (Mpa)		Area (sq. Inch)		Thickness (inch)		Percentage Change in	
				Initial	Final	Initial	Final	Initial	Final	Thickness	Area
105	60	300	2.00	3.13	3.32	0.99	1.05	0.12	0.11	2.59	6.02
105	60	300	2.50	3.91	4.16	0.99	1.05	0.12	0.11	2.59	6.25
105	60	300	3.00	4.70	5.09	0.99	1.07	0.12	0.11	6.03	8.43
105	60	300	3.50	5.48	5.93	0.99	1.07	0.12	0.11	6.90	8.32
105	60	300	4.00	6.26	6.89	0.99	1.09	0.12	0.11	7.76	10.11
105	60	300	4.50	6.98	8.00	0.99	1.13	0.12	0.11	8.62	14.58
105	60	300	5.00	7.83	9.23	0.99	1.17	0.12	0.10	11.21	17.94
105	60	300	5.50	8.61	10.27	0.99	1.18	0.12	0.10	12.07	19.35

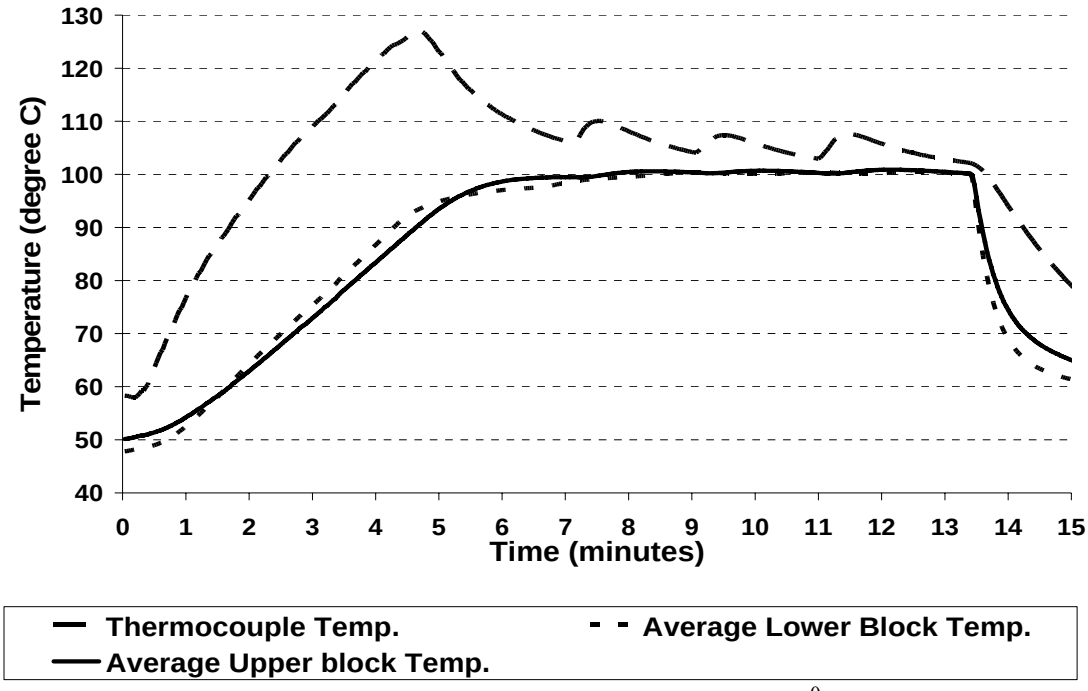

Figure 4.1. Plot for temperature profile for bonding at 100 ^{0}C, 300 sec and 5 MPa.

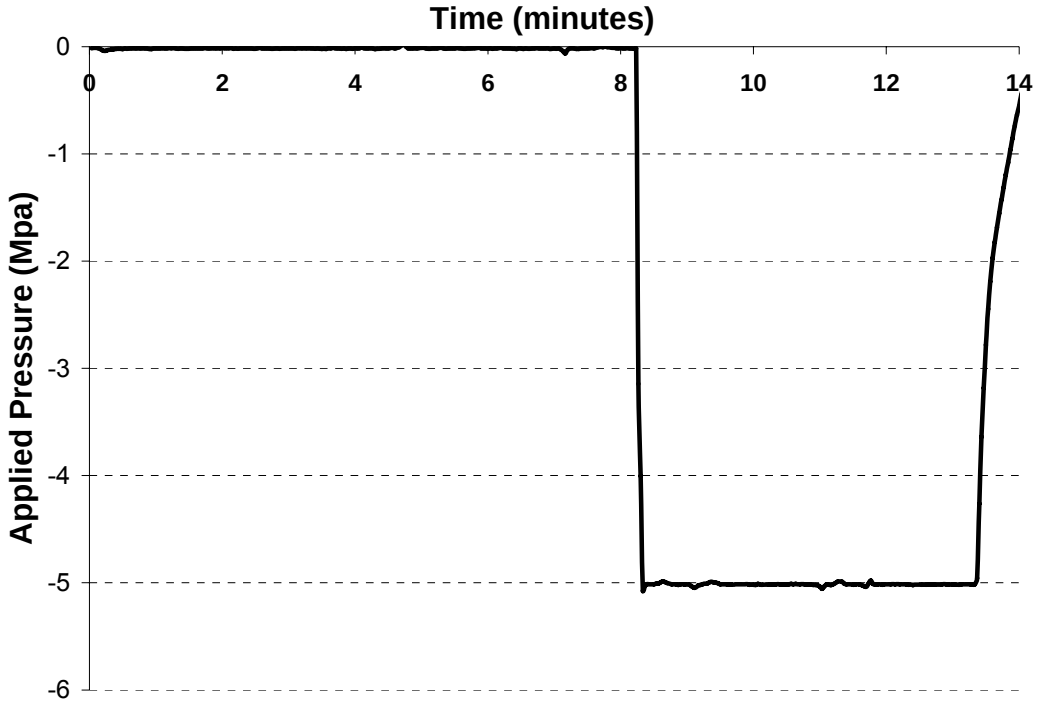

Figure 4.2. Applied pressure profile for bonding at 100 ^{0}C, 300 sec and 5 MPa.

Also, from the data at different process parameters, we can find out the relation between the applied pressure and percentage reduction in thickness.

The experimental data is also used to identify the relationship between the applied pressure and the percentage reduction in thickness. This is plotted in figure 4.3 for both temperatures. The temperature effect is more prevalent in the higher temperature, closer to the glass transition temperature. Also, the higher the thickness change the higher the area change will be since there is no material loss during bonding.

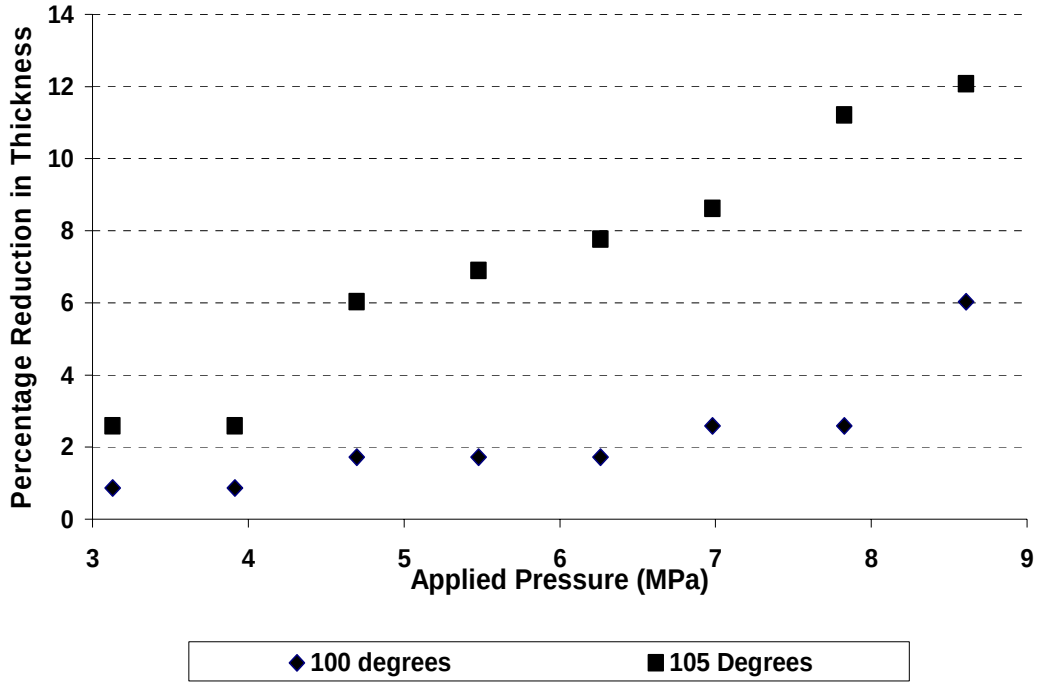

Figure 4.3. Plot for percentage change in thickness vs. applied pressure for two different process temperatures of 100 ^{0}C and 105 ^{0}C.

A set of additional experiments was performed with the following observations:

- No effective bonding takes place below 90 ^{0}C. At least a temperature above 90 ^{0}C and a pressure of approximately 1 MPa are required for bonding to take place unless the holding time increases considerably (about 2 hours for which a temperature of 85 ^{0}C could be used).
- The polymer thickness increases with an increase in temperature and/or pressure and is compounded when both temperature and pressure increase.

Therefore, keeping in mind the above observations, flat PMMA to PMMA bonding with good bond strength as well as minimum deformations could be obtained. These results

provided confidence to further pursue PMMA to PMMA bonding with features on one of the polymer substrates.

4.2 Flat PMMA to Featured PMMA Bonding

The initial sets of experiments utilized PMMA sheets without any features and aimed at providing an understanding of the deformation as a function of the process parameters of bond temperature, applied pressure and holding time. However, it is imperative to remember that polymeric microfluidic devices usually have reservoirs and channels for fluid storage, transportation and mixing. The next set of experiments was performed using PMMA sheets with pre-embossed channels in order to identify the geometry deformation and bonding strength as function of process parameters and PMMA sheet thicknesses (for both the flat and featured).

The channels were fabricated employing two different processes on square PMMA pieces with dimensions of approximately 25.4 mm^2 (1.0 $inch^2$). The first process used a milling machine to fabricate channels with larger dimensions of approximate depth of 650 μm and width of 900 μm. The second process utilized the HEMM system to replicate microchannels from a brass mold with approximate depth of 170 μm and width of 200 μm using process parameters as discussed in [51]. The channel geometry, width and depth, was measured using a Nikon Eclipse ME600 optical microscope with CCD camera for image analysis available in the Materials Science Characterization Lab.

The purpose of this bonding process was two fold; to seal and at the same time obtain microchannels that can be used in diagnostics, genomics, pharmacy, cell manipulation and many more micro-fluidic based applications [51]. The microchannels were characterized before and after bonding for various process parameters.

Subsequently, the geometry deformations were considered in the design of bonding rules and also could be used during the microchannel design stage.

4.2.1 Larger Geometry or Size Channels

The larger geometry microchannels were fabricated using a milling machine where the microchannel was running through the entire length of the PMMA piece used. After milling, the microchannels were washed with acetone to remove any material residue or particles due to the contact subtractive material process. The cleaned microchannels were then examined using optical microscopy and their width and depth were measured before bonding.

Another factored considered for bonding was the thickness of the flat sheet of PMMA to be bonded on the featured piece. The three thicknesses selected for the experiments were 1500 μm (original PMMA sheet thickness), 1000 μm and 400 μm.

These thicknesses were obtained from the original PMMA thickness of 1500 μm using the HEMM system. The 1000 μm thickness was obtained by flattening the original PMMA piece at a temperature of 115 ^{0}C (higher than the glass transition temperature for PMMA of 105 ^{0}C) and at a pressure of 35 to 40 MPa. The thickness of 400 μm a two step flattening process was employed by first obtaining the 1000 μm thickness and then the flattened PMMA was further flattened at high temperature and pressure (again at 115 ^{0}C and 35 to 40 MPa). Once the thicknesses were obtained, the surface area and dimensions of the final PMMA sheets were larger than 25.4 mm^2 (1.0 inch^2). The flattened PMMA pieces were machined to the desired dimensions and washed in acetone bath to remove unwanted material deposited due to machining.

Subsequently, bonding experiments were performed for different process parameters as follows:

Bond temperature:	100 ^{0}C, 105 ^{0}C
Bond pressure:	4 MPa, 5 MPa, 6 MPa
Holding Time:	5 min

The two PMMA substrates were positioned between two silicon wafers and placed on the HEMM system. Then, the cartridges are turned on so that the top and the bottom aluminum block reach the predetermined bond temperature, the desired force (calculated from a knowledge of area and desired applied pressure) is applied to the substrates and the system is held at the bond temperature and pressure for the desired holding time of 5 min. The substrates are cooled to the de-embossing temperature of 60 ^{0}C at which the upper and lower blocks separate and the bonded substrates are removed from the HEMM system. The stack thickness is measured and compared with the combined thickness of both substrates before bonding.

After bonding, the geometry of the channels was examined. The bonded PMMA pieces were measured using the optical microscope with the bonded channels side under focus (as shown in the Figure 4.4). Measuring the channels profiles provide information on the degradation of the channel width and height.

Measuring the bonded channels from the side gives an idea about the channel degradations, but to get the clear picture, we wanted to analyze the channel from the top along its full length (details shown by means of tables and plots in chapter 5) To accomplish this, the two substrates were separated on the MTS machine using the tensile testing fixture designed to analyze the bond strength of the bond. The tensile testing

fixture works on the principle that both substrates are held simultaneously in two different clamps of the MTS machine and pulled apart at a predetermined rate of 0.02 inch/min.

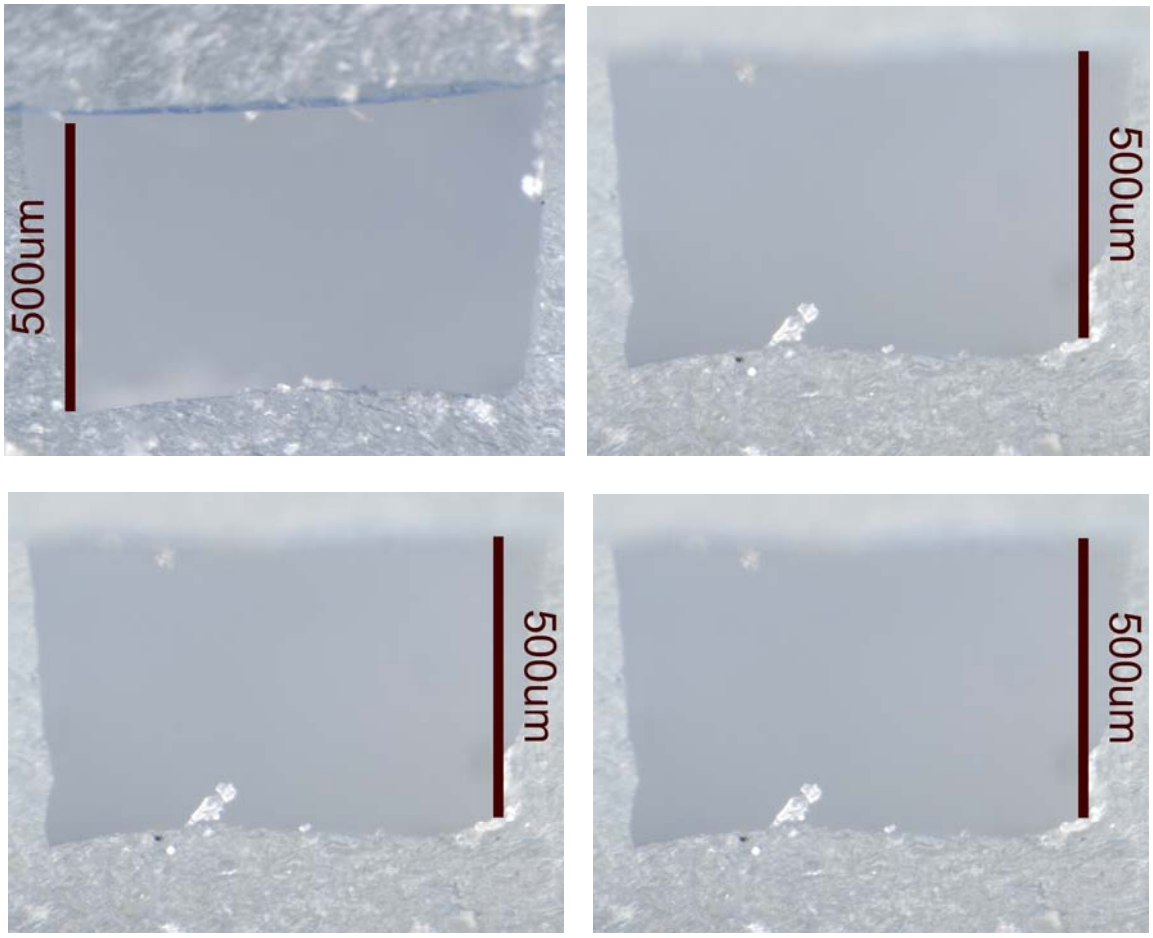

Figure 4.4. Picture showing bonded channels side-view taken from CCD camera attached to the optical microscope.

Once the substrates were separated/de-bonded, channels were analyzed for their thickness and depth after bonding. The thickness and depth were measured at three different points throughout the length of the channels, and the average value was taken for analysis.

The depth of the channels was measured by comparing the micrometer reading of the optical microscope at the top and bottom of the channels.

4.2.2 Smaller Channels

The channels on the polymer substrates were also made by embossing. In this method, a brass mold is prepared that contain the negative of the channels, and at high temperature (more than the glass transition temperature of PMMA) and on application of high pressure, the channels are completely replicated on to the PMMA substrates.

The channels produced using hot embossing were smaller than the ones produced by milling machine (width of the order of 200 μm and depth of the order of 170 μm. The brass mold was prepared using CNC milling machine and was 1*1 $inch^2$. The process parameters that were used during the embossing process were:

Embossing temperature:	115 ^{0}C
Applied Pressure:	2 MPa
Holding Time:	120 sec

It is interesting to note that at these process parameters, the channels were completely replicated from the mold to PMMA substrate. The bonding of these PMMA substrates with channels was performed at the same range of temperature as done for the bigger channels.

Bond temperature:	100 ^{0}C, 105 ^{0}C
Bond pressure:	3.1 MPa, 4.7 MPa, 6.3 MPa
Holding Time:	2 min

When the bond temperature was 105 ^{0}C, the channels were degraded to such an extent that there were physically no channels left. This is due to the reason that at the

temperature near the glass transition temperature, the PMMA behaves viscous and at high pressure, the material flow is such that the channels are completely filled.

Even at the bond temperature of 100 ^{0}C, the degradation in the channel depth is about 80 %. And the top cover PMMA substrate material flow into the channels is such that there are practically negligible channels left. Even to take into account the top plate that goes into the channels, three different thicknesses of the top plates PMMA Substrates was used: 400 μm, 1000 μm and 1500 μm. These thin PMMA substrates were prepared by flattening using the hot embossing setup at high temperature and pressure (115 ^{0}C and 25 MPa respectively for 1000 μm thickness). To get even smaller thicknesses, the flattening experiment was repeated. The bonding results are presented in figures 4.5 and 4.6.

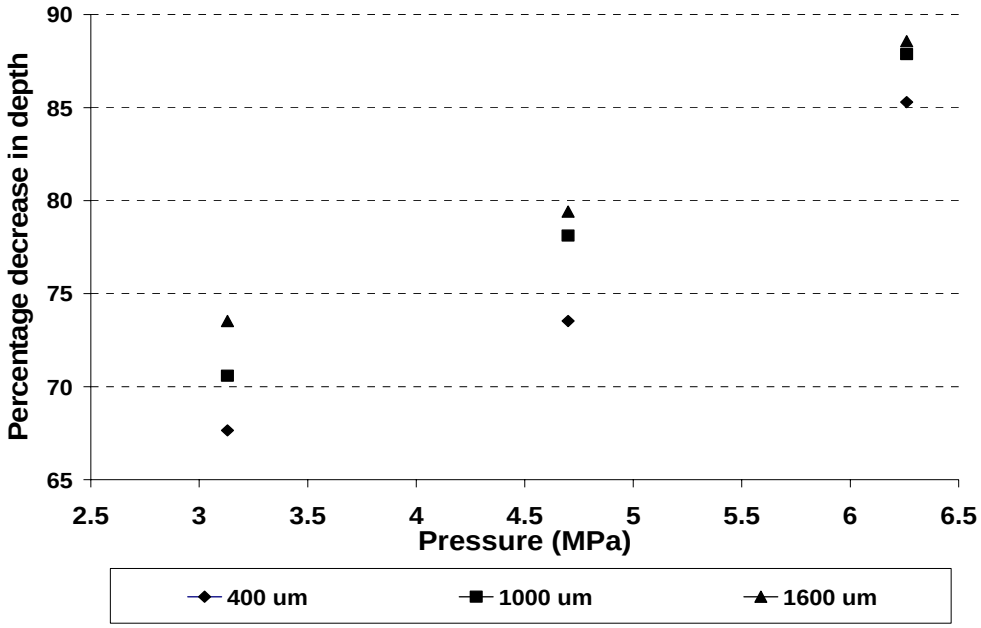

Figure 4.5. Plot for percentage decrease in channel depth for smaller channels at 100 ^0C and varying pressure.

It is observed that for smaller channels the bond temperature needs to be less than the range of glass transition temperature (even less than 100^0C) to reduce degradation in channel depth. But at the same time, the stress is on the bond strength of the PMMA bonding.

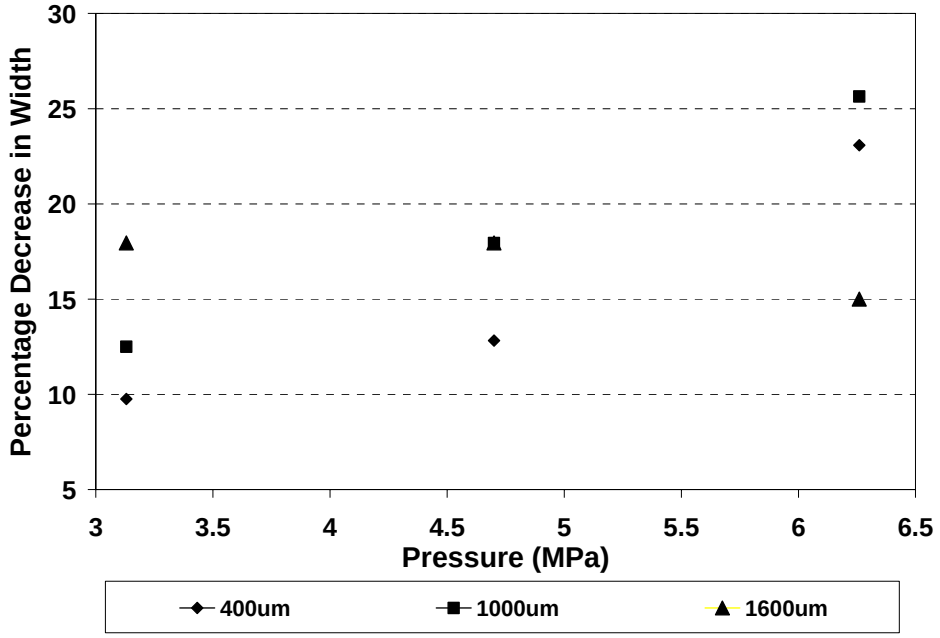

Figure 4.6. Plot for percentage decrease in channel width for smaller channels at 100 ^0C and varying pressure.

Therefore, to achieve both (reduced degradation and good bond strength), a series of new experiments was performed to bond the smaller channels PMMA substrate with non-featured top PMMA substrate using the following bonding parameters.

Bond temperature:	95 ^{0}C
Bond pressure:	2 MPa, 4 MPa and 6 MPa
Holding Time:	4 min, 8 min and 16 min

CHAPTER 5

DISCUSSION OF EXPERIMENTAL RESULTS

Bonding of featured and non-featured PMMA substrates was performed at various combinations of process parameters: Bond temperature, holding time and applied pressure. In addition to the process parameters, the thickness of the top PMMA substrate was varied from 400 μm -1600 μm and the corresponding effect on the geometry of the channels and bond strength has been studied. The following sections discuss the experiments and experimentally obtained results and the effect of the various parameters on the bond strength and channel geometry changes.

5.1 Bonding Pressure

The desired applied bonding pressure along with the surface area of the substrates was used to find the force to be applied by the HEMM system. This force is measured by a load cell and monitored through the force control VI. A good and stable bond was generally obtained by considering the applied pressure and bond temperature according to the following rule of thumb;

- High temperature and low pressure.
- Low temperature and high pressure

Different loads were applied during the bonding at different temperatures and the effects on microchannels dimensions are measured. Also extensive experiments were performed by considering and changing the top PMMA thickness.

The percentage change (decrease) in channel geometry and the increase in bond strength of microchannels at three different bond pressures (2, 4 and 6 MPa) are shown in Tables A.1 to A.3 and Figures 5.1 to 5.9. Each of these figures shows the effect of bond pressure for three sets of experiments (series 1, series 2 and series 3). Also the top PMMA substrate thickness was varied for this set of experiments and its effects are discussed.

It is interesting to note that by varying the bond pressure, there is more effect on the channel depth as compared to the width of microchannels. The percentage decrease in depth increases from 11 % to 73 % by increasing the bond pressure from 2 MPa to 6 MPa, where the corresponding percentage decrease in width increases from 2.5 % to 9.25 %. The bond strength increases when the top PMMA thickness is more. An increase in the bond pressure for the 400 μm top PMMA thickness increases the bond strength from 0.74 MPa to 0.97 MPa (31 % increase), whereas the same increase in bond pressure for the 1600 μm top PMMA substrate causes an increase from 1.63 MPa to 1.99 MPa (18 % increase).

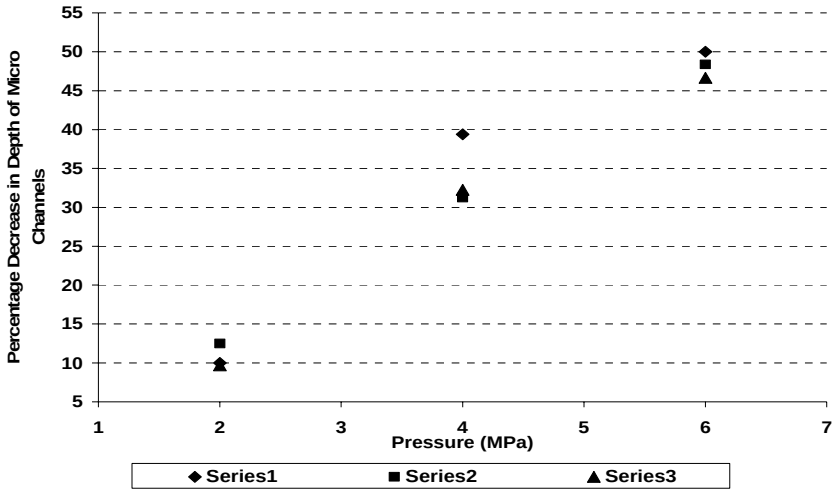

Figure 5.1. Plot of bond pressure vs. percentage decrease in depth of microchannels at 95 ^{0}C and 480 sec for 400 μm top PMMA thickness.

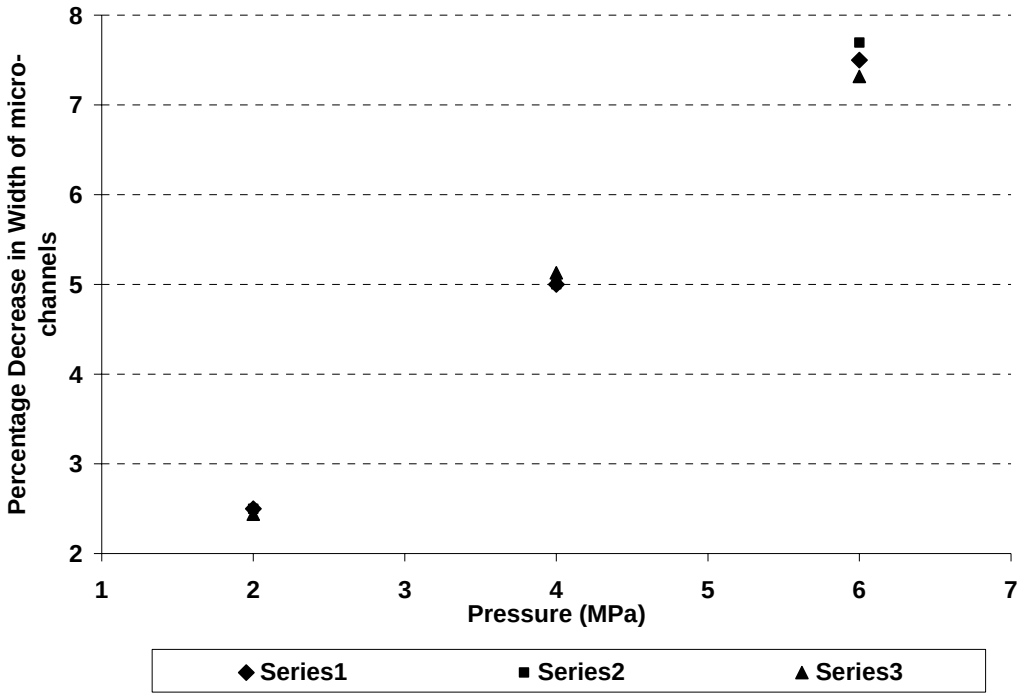

Figure 5.2. Plot of bond pressure vs. percentage decrease in width of microchannels at 95 ^{0}C and 480 sec for 400 μm top PMMA thickness.

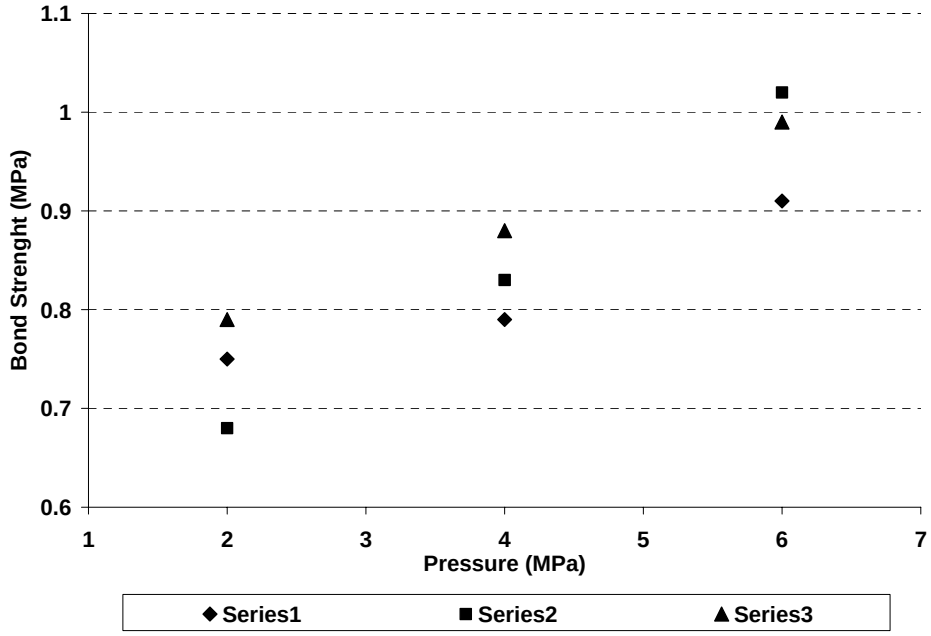

Figure 5.3. Plot of bond pressure vs. bond strength of microchannels at 95 ^{0}C and 480 sec for 400 μm top PMMA thickness.

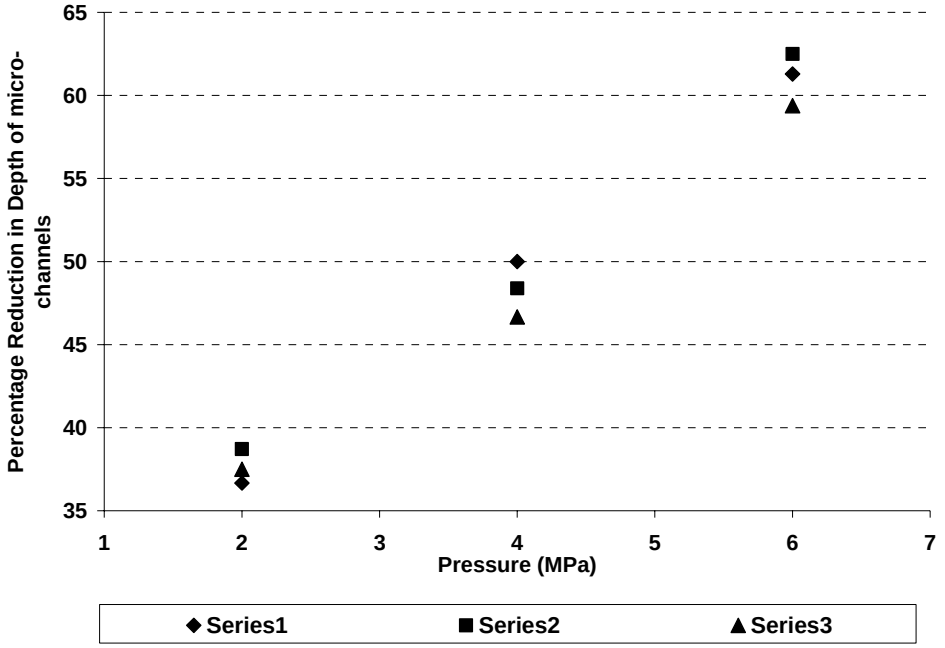

Figure 5.4. Plot of bond pressure vs. percentage decrease in depth of microchannels at 95 ^{0}C and 480 sec for 1000 μm top PMMA thickness.

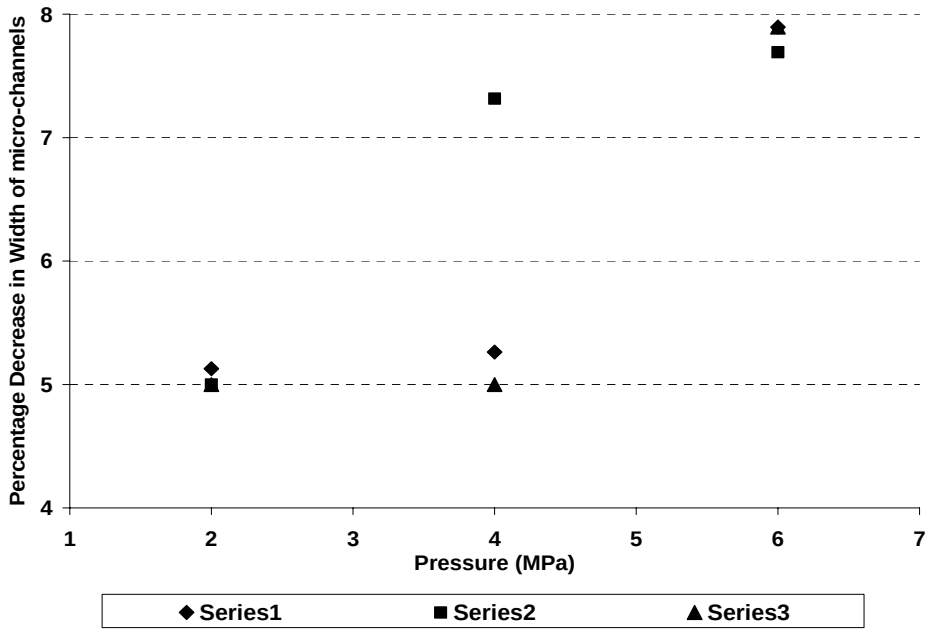

Figure 5.5. Plot of bond pressure vs. percentage decrease in width of microchannels at 95 ^{0}C and 480 sec for 100 μm top PMMA thickness.

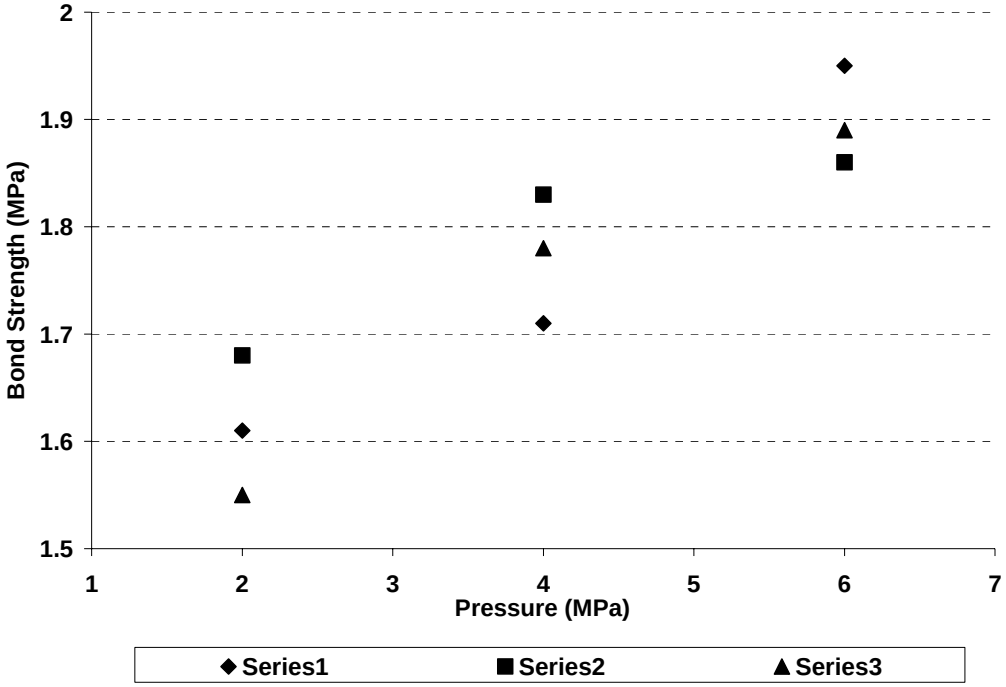

Figure 5.6. Plot of bond pressure vs. bond strength of microchannels at 95 ^{0}C and 480 sec for 1000 μm top PMMA thickness.

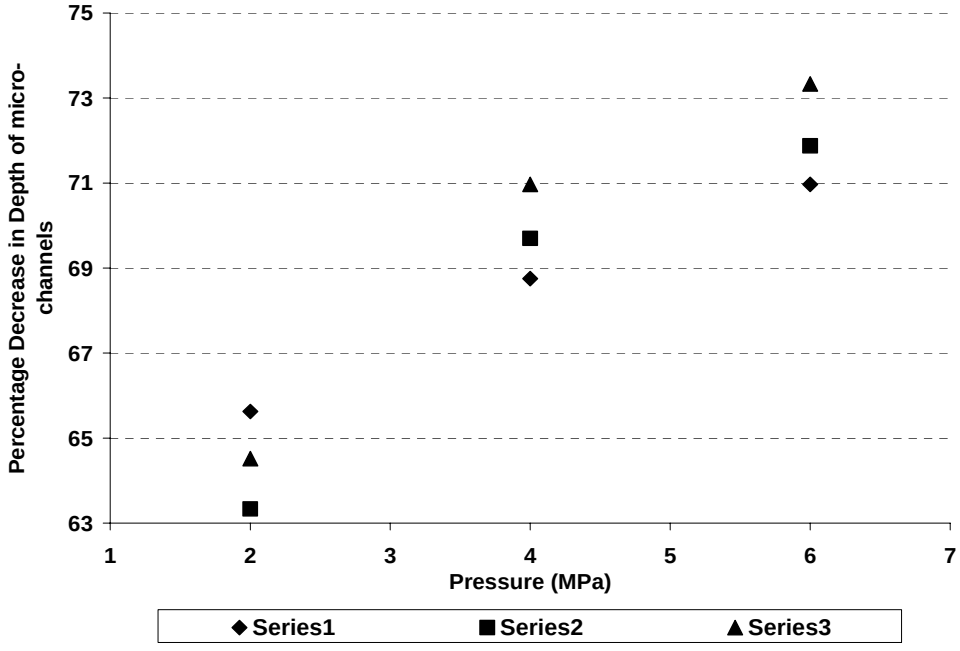

Figure 5.7. Plot of bond pressure vs. percentage decrease in depth of microchannels at 95 ^{0}C and 480 sec for 1600 μm top PMMA thickness.

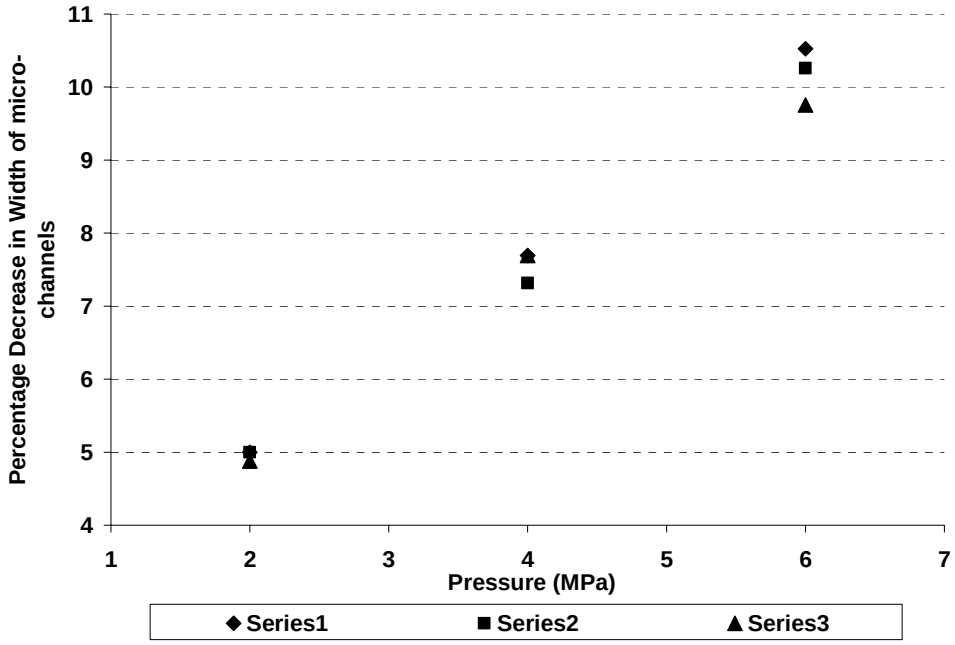

Figure 5.8. Plot of bond pressure vs. percentage decrease in width of microchannels at 95 ^{0}C and 480 sec for 1600 μm top PMMA thickness.

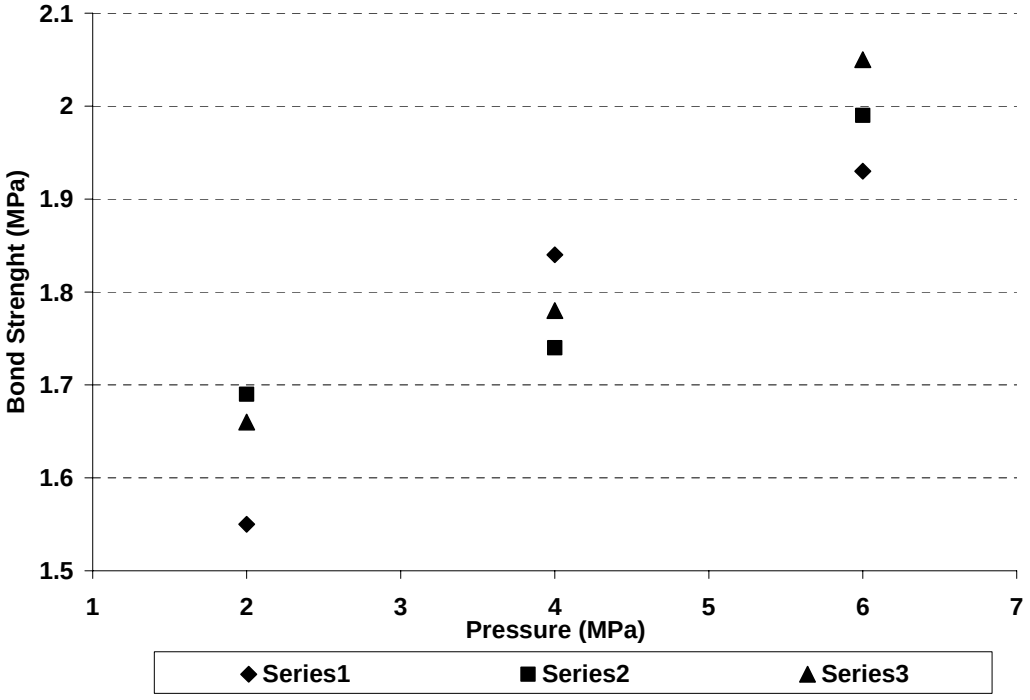

Figure 5.9. Plot of bond pressure vs. bond strength of microchannels at 95 ^{0}C and 480 sec for 1600 μm top PMMA thickness.

Examining the average values of degradation in channels and bond strength variations due to increase in bond pressure, it is clear that the effect is more on the channels depth as compared to the width (shown by table A.4 and figures 5.10 to 5.12). This effect is even more when the top PMMA thickness increases. The reason that accounts for this is that more thickness of top PMMA substrate when heated to the bond temperature causes more material flow into the channels, thus resulting in degradation in channel depth more than the width. Also the bond strength is affected more when the top PMMA thickness is more. The maximum bond strength obtained at higher bond pressure (6 MPa) is 1.99 MPa.

The average values of percentage degradation in channels geometry and bond strength by increasing bond pressure at two different bond temperatures (95^0C and 100^0C) are presented in Table A.5 and Figures 5.13 to 5.15.

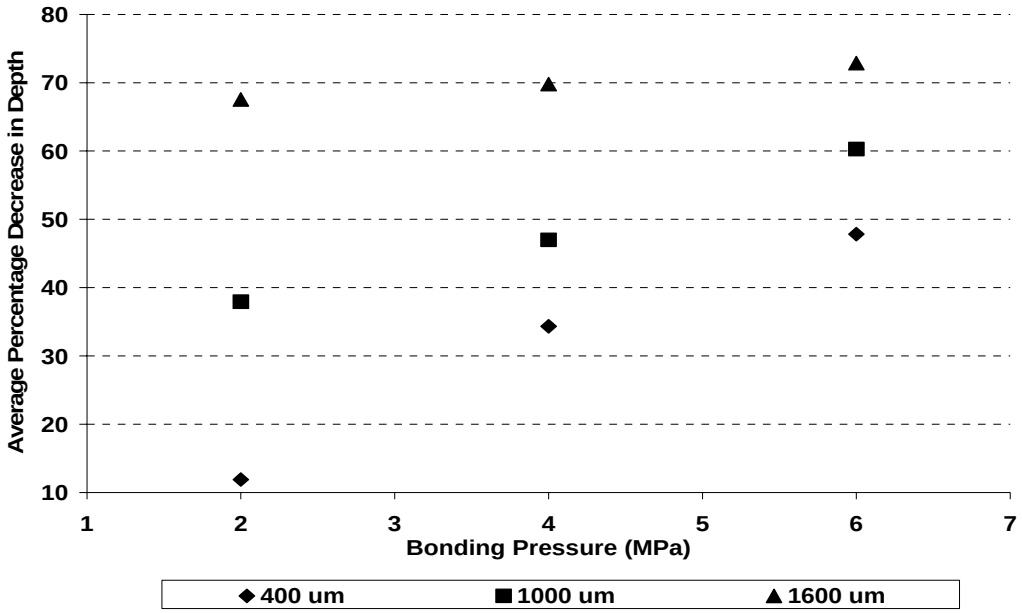

Figure 5.10. Plot for bond pressure vs. average percentage decrease in channel depth of PMMA micro-devices at 95 ^{0}C and 480 sec for varying top PMMA thickness.

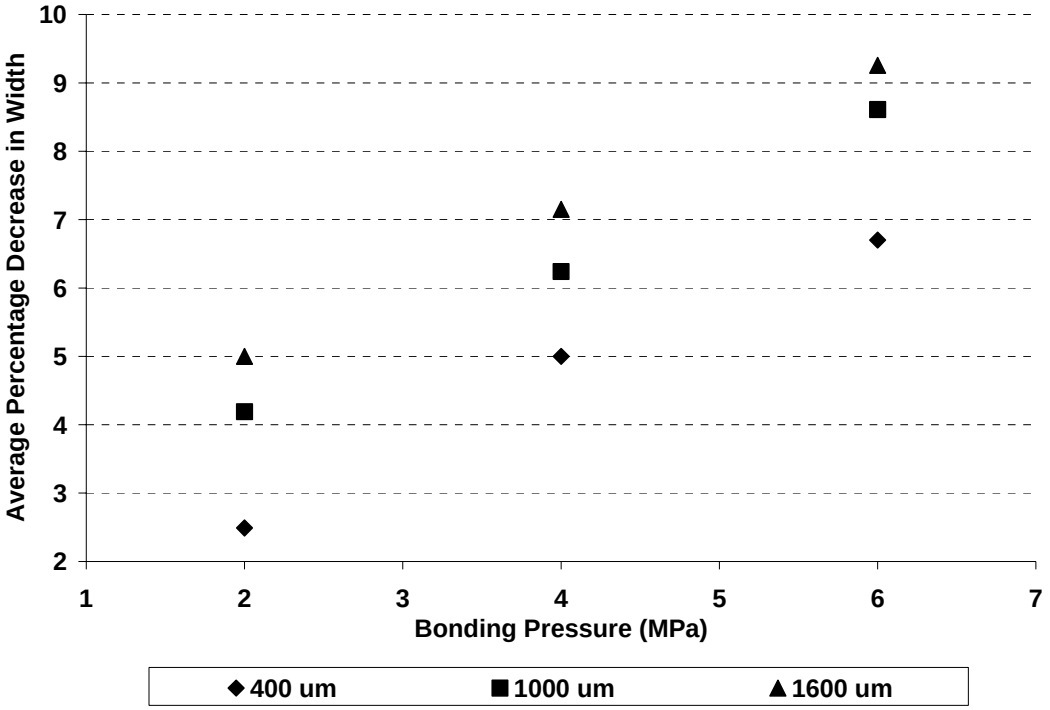

Figure 5.11. Plot for bond pressure vs. average percentage decrease in channel width of PMMA micro-devices at 95 ^{0}C and 480 sec for varying top PMMA thickness.

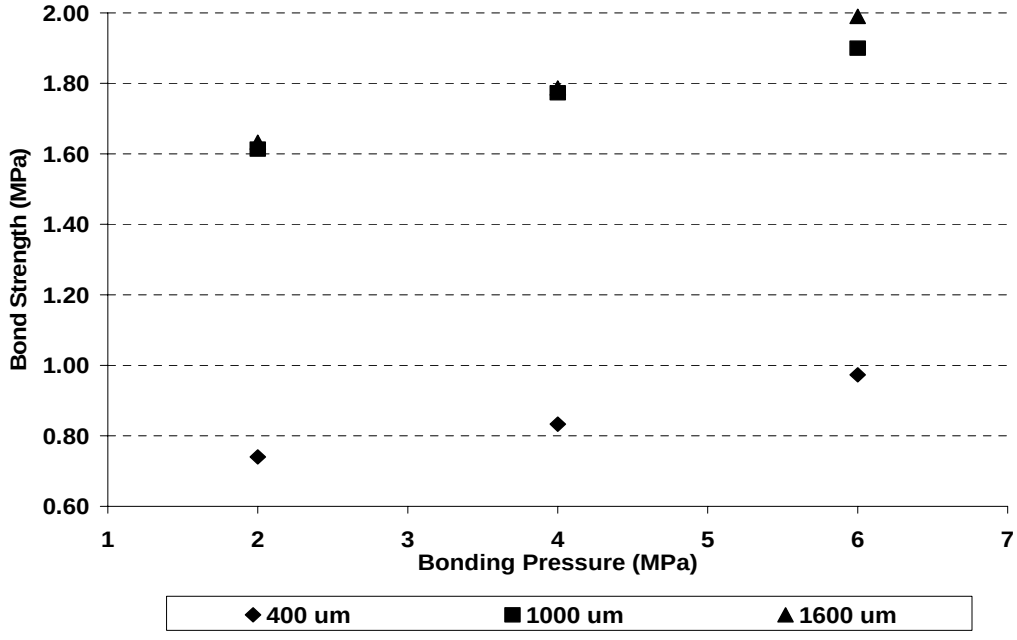

Figure 5.12. Plot for bond pressure vs. average bond strength of PMMA micro-devices at 95 ^{0}C and 480 sec for varying top PMMA thickness.

For same low temperature (95 ^{0}C), the percentage decrease in depth of channels is as low as 11.9 % for a 400 μm thin top PMMA substrate at pressure of 2 MPa while it increased to about 47.83 % for the same top PMMA substrates by increasing the applied pressure to 6 MPa. It increases even more to 72.88 % for thicker top PMMA substrate at higher pressure and same low temperature. The effect on width of microchannels is very small at low pressure (2 MPa), but at higher pressure the degradation is about 9.26 %.

For higher temperature (100 ^{0}C), the degradation is more under the same process parameters. For low pressures the degradation in depth of microchannels is 68.2 – 83.55 % for thin top PMMA substrate, which increased to 91.3 % for higher pressure (6 MPa). Also the channel width degradation increases from 7.4 % at low pressure to 26.55 % at higher pressure. But apart from all these changes, the effect of increasing bond pressure is increased bond strength (0.74 MPa at low pressure to 1.99 MPa at higher pressure). At even higher temperature, the bond strength increases as well to 2.13 MPa.

Hence, varying the pressure by keeping the remaining process parameters same has more effect on depth of microchannels rather than on their width and it also increases the bond strength. Therefore, considering the desired outputs it is recommended to use:

- Lower bond pressure for minimum channel degradations.
- Intermediate value for getting less degradations and good bond strength.
- Higher bond pressure for higher bond strength.

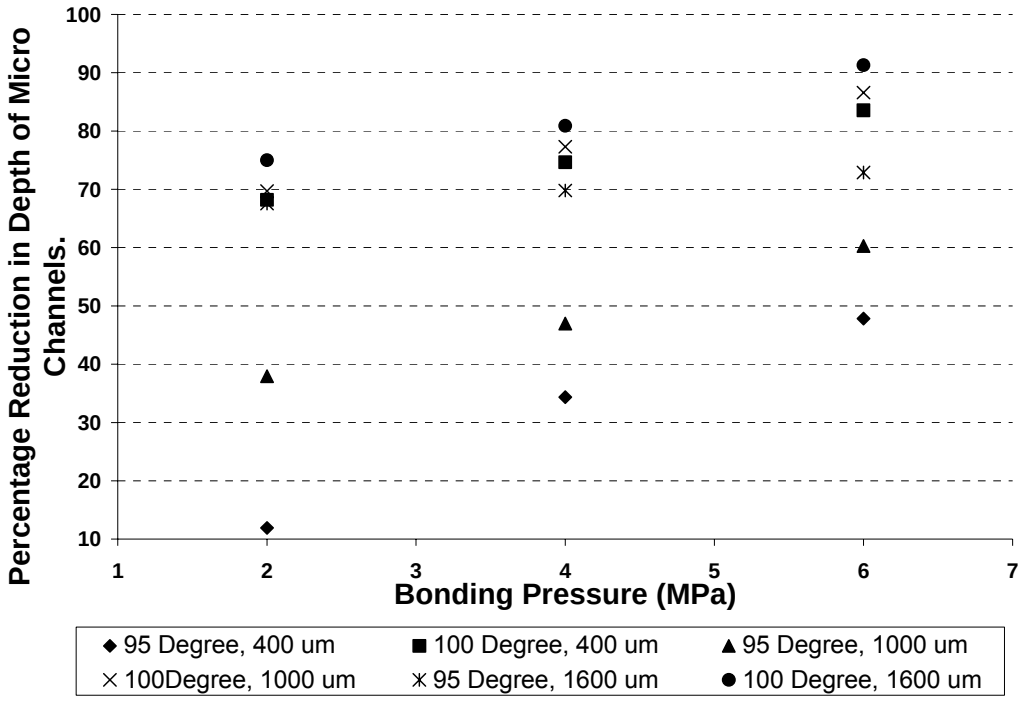

Figure 5.13. Plot of bond pressure vs. average percentage decrease in channel depth of PMMA microchannels at 480 sec holding time, 95 ^{0}C and 100 ^{0}C bond temperature and varying top PMMA thickness.

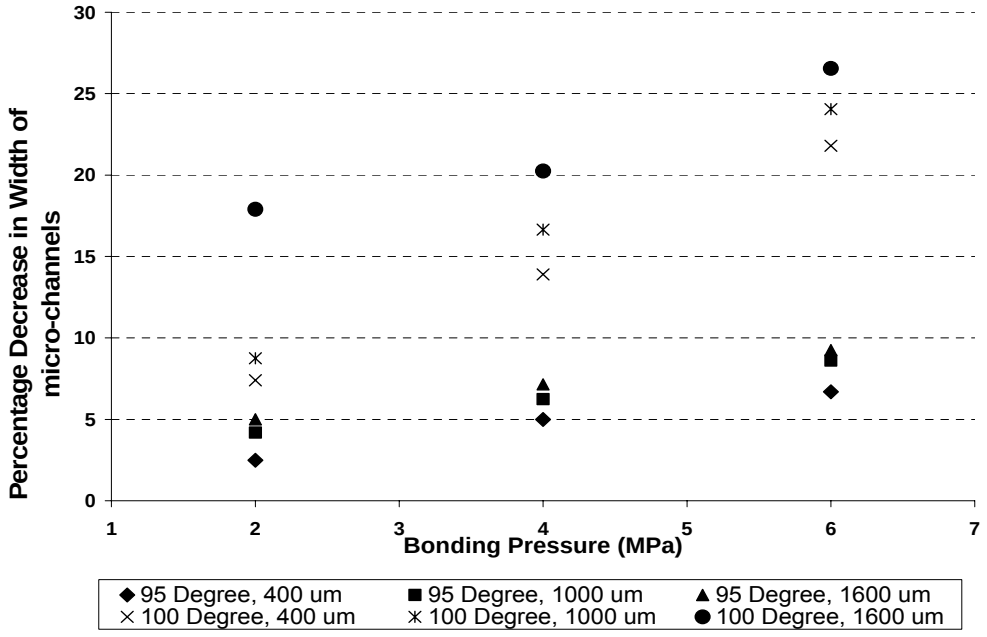

Figure 5.14. Plot of bond pressure vs. average percentage decrease in channel width of PMMA microchannels at 480 sec holding time, 95 ^{0}C and 100 ^{0}C bond temperature and varying top PMMA thickness.

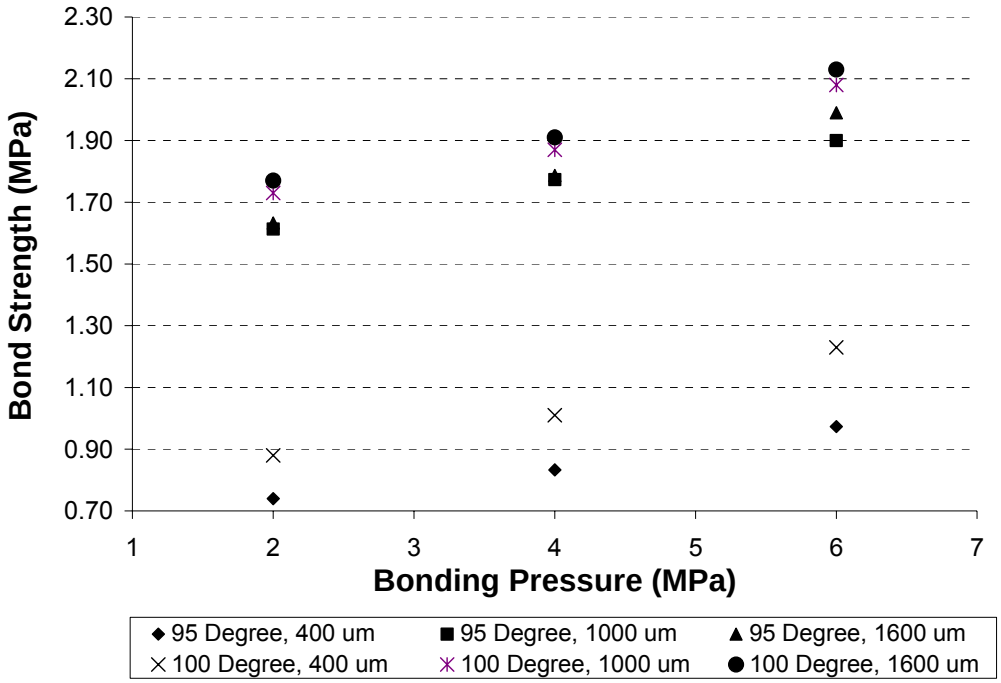

Figure 5.15. Plot of bond pressure vs. average bond strength of PMMA microchannels at 480 sec holding time, 95 ^{0}C and 100 ^{0}C bond temperature and varying top PMMA thickness.

5.2 Bonding Temperature

The bonding temperature played a major role in the bond strength and microchannels degradations. Heating at a temperature near or above the glass transition temperature of PMMA yields good bond strength, but on the other hand, at such a higher temperature, PMMA becomes viscous. Therefore, a small pressure is enough to result in a major degradation in microchannels.

Therefore, a temperature that is below the glass transition temperature of PMMA was used. Experiments were performed at 95 ^{0}C, 100 ^{0}C and 105 ^{0}C for various holding times and applied pressures and different top PMMA substrate thickness. Tables A.6 to A.8 and figures 5.16 to 5.24 show the effects of varying temperature on microchannels depth, width and bond strength.

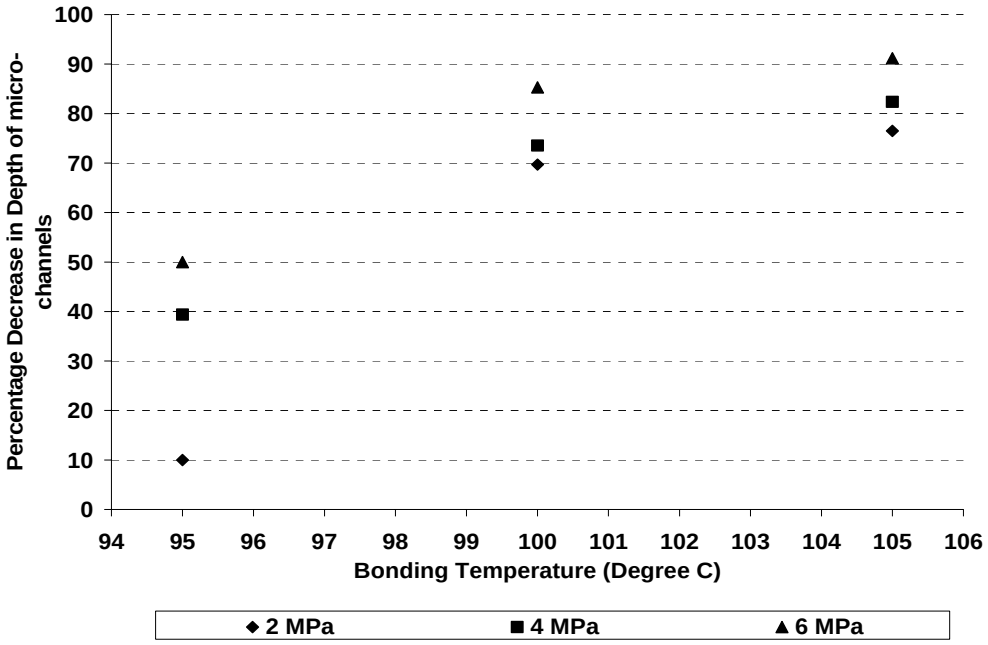

Figure 5.16. Plot of bond temperature vs. percentage decrease in depth of microchannels at 2 MPa and 120 sec for 400 μm top PMMA thickness.

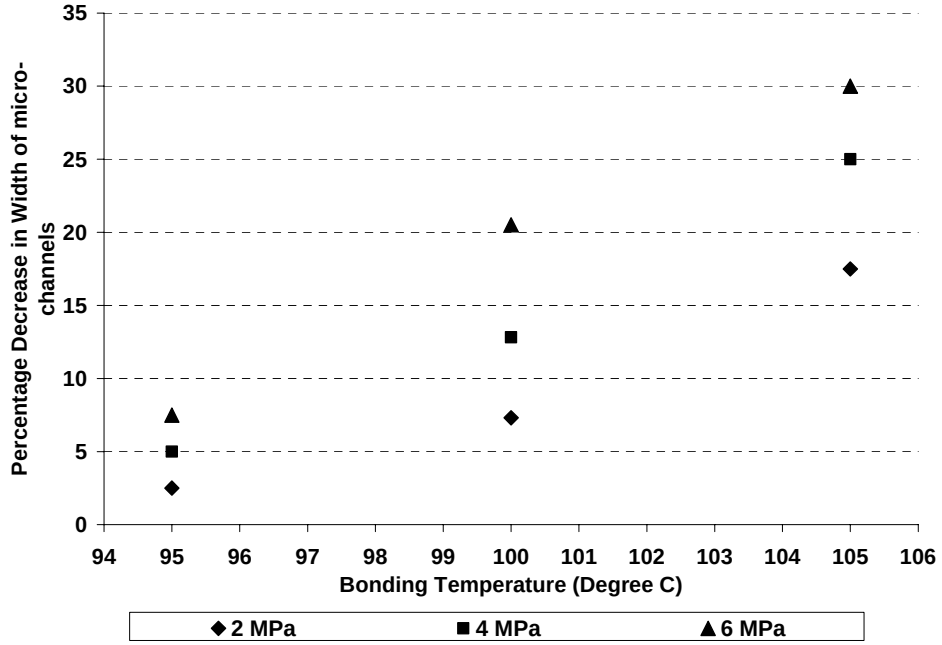

Figure 5.17. Plot of bond temperature vs. percentage decrease in width of microchannels at 2 MPa and 120 sec for 400 μm top PMMA thickness.

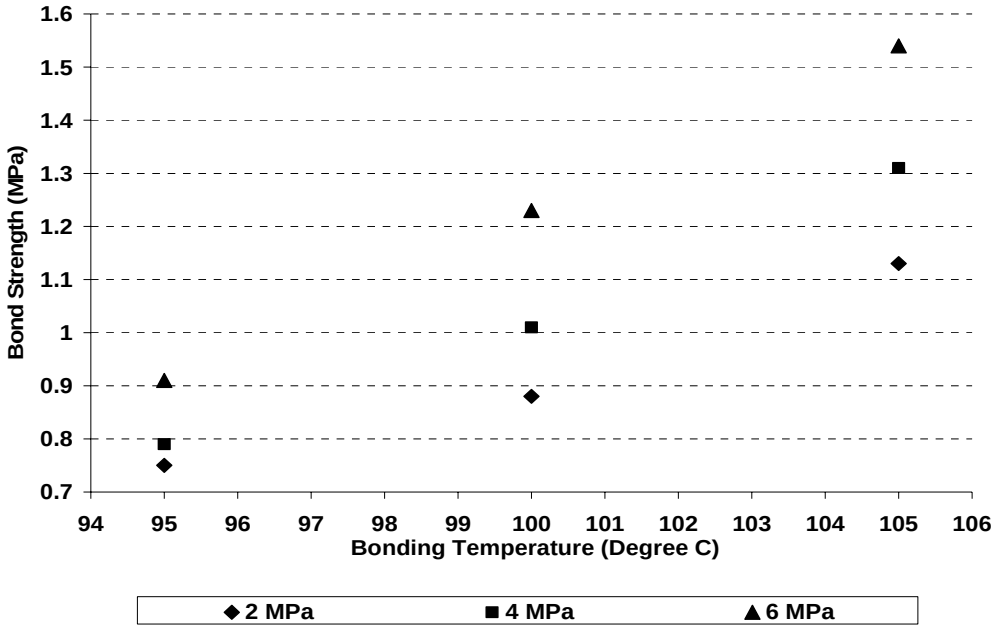

Figure 5.18. Plot of bond temperature vs. bond strength of microchannels at 2 MPa and 120 sec for 400 μm top PMMA thickness.

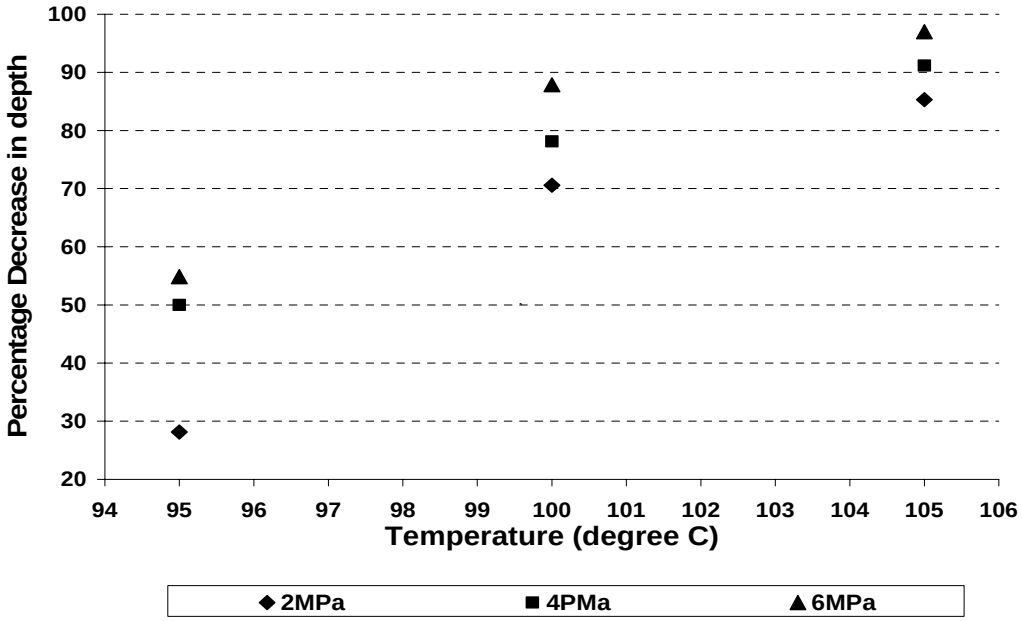

Figure 5.19. Plot of bond temperature vs. percentage decrease in depth of microchannels at 2 MPa and 120 sec for 1000 μm top PMMA thickness.

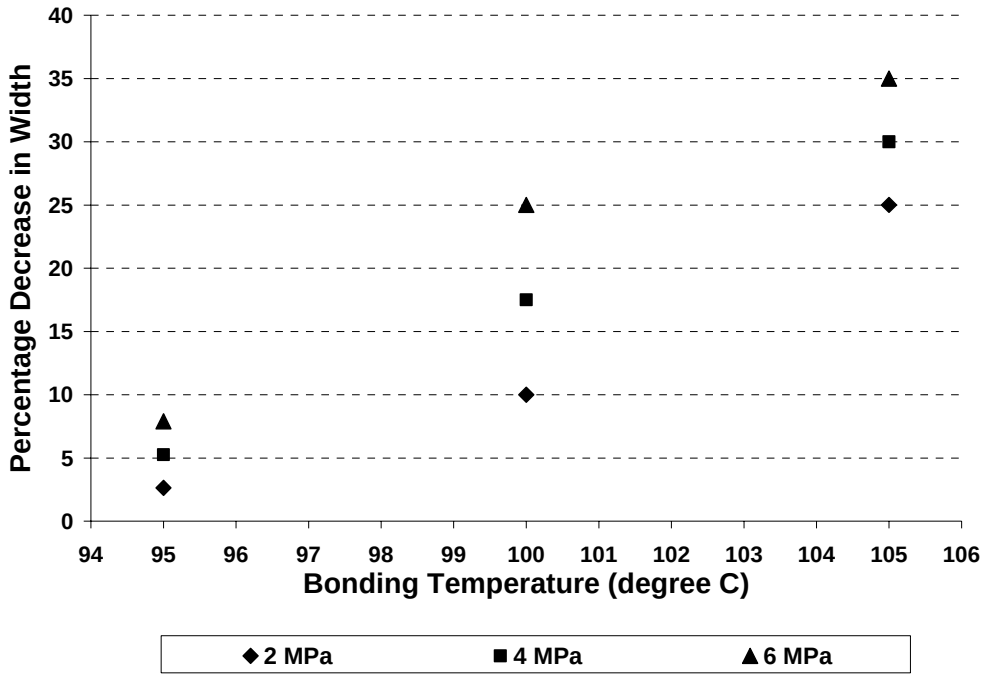

Figure 5.20. Plot of bond temperature vs. percentage decrease in width of microchannels at 2 MPa and 120 sec for 1000 μm top PMMA thickness.

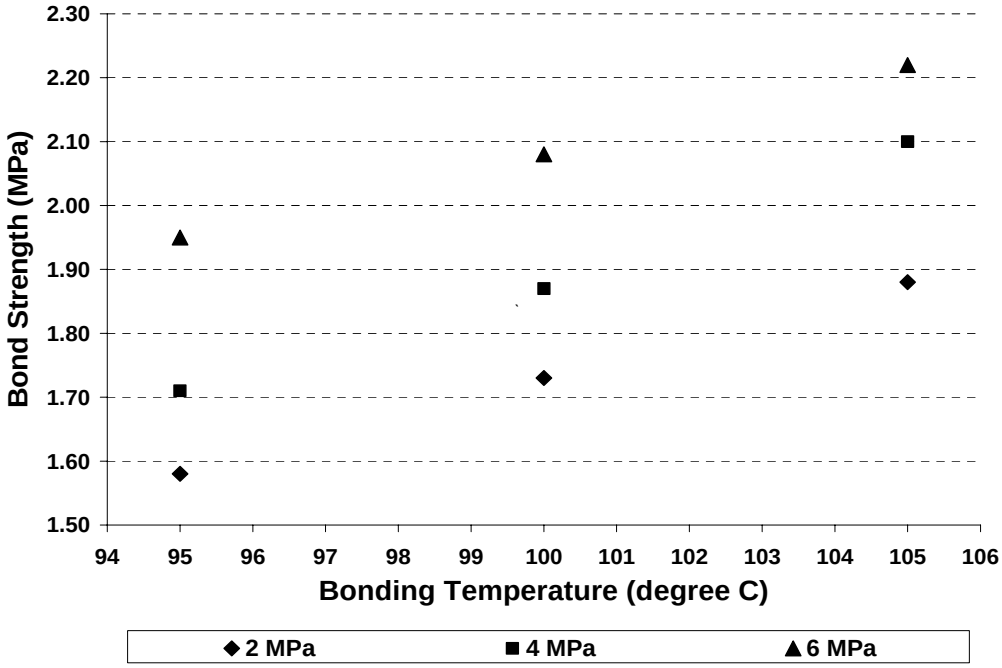

Figure 5.21. Plot of bond temperature vs. bond strength of microchannels at 2 MPa and 120 sec for 1000 μm top PMMA thickness.

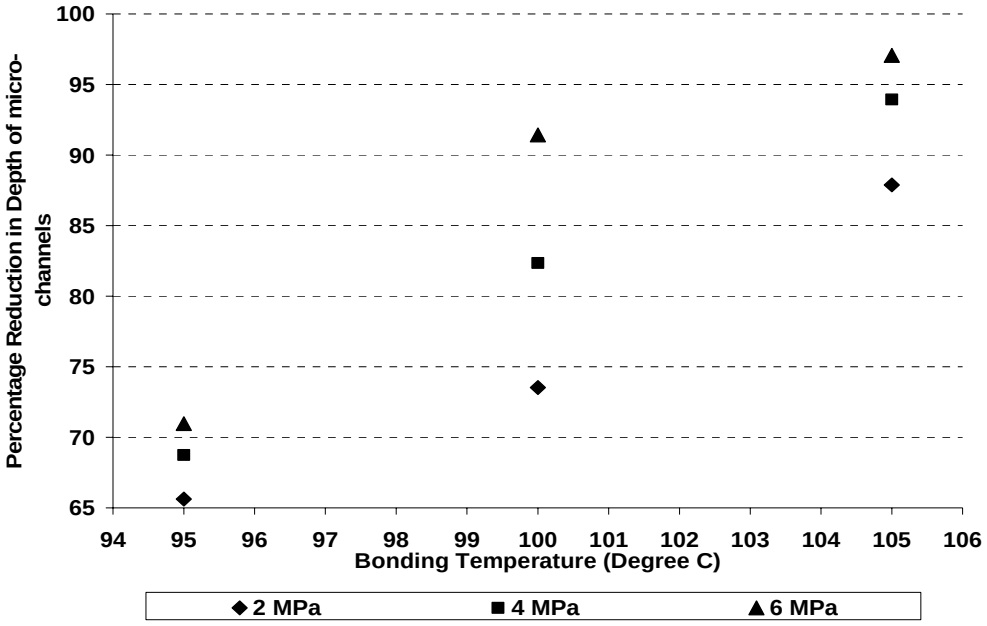

Figure 5.22. Plot of bond temperature vs. percentage decrease in depth of microchannels at 2 MPa and 120 sec for 1600 μm top PMMA thickness.

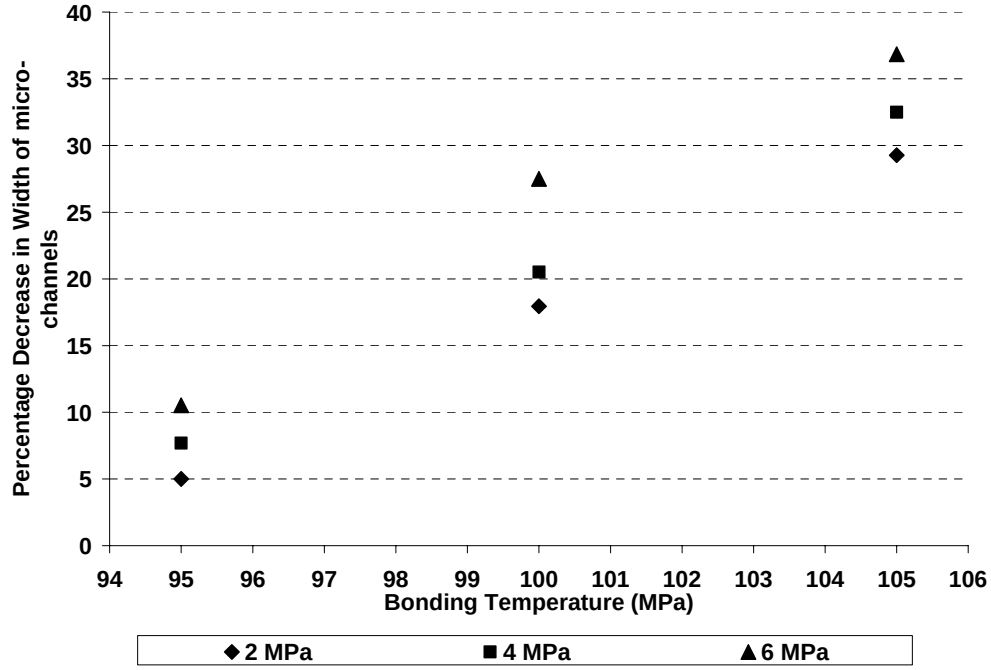

Figure 5.23. Plot of bond temperature vs. percentage decrease in width of microchannels at 2 MPa and 120 sec for 1600 μm top PMMA thickness.

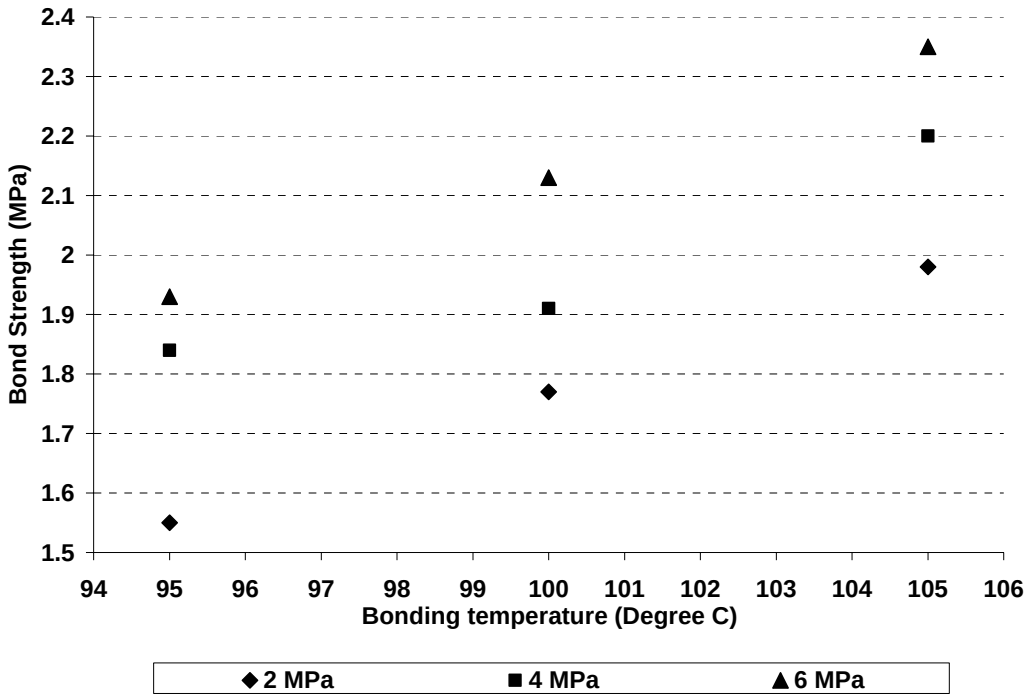

Figure 5.24. Plot of bond temperature vs. bond strength of microchannels at 2 MPa and 120 sec for 1600 μm top PMMA thickness.

It is observed that as the temperature increases, keeping the rest of parameters the same, the degradation in the microchannels also increase. The percentage change in depth is nearly 30 % for 95 ^{0}C but it increases and reaches almost to a level of full degradation of channels at higher temperature of 105 ^{0}C.

Also, the percentage change in width is negligible at lower temperatures, but at higher temperatures, there is nearly 30 % to 36 % degradation in microchannels width depending on the top PMMA thickness.

Also the bond temperature has a major effect on the bond strength. No wonder, the bond strength is higher at higher temperatures as it is clear from the given table. A bond strength of 2.35 MPa is achieved at a bond temperature of 105 ^{0}C using 6 MPa of

pressure as compared to 1.54 MPa for the bond temperature of 95 ^{0}C at the same pressure. But the degradations are more at higher temperature.

From the above data, it is inferred that the increase in degradation in channels is very high (increase from as low as 10 % to an almost full degradation) when we increase temperature form 95 ^{0}C to 105 ^{0}C but under same change in temperature, the improvement in bond strength is also effective (increase from 0.75 MPa to 2.35 MPa). Thus, increase in bond temperature plays a major role in microchannels degradations. Also, the effective microchannels left for fluidic movement is negligible at higher temperature, whereas at lower temperature, there is more than 70 % of the original channel left for fluid flow.

Therefore, for micro-fluidic devices, it is recommended to use a temperature of 95^{0}C for bonding PMMA substrates with channels in order to obtain minimum channel degradations and achieve considerably good bond.

5.3 Holding Time

Holding time refers to the time from reaching the desired process temperature for the first time and applying the desired pressure to the time at which the cooling starts. Generally for a bonding process this time is more than 120 sec. A series of experiments was performed at different holding times (240 sec, 480 sec and 960 sec) and varying the top PMMA substrate thickness to account for the effect of holding time on the microchannels degradations and also its effect on bond strength as shown by Tables A.9 to A.11 and Figures 5.25 to 5.33.

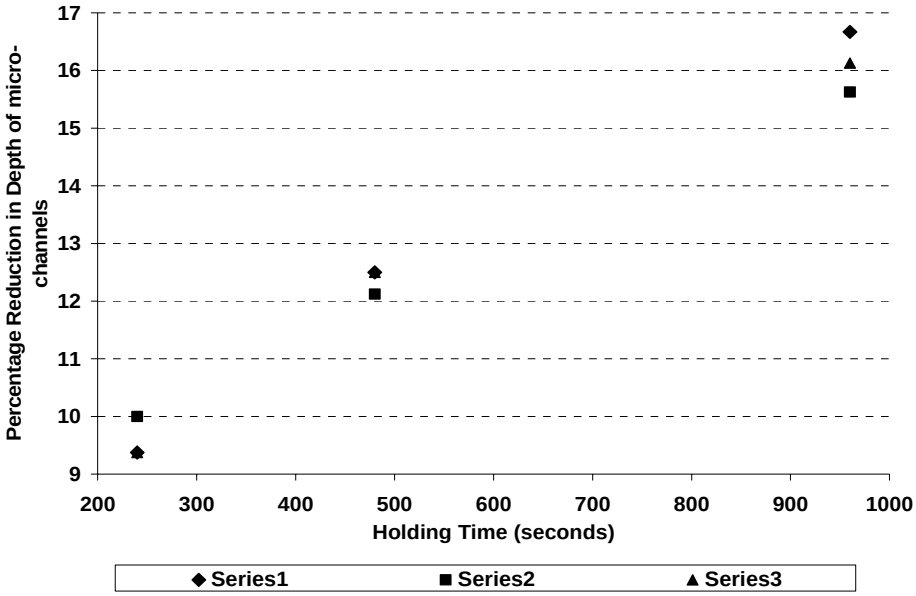

Figure 5.25. Plot of holding time vs. percentage decrease in depth of microchannels at 95 ^{0}C bond temperature and 2 MPa bond pressure for 400 μm top PMMA thickness.

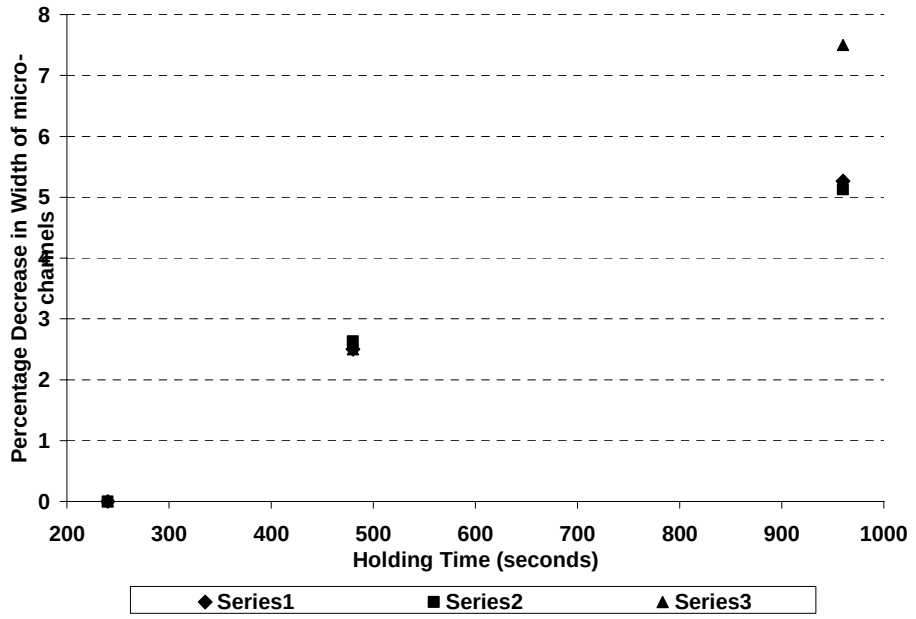

Figure 5.26. Plot of holding time vs. percentage decrease in width of microchannels at 95 ^{0}C bond temperature and 2 MPa bond pressure for 400 μm top PMMA thickness.

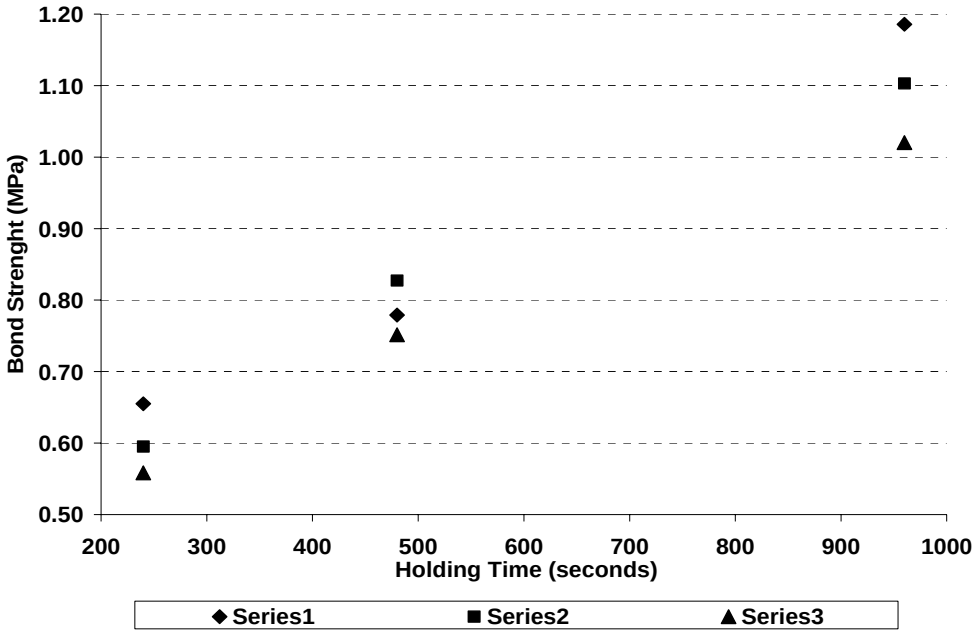

Figure 5.27. Plot of holding time vs. bond strength of microchannels at 95 ^{0}C bond temperature and 2 MPa bond pressure for 400 μm top PMMA thickness.

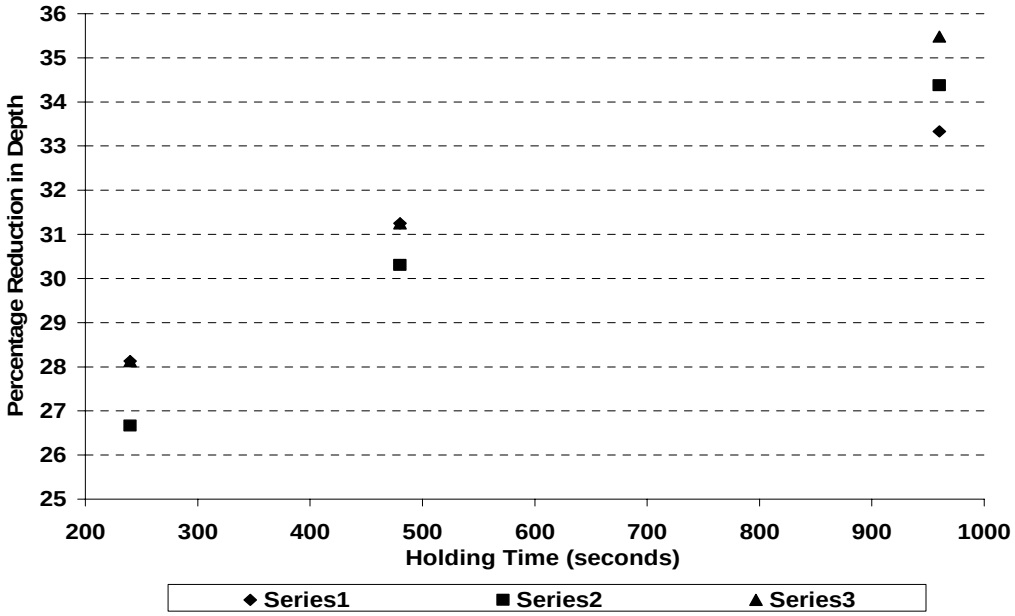

Figure 5.28. Plot of holding time vs. percentage decrease in depth of microchannels at 95 ^{0}C bond temperature and 2 MPa bond pressure for 1000 μm top PMMA thickness.

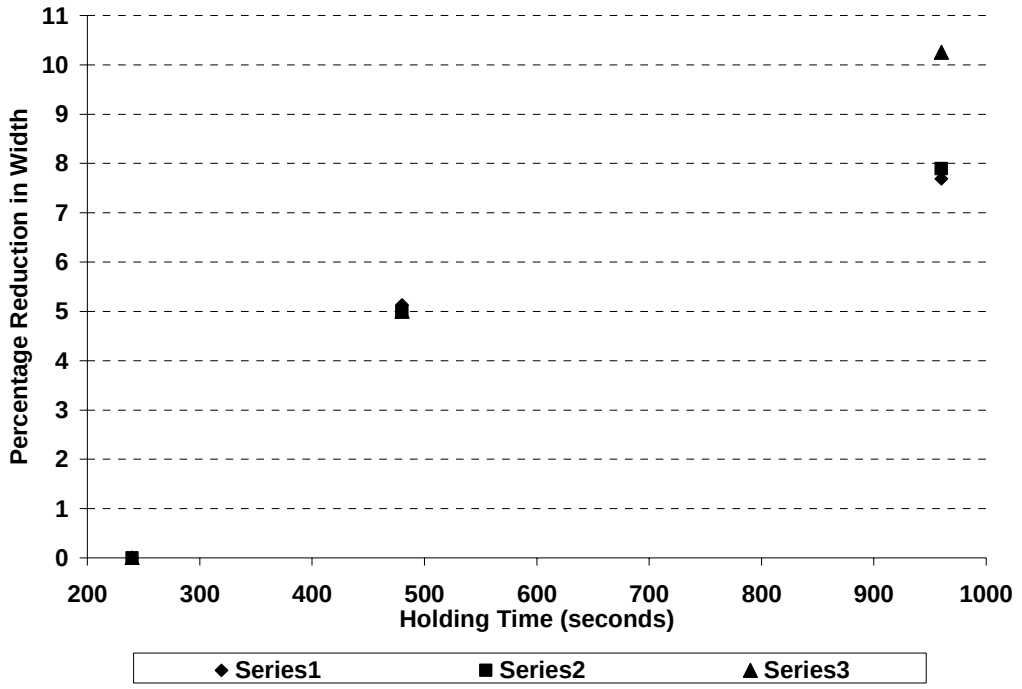

Figure 5.29. Plot of holding time vs. percentage decrease in width of microchannels at 95 ^{0}C bond temperature and 2 MPa bond pressure for 1000 μm top PMMA thickness.

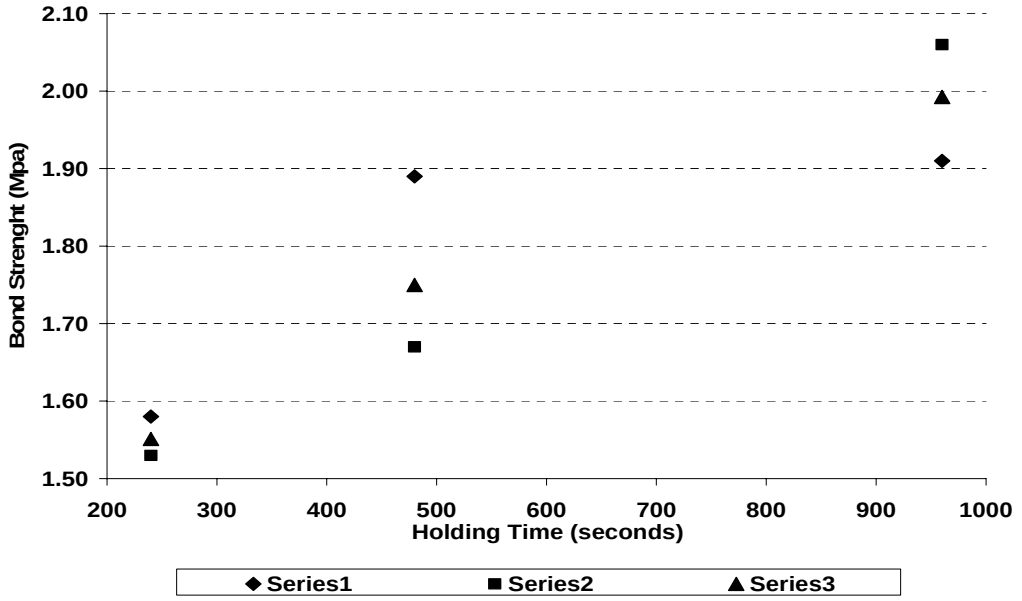

Figure 5.30. Plot of holding time vs. bond strength of microchannels at 95 ^{0}C bond temperature and 2 MPa bond pressure for 1000 μm top PMMA thickness.

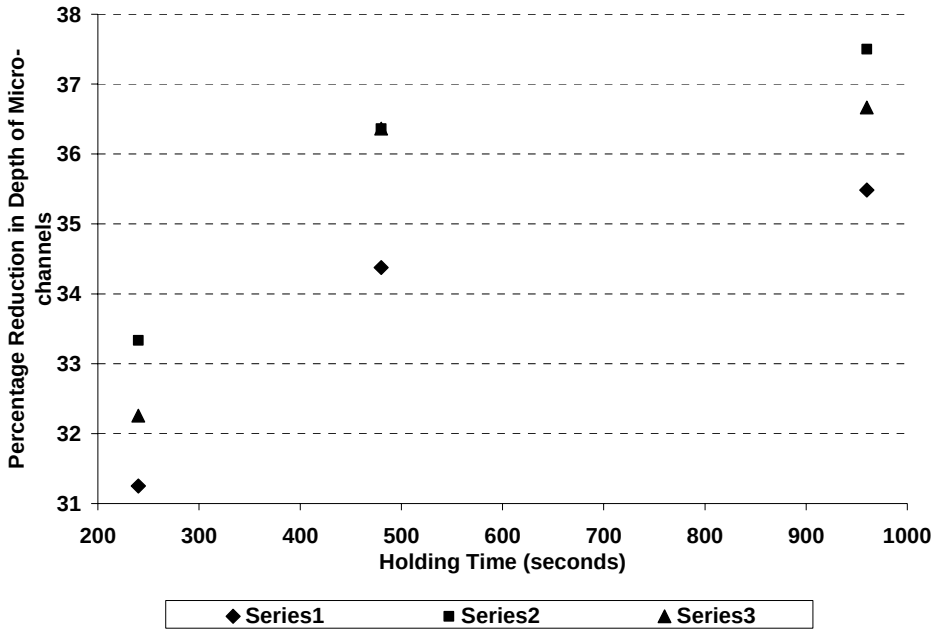

Figure 5.31. Plot of holding time vs. percentage decrease in depth of microchannels at 95 ^{0}C bond temperature and 2 MPa bond pressure for 1600 μm top PMMA thickness.

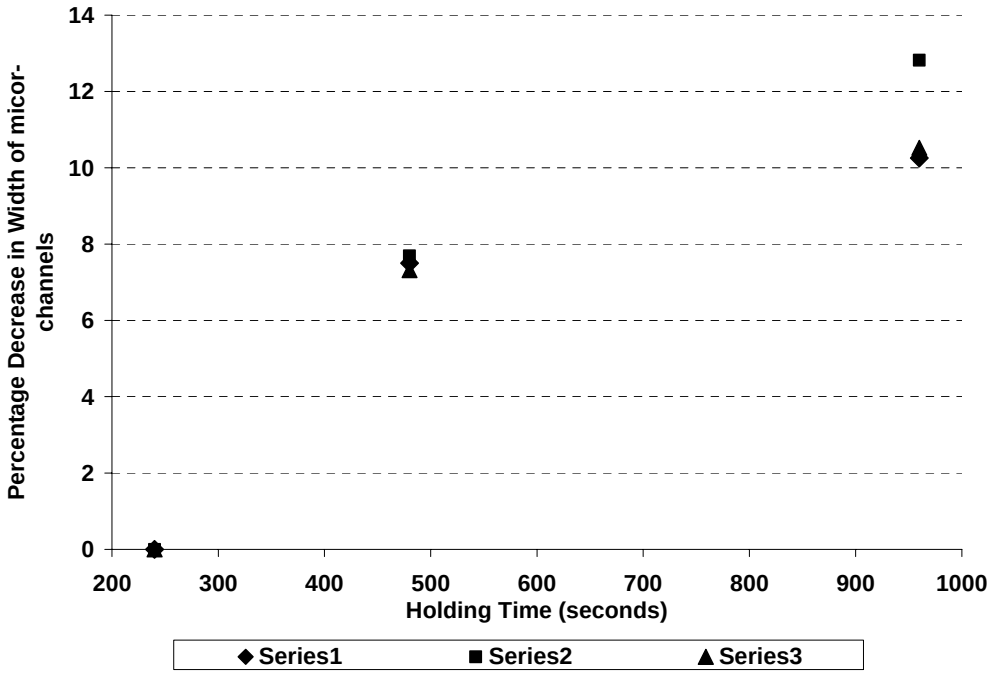

Figure 5.32. Plot of holding time vs. percentage decrease in width of microchannels at 95 ^{0}C bond temperature and 2 MPa bond pressure for 1600 μm top PMMA thickness.

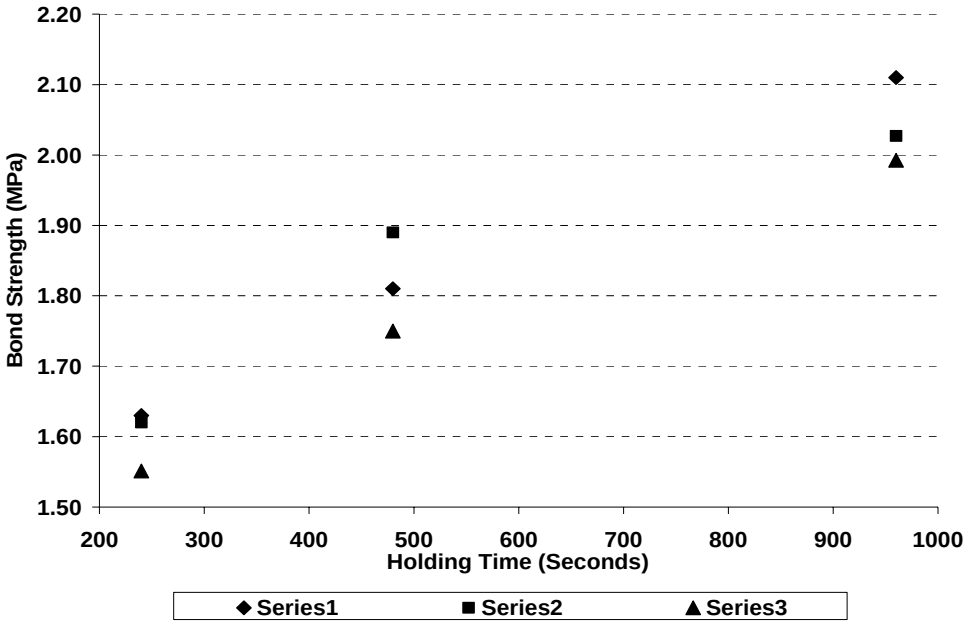

Figure 5.33. Plot of holding time vs. bond strength of microchannels at 95 ^{0}C bond temperature and 2 MPa bond pressure for 1600 μm top PMMA thickness.

The effect of varying holding time on microchannels geometry and PMMA thermal bond strength are presented in Table A.12 and figures 5.34 to 5.36.

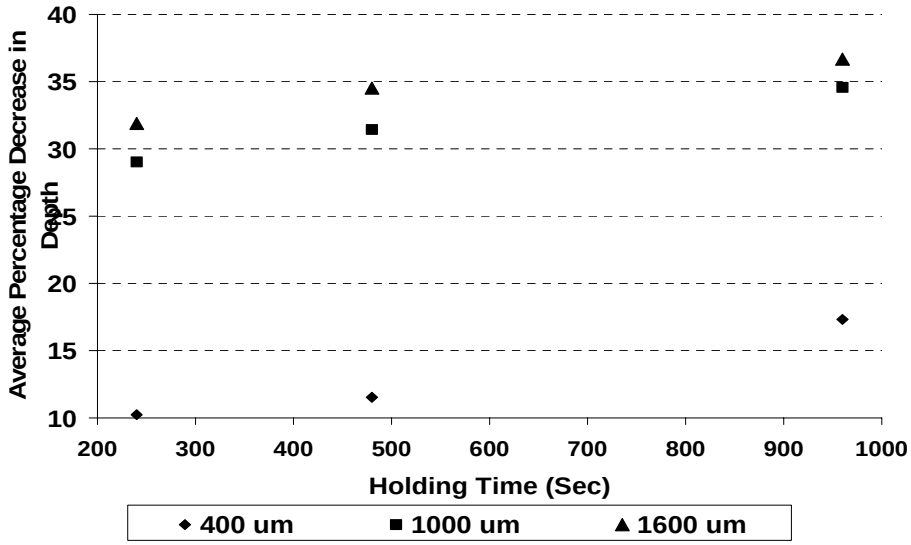

Figure 5.34. Plot of holding time vs. average percentage change in depth of microchannels at 95 ^{0}C bond temperature and 2 MPa bond pressure for varying top PMMA thickness.

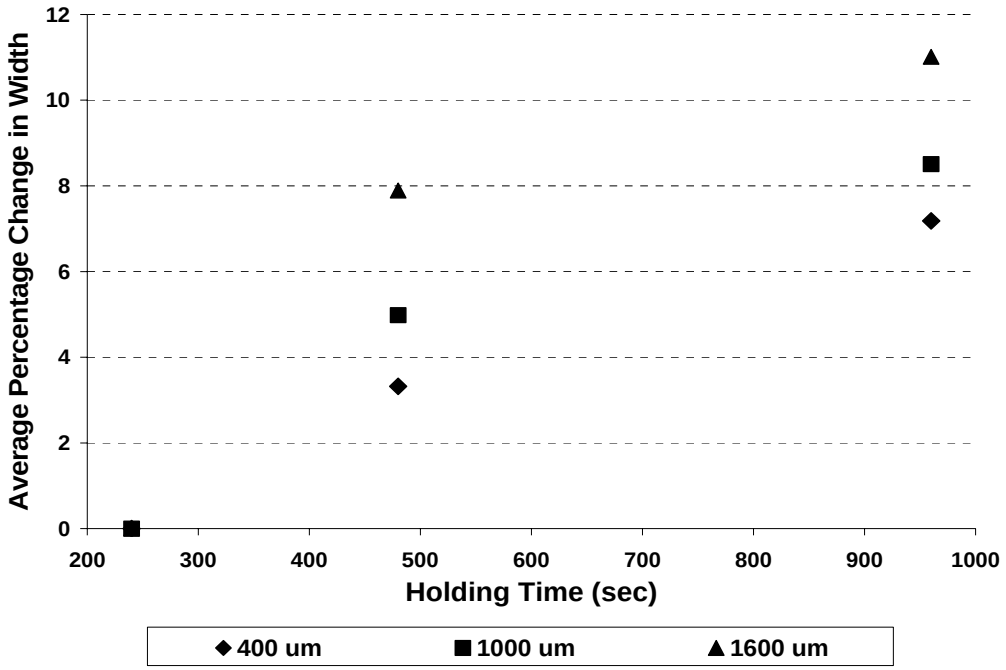

Figure 5.35. Plot of holding time vs. average percentage change in width of microchannels at 95 ^{0}C bond temperature and 2 MPa bond pressure for varying top PMMA thickness.

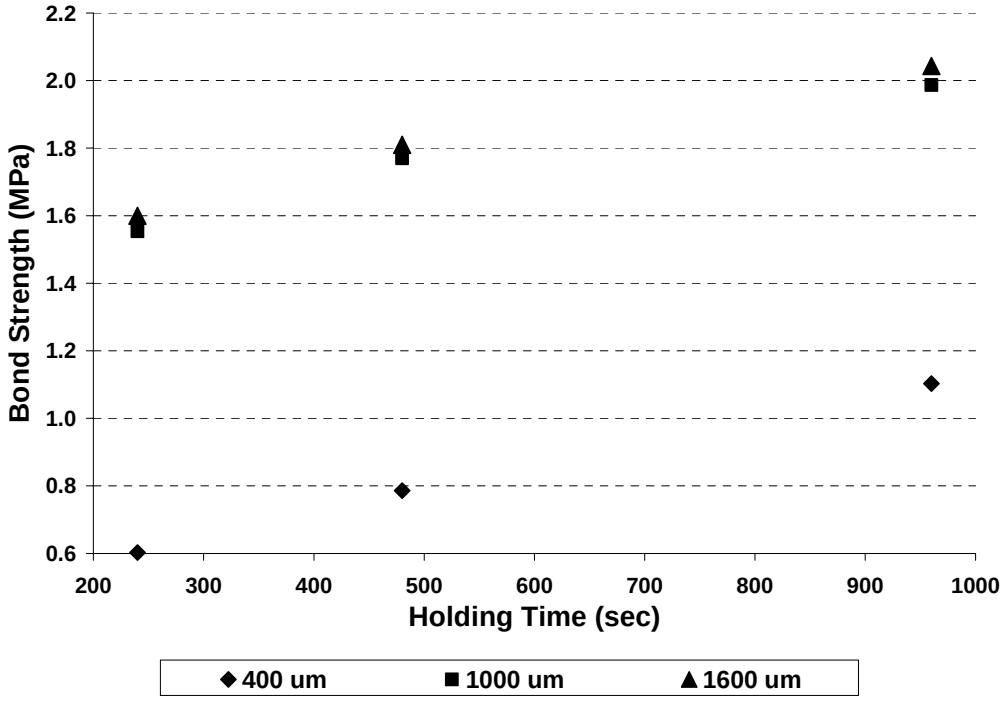

Figure 5.36. Plot of holding time vs. average bond strength of microchannels at 95 ^{0}C bond temperature and 2 MPa bond pressure for varying top PMMA thickness.

It is observed that by increasing the holding time, the degradation in depth and width of microchannels increases, but the bond strength of the PMMA bond also increases.

The decrease in channel depth is less at lower temperatures, but as the time increases, the decrease in channel depth also increases. For the same top PMMA thickness (400 μm), the percentage reduction in depth increases from 10.24 % to 17.32 % by increasing the holding time from 4 minutes to 16 minutes. This percentage increase in depth reduction is almost 60 %. The percentage decrease in width is a maximum of 7 %. But the major change is in the bond strength. The bond strength increases from 0.6 MPa to 1.1 MPa (which is almost an increase of 85 %) by increasing the holding time from 4 min to 16 min.

Thus, the increase in holding time has more effect on the bond strength than on channel degradations. Considering the desired outputs, it is recommend to use:

- Smaller holding time for minimum channel degradations.
- Larger holding time for higher bond strength.
- Holding time of about 10-12 minutes will provide a combination of good bond strength and less degradation as there is not much change in channel depth and width, but there is considerable increase in bond strength.

5.4 Top PMMA Substrate Thickness

Different thickness of top PMMA substrates were used in the experiments discussed above to study the effect of various process parameters (temperature, pressure and holding time). The different top PMMA thickness had effects on both channel degradations and bond strength.

Increase in the top PMMA substrate thickness leads to more degradation in depth of microchannels. For lesser top PMMA thickness (400 μm), the percentage decrease in depth has an average value of 12.5 %. As the top PMMA thickness increases, this degradation increases to a value of around 34.23 % for a thickness of 1000 μm and increases further to 63.47 % for the top substrate thickness being 1600 μm.

The effect of top PMMA thickness on the percentage change in width of microchannels is 2.5 % at less thickness (400 μm), 5 % at medium thickness (1000 μm) and about 7.8 % at full thickness (1600 μm).

The bond strength of PMMA-PMMA thermal bond also varies with top PMMA substrate thickness. The strength is 0.74 MPa at less thickness (400 μm), 1.66 MPa at medium thickness (1000 μm) and about 1.76 MPa at full thickness (1600 μm) (shown by Table A.13 and Figures 5.37 to 5.39). It is to be noted that the above data is for the following process parameters:

Bond temperature: 95 ^{0}C

Holding Time: 480 sec

Bond pressure: 2 MPa

At larger values of these process parameters, the microchannel degradations and bond strength values are even higher as discussed earlier during discussion of effect of other parameters.

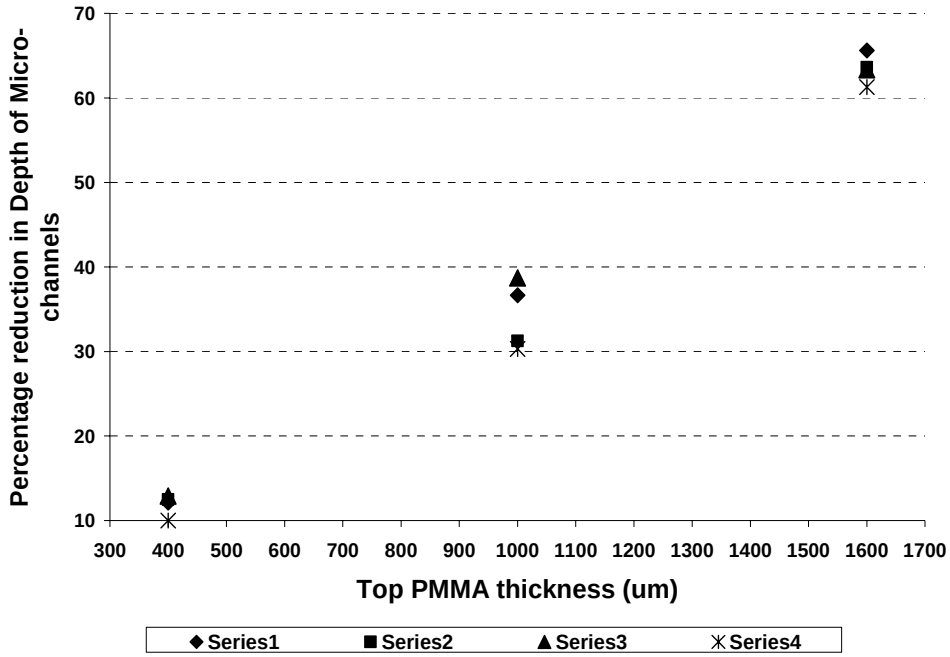

Figure 5.37. Plot of top PMMA thickness vs. percentage decrease in depth of microchannels at 95 ^{0}C bond temperature, 2 MPa bond pressure & 480 sec holding time.

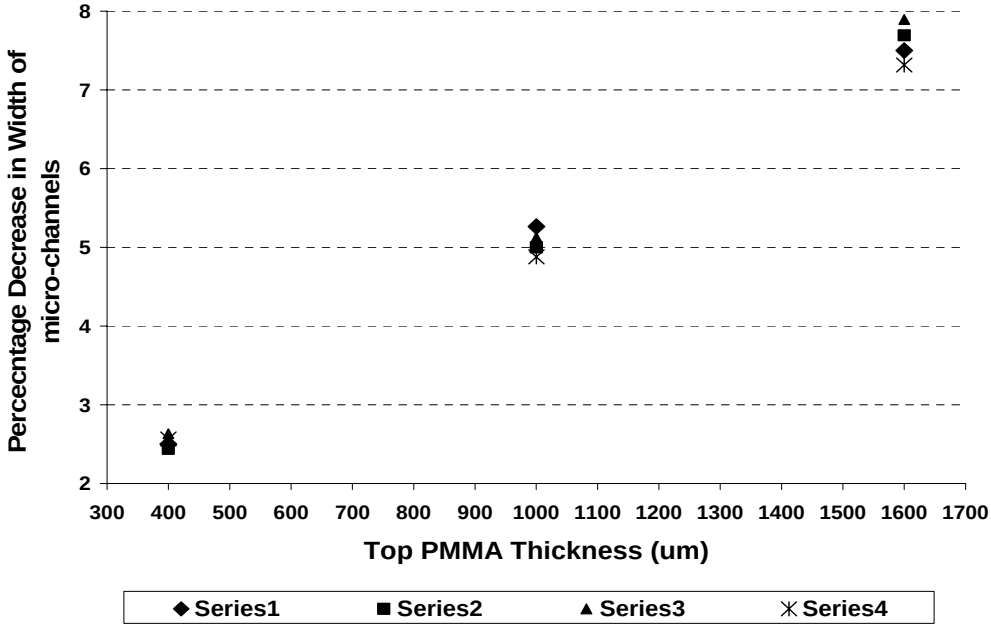

Figure 5.38. Plot of top PMMA thickness vs. percentage decrease in width of microchannels at 95 ^{0}C bond temperature, 2 MPa bond pressure and 480 sec holding time.

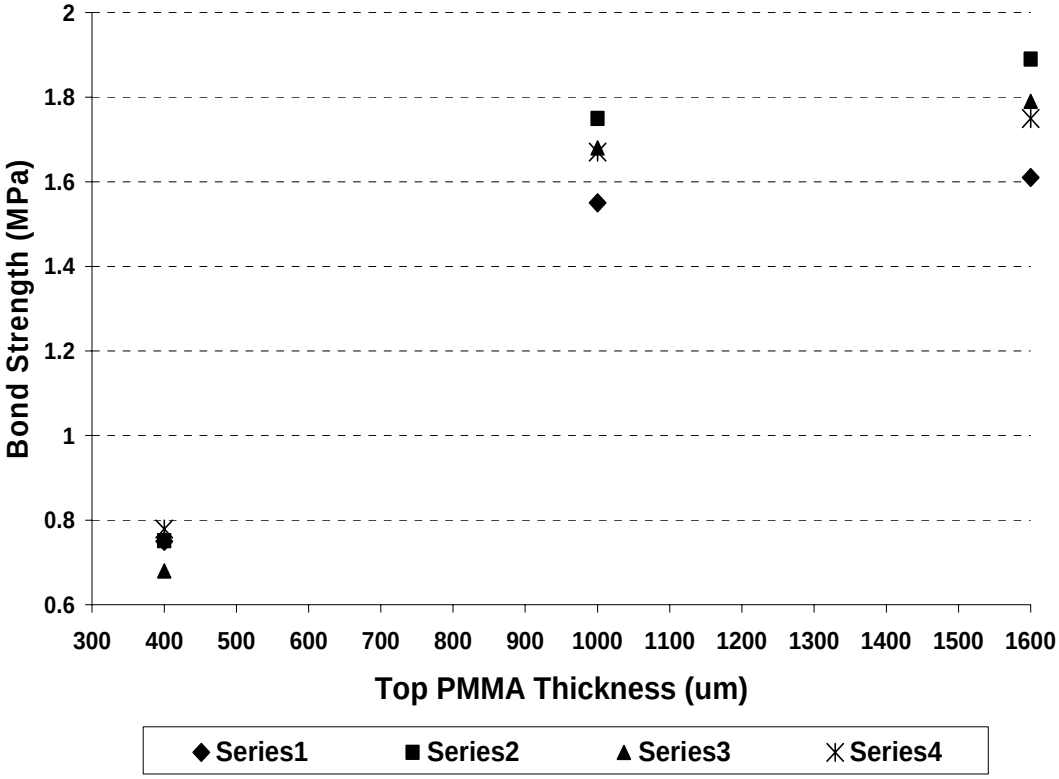

Figure 5.39. Plot of top PMMA thickness vs. bond strength of microchannels at 95 ^{0}C bond temperature, 2 MPa bond pressure and 480 sec holding time.

5.5 Regression Analysis

The completion of the experiments, the analysis of the collected data for the various combinations of process parameters and top PMMA thickness allowed for the analysis of the effect of each of the parameters individually. However, it is important that the effect of the parameters as a whole to the bonding strength and channel geometry change understood as well. The collected data was used in the Statistical Analysis Software (SAS) [53] to perform regression analysis in an attempt to identify a model that could be used to understand the relative effect of the process parameters and predict the bond strength and geometry changes.

The dependent-sample *t-test* compares the difference in the means from the two variables to a given number (usually 0), while taking into account the fact that the scores are not independent. The *t-value* or *t-statistic* is the ratio of the mean of the difference in means to the standard error of the difference. A ***p-value*** is the probability of observing a greater absolute *t-value* under the null hypothesis. The smaller the ***p-value*** the stronger is the evidence for rejecting the null hypothesis. The regression model considered the individual linear and quadratic interaction of the four process parameters (temperature, pressure, time and top PMMA thickness) with a 95% confidence interval. This meant that parameters with ***p-value*** greater than 0.05 were neglected. The results of the ***t-test*** in SAS for bond strength percentage change in depth and percentage decrease in width of microchannels due to thermal bonding are shown in Tables 5.1 to 5.3. To account for accuracy of the model, the estimated coefficients and *p-values* were taken to the 4th significant digit, while the *t-values* were kept to 2 decimal places. The probability was also taken to the 4 decimal places, accounting for the confidence interval of 95%.

Table 5.1. Percentage reduction in microchannel width for *t-type* regression analysis

Width Percent Reduction				
Parameter	**Estimate**	**Error**	**t-value**	**Pr > |t|**
INTERCEPT	-861.2596	239.6103	-3.59	0.0006
TEMP (^{0}C)	15.7401	4.8050	3.28	0.0016
PRESS (MPa)	-14.9795	3.0879	-4.85	<0.0001
TIME (sec)	0.0108	0.0009	12.30	<0.0001
THICK (mm)	-0.0399	0.0101	-3.96	0.0002
TEMP2	-0.0709	0.0241	-2.95	0.0043
TEMPRESS	0.1708	0.0318	5.37	<0.0001
TEMPTHICK	0.0005	0.0001	4.27	<0.0001

Table 5.2. Percentage reduction in microchannel depth for *t-type* regression analysis

Depth Percent Reduction				
Parameter	**Estimate**	**Error**	**t-value**	**Pr > |t|**
INTERCEPT	-8087.8683	1344.3775	-6.02	<0.0001
TEMP (^{0}C)	152.9852	26.7631	5.72	<0.0001
PRESS (MPa)	50.1699	14.3588	3.49	0.0008
TIME (sec)	0.0752	0.0231	3.26	0.0017
THICK (mm)	0.2188	0.0456	4.80	<0.0001
TEMP2	-0.7174	0.1333	-5.38	<0.0001
TIME2	-0.0001	0.00001	-3.10	0.0027
TEMPRESS	-0.4528	0.1474	-3.07	0.003
TEMPTHICK	-0.0021	0.0004	-4.35	<0.0001

Table 5.3. Microchannel bond strength for *t-type* regression analysis

Bond Strength (MPa)				
Parameter	**Estimate**	**Error**	**t-value**	**Pr > |t|**
INTERCEPT	-4.3122	0.7237	-5.96	<0.0001
TEMP (^{0}C)	0.0379	0.0074	5.13	<0.0001
PRESS (MPa)	-0.6125	0.1647	-3.72	0.0004
TIME (sec)	0.0007	0.0001	14.20	<0.0001
THICK (mm)	0.0031	0.0001	27.95	<0.0001
THICK2	-0.000001	0.00000005	-21.03	<0.0001
TEMPRESS	0.0071	0.0017	4.16	<0.0001

The regression model for each of the outputs is obtained using the regression analysis results in SAS. The estimator or predictor models for depth, width and bond strength are shown in equations 5.1 to 5.3 respectively.

$$\hat{y}_{Depth} = -8087.8683 + 152.9852 * Temp + 50.1699 * \Pr ess + 0.07516 * Time + 0.218815 * Thick$$
$$-0.7174 * Temp^2 - 0.000056 * Time^2 - 0.45275 * Temp * \Pr ess - 0.00205 * Temp * Thick \quad (5.1)$$

$$\hat{y}_{Width} = -861.2596 + 15.7401 * Temp - 14.9795 * Press + 0.01075 * Time - 0.039975 * Thick$$
$$-0.07095 * Temp^2 + 0.17075 * Temp * Press + 0.00045 * Temp * Thick \quad (5.2)$$

$$\hat{y}_{BondStrength} = -4.31222 + 0.037967 * Temp - 0.612512 * Press +$$
$$0.000662 * Time + 0.003065 * Thick - 0.0000011 * Thick^2 + 0.007046 * Temp * Press \quad (5.3)$$

These estimator models allow one to predict the outputs (bond strength and channel degradations) given a set of known inputs or process parameters within the analyzed ranges.

The estimator models also show the sensitivity of the respective output to a particular process parameter and also which process parameter has the maximum effect on the output. It is observed that bonding temperature and pressure have the major effect on the outputs; the temperature has more effect on the degradations as compared to the pressure whereas the effect of pressure on the bond strength is more than the effect of temperature. All the other parameters and their interactions do affect the outputs but the effect is not as prominent as that for temperature and pressure.

5.6 Estimator or Predictor Model Analysis

In manufacturing operations one would like to estimate or predict the process parameters for a desired or acceptable result or output. In this particular research, the derived regression models were used to identify the set of process parameters for a set of outputs. Subsequently, experiments were performed with the defined process parameters and the experimental results compared with the predicted ones from the regression analysis. The estimator equations were linearized using Taylor series expansion with the linearization points selected to be the average of the values used in the experiments. In this example,

the linearization points were selected to be Temperature = 95 ^{0}C, Pressure = 2 MPa, Time = 480 sec, and Top PMMA Thickness = 1000 μm. Using these values as the operating point the linearized equations are given by:

$$\begin{aligned}\Delta\hat{y}_{depth} &= (152.9852 - 1.4348 * Temp - 0.4528 * \Pr ess - 0.0021 * Thick)_0 * \Delta Temp \\ &+ (50.1699 - 0.4528 * Temp)_0 * \Delta \Pr ess + (0.0752 - 0.0002 * Time) * \Delta Time \\ &+ (0.2188 - 0.0021 * Temp)_0 * \Delta Thick\end{aligned} \quad (5.4)$$

$$\begin{aligned}\Delta\hat{y}_{width} &= (15.7401 - 0.1418 * Temp + 0.1708 * \Pr ess + 0.0005 * Thick)_0 * \Delta Temp \\ &+ (-14.9796 + 0.1708 * Temp)_0 * \Delta \Pr ess + 0.0108 * \Delta Time \\ &+ (-0.0399 + 0.0005 * Temp)_0 * \Delta Thick\end{aligned} \quad (5.5)$$

$$\begin{aligned}\Delta\hat{y}_{Bondstrength} &= (0.0379 + 0.0071 * \Pr ess)_0 * \Delta Temp + (-0.6125 + 0.0071 * Temp)_0 \\ &* \Delta \Pr ess + 0.0007 * \Delta Time + (0.0031 - 0.000002 * Thick)_0 * \Delta Thick\end{aligned} \quad (5.6)$$

The linearized equations 5.4 through 5.6 could be treated as a set of three unknowns (desired outputs) and four inputs (process parameters). These equations could be used to estimate the process parameters for a desired set of outputs. This is accomplished by defining one of the process parameters apriori yielding a set of three linear equations with three unknowns. The desired outputs are defined and the solution of the set of equations yields the process parameters to be used. This procedure was followed to identify the process parameters in a series of experiments to verify the proposed estimator models or inverse analysis. A comparison of the experimentally obtained results from the predicted

output values is shown in Table 5. 4. It is interesting to note that the model provides estimates of within ±5 % of the experimentally obtained results.

Table 5.4. Comparison experimental and predicted results from regression models at the same process parameters for bond strength and percentage degradation in microchannels

Temp (Deg C)	Press (MPa)	Time (sec)	Thick (um)	Bond Strength (MPa)		Percentage Reduction in				Percentage change in Estimate from actual of		
						Width		Depth				
				Estimate	Experimental	Estimate	Experimental	Estimate	Experimental	Bond Strength (Mpa)	Reduction in Width	Reduction in Depth
95	2	240	1000	1.50	1.54	1.11	0.98	28.35	26.58	-2.67	11.71	6.24
95	4	480	1600	1.84	1.79	7.57	7.15	62.10	65.08	2.72	5.55	-4.80
95	6	480	400	1.00	0.97	7.26	7.12	46.96	47.83	3.00	1.93	-1.85
95	2	960	1000	1.97	2.00	8.85	7.69	30.43	32.02	-1.52	13.11	-5.23
100	2	120	1000	1.68	1.73	13.28	11.75	68.78	69.60	-2.98	11.52	-1.19
100	6	120	1600	1.92	2.04	24.39	26.55	96.95	92.30	-6.25	-8.86	4.80

CHAPTER 6

CONCLUSIONS AND RECOMMENDATIONS

This chapter concludes this report by summarizing the conclusions drawn from the earlier chapters while suggesting recommendations that can be incorporated for future research work

6.1 Conclusions

6.1.1 Polymer Bonding Techniques

MicroElectroMechanical systems were discussed with their benefits and applications and stress was given on use of polymers as a substrate. Different bonding techniques were studied with their effects on substrate thickness and bond strength. Study was also carried out for the micro-channel fabrication and their degradations due to thermal bonding.

6.1.2 Characterization of HEMM

Basic configuration and functioning of various subsystems of a developed HEMM system were discussed along with their ability for hot-embossing. The current state was studied and its limitation to keep the temperature at the desired value for a larger duration of time (more than 2 min) was overcome by introducing the ON/OFF control sequence for the heating cartridges. Also modifications were done in the temperature VI to introduce a ¼ inch plate on the bottom heating block and the temperature and force VI were modified and combined to accommodate this control sequence.

6.1.3 Thermal Bonding of PMMA

The micro channels on PMMA were prepared using end milling and also using embossing by means of a brass mold. The channels dimensions (width and depth) were characterized using the optical microscope. The three process parameters for the thermal bonding: bond pressure, bonding temperature and holding time were discussed and their effects on the channel degradations and bond strength were reviewed and compared with results from others. To facilitate this, experiments were performed using different process parameter combinations and results were plotted and studied. Also top PMMA substrate thickness was also varied and its effect on micro-channels was discussed. Bond strength was evaluated using the MTS tensile testing machine. Rise in bond temperature and bond pressure mainly affect the channel degradations than they affect the bond strength. The degradation in depth of microchannels increased tremendously at high temperature and pressure. Holding time has maximum affects on the bond strength. Increasing top PMMA thickness also increases degradations in channel dimensions as well as the bond strength, but the influence is not much as compared to other parameters.

6.1.4 Regression analysis

Having all the experimental data, regression models were developed for relation of output with process parameters and their interactions with each other, and these regression models could be used to evaluate the degradations in micro-channels and also the bond strength of thermal bond. Also linearization was performed for these models to obtain equations which could be used to predict the value of process parameters to be applied during the thermal bonding process to achieve desired micro-channel geometry or desired bond strength or a combination of both.

6.2 Recommendations for Future Research

6.2.1 Surface Modifications

Thermal bonding has considerable effect on microchannels, bond strength and also affects the polymer thickness. As discussed, the PMMA bonding takes place by forming some bonds between the monomers. Hence, it is important to discuss the change in material properties and also surface modifications after thermal bonding. The effect of various process parameters on the material properties of PMMA need to be discussed.

6.2.2 Analysis for other Polymers

Apart from PMMA, other polymers like PLLA can be studied for the effects of thermal bonding. The study on micro-channels on these new polymers can also be considered for this purpose.

6.2.3 Effect of Storage Time

There is effect of storage time on the bond strength of the bonds formed by thermal bonding. So, work could be carried out to study the effect of this storage time.

6.2.4 Sealing Efficiency

Once the thermal bonding with micro-channels on polymers is done, the bond can be checked for the sealing efficiency for any leaks or so. This can be performed by passing fluid through these micro channels at some pressure to check for leak-proof bonding.

APPENDIX A

TABLES FOR THERMAL BONDING EXPERIMENTAL RESULTS

In this appendix, the tables for thermal bonding experiment results are presented.

Table A.1. Bond pressure effect on PMMA microchannels and thermal bond strength at 95^0C, 480 sec and 400 μm.

Exp. No.		Bonding Temp.	Plate Seperation Temp.	Holding Time (sec.)	INITIAL					FINAL					PERCENTAGE CHANGE				Effective channel Left	Tensile Bond Strength (Mpa)	
					Channel		Top Thin PMMA Thickness (μm)	Thickness of PMMA with channel (μm)	Pressure (Mpa)	Channel		Top Thin PMMA Thickness (μm)	Depth that top goes into the channel (μm)	Thickness of PMMA with channel (μm)	Channel		Top Thin PMMA Thickness (μm)	Bottom PMMA thickness (μm)			
					Width (μm)	Depth (μm)				Width (μm)	Depth (μm)				Width (μm)	Depth (μm)					
10	Left	95	50	480	200	150	440	1400	2	195	135	430	20	1360	2.50	10.00	2.27	2.86	115	0.75	400μm thick Top PMMA
	Right				200	150				195	125		15		2.50	16.67			110		
11	Left	95	50	480	200	165	460	1410	4	190	100	435	15	1350	5.00	39.39	5.43	4.26	85	0.79	
	Right				200	160				190	100		15		5.00	37.50			85		
12	Left	95	50	480	200	160	490	1370	6	185	80	405	25	1175	7.50	50.00	17.35	14.23	55	0.91	
	Right				200	155				195	90		25		2.50	41.94			65		
46	Left	95	50	480	200	160	450	1380	2	195	140	440	15	1350	2.50	12.50	2.22	2.17	125	0.68	
	Right				200	155				195	140		15		2.50	9.68			125		
47	Left	95	50	480	200	160	605	1425	4	190	110	555	15	1360	5.00	31.25	8.26	4.56	95	0.83	
	Right				205	160				195	110		20		4.88	31.25			90		
48	Left	95	50	480	195	155	565	1395	6	180	80	455	25	1180	7.69	48.39	19.47	15.41	55	1.02	
	Right				195	155				180	75		20		7.69	51.61			55		
62	Left	95	50	480	205	155	525	1420	2	200	140	505	15	1375	2.44	9.68	3.81	3.17	125	0.79	
	Right				200	155				195	135		15		2.50	12.90			120		
63	Left	95	50	480	195	155	450	1440	4	185	105	420	15	1380	5.13	32.26	6.67	4.17	90	0.88	
	Right				200	160				190	105		20		5.00	34.38			85		
64	Left	95	50	480	205	150	500	1390	6	190	80	410	25	1185	7.32	46.67	18.00	14.75	55	0.99	
	Right				200	155				185	80		25		7.50	48.39			55		

Table A.2. Bond pressure effect on PMMA microchannels and thermal bond strength at 95 ^{0}C, 480 sec and 1000 μm.

Exp. No.		Bonding Temp.	Plate Seperation Temp.	Holding Time (sec.)	INITIAL					FINAL					PERCENTAGE CHANGE				Effective channel Left	Tensile Bond Strength (Mpa)	
					Channel		Top Thin PMMA Thickness (μm)	Thickness of PMMA with channel (μm)	Pressure (Mpa)	Channel		Top Thin PMMA Thickness (μm)	Depth that top goes into the channel (μm)	Thickness of PMMA with channel (μm)	Channel		Top Thin PMMA Thickness (μm)	Bottom PMMA thickness (μm)			
					Width (μm)	Depth (μm)				Width (μm)	Depth (μm)				Width (μm)	Depth (μm)					
13	Left	95	50	480	195	150	1045	1280	2	185	95	990	20	1225	5.13	36.67	5.26	4.30	75	1.61	1000μm thick Top PMMA
	Right				190	150				185	95		20		2.63	36.67			75		
14	Left	95	50	480	190	160	1045	1425	4	180	80	940	40	1285	5.26	50.00	10.05	9.82	40	1.71	
	Right				205	150				190	90		40		7.32	40.00			50		
15	Left	95	50	480	190	155	1070	1510	6	175	60	890	55	1210	7.89	61.29	16.82	19.87	5	1.95	
	Right				190	160				175	55		50		7.89	65.63			5		
49	Left	95	50	480	200	155	1040	1320	2	190	95	990	20	1260	5.00	38.71	4.81	4.55	75	1.68	
	Right				200	160				195	95		15		2.50	40.63			80		
50	Left	95	50	480	205	155	1025	1445	4	190	80	925	40	1295	7.32	48.39	9.76	10.38	40	1.83	
	Right				205	160				195	85		40		4.88	46.88			45		
51	Left	95	50	480	195	160	1025	1405	6	180	60	870	50	1170	7.69	62.50	15.12	16.73	10	1.86	
	Right				195	155				175	65		55		10.26	58.06			10		
65	Left	95	50	480	200	160	1005	1370	2	190	100	940	20	1300	5.00	37.50	6.47	5.11	80	1.55	
	Right				205	160				195	100		15		4.88	37.50			85		
66	Left	95	50	480	200	150	1090	1440	4	190	80	1000	35	1310	5.00	46.67	8.26	9.03	45	1.78	
	Right				195	150				180	75		40		7.69	50.00			35		
67	Left	95	50	480	190	160	930	1475	6	175	65	795	55	1240	7.89	59.38	14.52	15.93	10	1.89	
	Right				200	155				180	70		50		10.00	54.84			20		

Table A.3. Bond pressure effect on PMMA microchannels and thermal bond strength at 95 ^{0}C, 480 sec and 1600 μm.

Exp. No.		Bonding Temp.	Plate Seperation Temp.	Holding Time (sec.)	INITIAL					FINAL					PERCENTAGE CHANGE				Effective channel Left	Tensile Bond Strength (Mpa)	
					Channel		Top Thin PMMA Thickness (μm)	Thickness of PMMA with channel (μm)	Pressure (Mpa)	Channel		Top Thin PMMA Thickness (μm)	Depth that top goes into the channel (μm)	Thickness of PMMA with channel (μm)	Channel		Top Thin PMMA Thickness (μm)	Bottom PMMA thickness (μm)			
					Width (μm)	Depth (μm)				Width (μm)	Depth (μm)				Width (μm)	Depth (μm)					
16	Left	95	50	480	200	160	1600	1515	2	190	55	1460	25	1450	5.00	65.63	8.75	4.29	30	1.55	1600μm thick Top PMMA
	Right				200	155				190	40		25		5.00	74.19			15		
17	Left	95	50	480	195	160	1600	1470	4	180	50	1340	40	1310	7.69	68.75	16.25	10.88	10	1.84	
	Right				195	160				180	45		45		7.69	71.88			0		
18	Left	95	50	480	190	155	1600	1470	6	170	45	1225	55	1180	10.53	70.97	23.44	19.73	-10	1.93	
	Right				200	155				185	40		55		7.50	74.19			-15		
52	Left	95	50	480	200	150	1600	1420	2	190	55	1435	25	1365	5.00	63.33	10.31	3.87	30	1.69	
	Right				195	150				185	50		25		5.13	66.67			25		
53	Left	95	50	480	205	165	1600	1430	4	190	50	1345	45	1295	7.32	69.70	15.94	9.44	5	1.74	
	Right				200	160				185	50		40		7.50	68.75			10		
54	Left	95	50	480	195	160	1600	1440	6	175	45	1230	50	1170	10.26	71.88	23.13	18.75	-5	1.99	
	Right				200	165				185	45		55		7.50	72.73			-10		
68	Left	95	50	480	205	155	1600	1370	2	195	55	1430	25	1310	4.88	64.52	10.63	4.38	30	1.66	
	Right				200	155				190	45		30		5.00	70.97			15		
69	Left	95	50	480	195	155	1600	1420	4	180	45	1330	45	1305	7.69	70.97	16.88	8.10	0	1.78	
	Right				200	160				190	50		45		5.00	68.75			5		
70	Left	95	50	480	205	150	1600	1410	6	185	40	1250	55	1180	9.76	73.33	21.88	16.31	-15	2.05	
	Right				200	155				180	40		50		10.00	74.19			-10		

Table A.4. Average value of PMMA microchannels degradation in width and depth and thermal bond strength due to effect of bond pressure at 95 ^{0}C, 480 sec and different top PMMA substrate thickness.

AVERAGE				Top PMMA Thickness
Pressure (Mpa)	Percentage Decrease		Bond Strength	
	Depth	Width		
2	11.904	2.49	0.74	400 µm
4	34.338	5	0.833	
6	47.832	6.7	0.9733	
2	37.94	4.19	1.6133	1000 µm
4	46.99	6.24	1.7733	
6	60.28	8.61	1.9	
2	67.55	5.001	1.633	1600 µm
4	69.8	7.15	1.787	
6	72.88	9.256	1.99	

Table A.5. Average value of PMMA microchannels degradation in width and depth and thermal bond strength due to effect of bond pressure at 480 sec holding time, 95 ^{0}C and 100 ^{0}C of bond temperature, and different top PMMA substrate thickness.

AVERAGE

Pressure (MPa)	95 Degree C				100 Degree C			Top PMMA Thickness
	Percentage Decrease		Bond Strength		Percentage Decrease		Bond Strength	
	Depth	Width			Depth	Width		
2	11.90	2.49	0.74		68.20	7.40	0.88	400 µm
4	34.34	5.00	0.83		74.65	13.90	1.01	
6	47.83	6.70	0.97		83.55	21.80	1.23	
2	37.94	4.19	1.61		69.70	8.75	1.73	1000 µm
4	46.99	6.24	1.77		77.30	16.65	1.87	
6	60.28	8.61	1.90		86.60	24.05	2.08	
2	67.55	5.00	1.63		75.00	17.90	1.77	1600 µm
4	69.80	7.15	1.79		80.90	20.25	1.91	
6	72.88	9.26	1.99		91.30	26.55	2.13	

Table A.6. Bond temperature effects on PMMA microchannels and thermal bond strength at 2 MPa bond pressure, 120 sec holding time and 400 μm top PMMA thickness.

Exp. No.		Bonding Temp.	Plate Seperation Temp.	Holding Time (sec.)	INITIAL					FINAL					PERCENTAGE				Effective channel Left	Tensile Bond Strength (Mpa)	
					Channel		Top Thin PMMA Thickness (um)	Thickness of PMMA with channel (um)	Pressure (Mpa)	Channel		Top Thin PMMA Thickness (um)	Depth that top goes into the channel (um)	Thickness of PMMA with channel (um)	Channel		Top Thin PMMA Thickness (um)	Bottom PMMA thickness (um)			
					Width (μm)	Depth (μm)				Width (μm)	Depth (μm)				Width (μm)	Depth (μm)					
10	Left	95	50	480	200	150	440	1400	2	195	135	430	20	1360	2.50	10.00	2.27	2.86	115	0.75	400μm thick top PMMA
	Right				200	150				195	125		15		2.50	16.67			110		
71	Left	100	60	120	205	165	460	1440	2	190	50	445	10	1390	7.32	69.70	3.26	3.47	40	0.88	
	Right				200	165				185	55		10		7.50	66.67			45		
2_1	Left	105	60	120	200	170	490	1425	2	165	40	445	20	1310	17.50	76.47	9.18	8.07	20	1.13	
	Right				200	160				160	40		20		20.00	75.00			20		
11	Left	95	50	480	200	165	460	1410	4	190	100	435	15	1350	5.00	39.39	5.43	4.26	85	0.79	
	Right				200	160				190	100		15		5.00	37.50			85		
72	Left	100	60	120	195	170	470	1340	4	170	45	440	10	1155	12.82	73.53	6.38	13.81	35	1.01	
	Right				200	165				170	40		10		15.00	75.76			30		
2_2	Left	105	60	120	200	170	440	1380	4	150	30	370	15	1230	25.00	82.35	15.91	10.87	15	1.31	
	Right				200	160				145	30		15		27.50	81.25			15		
12	Left	95	50	480	200	160	490	1370	6	185	80	405	25	1175	7.50	50.00	17.35	14.23	55	0.91	
	Right				200	155				195	90		25		2.50	41.94			65		
73	Left	100	60	120	195	170	450	1390	6	155	25	381	20	1110	20.51	85.29	15.33	20.14	5	1.23	
	Right				195	165				150	30		25		23.08	81.82			5		
2_3	Left	105	60	120	200	170	470	1420	6	140	15	370	10	1190	30.00	91.18	21.28	16.20	5	1.54	
	Right				200	160				140	15		10		30.00	90.63			5		

Table A.7. Bond temperature effects on PMMA microchannels and thermal bond strength at 2 MPa Bond Pressure, 120 sec holding time and 1000 μm top PMMA thickness.

Exp. No.		Bonding Temp.	Plate Seperation Temp.	Holding Time (sec.)	INITIAL					FINAL					PERCENTAGE CHANGE				Effective channel Left	Tensile Bond Strength (Mpa)	
					Channel		Top Thin PMMA Thickness (um)	Thickness of PMMA with channel (um)	Pressure (Mpa)	Channel		Top Thin PMMA Thickness (um)	Depth that top goes into the channel (um)	Thickness of PMMA with channel (um)	Channel		Top Thin PMMA Thickness (um)	Bottom PMMA thickness (um)			
					Width (μm)	Depth (μm)				Width (μm)	Depth (μm)				Width (μm)	Depth (μm)					
13	Left	95	50	120	190	160	1045	1280	2	185	115	990	20	1250	2.63	28.13	5.26	2.34	95	1.58	1000μm thick top PMMA
	Right				190	160				185	115		20		2.63	28.13			95		
74	Left	100	60	120	200	170	1040	1450	2	180	50	980	15	1370	10.00	70.59	5.77	5.52	35	1.73	
	Right				200	160				185	50		15		7.50	68.75			35		
2_4	Left	105	60	120	200	170	1045	1425	2	150	25	910	20	1270	25.00	85.29	12.92	10.88	5	1.88	
	Right				200	160				145	25		20		27.50	84.38			5		
14	Left	95	50	480	190	160	1045	1425	4	180	80	940	40	1285	5.26	50.00	10.05	9.82	40	1.71	
	Right				205	150				190	90		40		7.32	40.00			50		
75	Left	100	60	120	200	160	1040	1419	4	165	35	890	15	1100	17.50	78.13	14.42	22.48	20	1.87	
	Right				190	170				160	40		15		15.79	76.47			25		
2_5	Left	105	60	120	200	170	1060	1420	4	140	15	830	15	1200	30.00	91.18	21.70	15.49	0	2.10	
	Right				200	160				145	15		15		27.50	90.63			0		
15	Left	95	50	480	190	155	1070	1510	6	175	70	890	55	1210	7.89	54.84	16.82	19.87	15	1.95	
	Right				190	160				175	65		50		7.89	59.38			15		
76	Left	100	60	120	200	165	870	1390	6	150	20	725	20	1100	25.00	87.88	16.67	20.86	0	2.08	
	Right				195	170				150	25		20		23.08	85.29			5		
2_6	Left	105	60	120	200	165	1040	1400	6	130	5	760	10	1130	35.00	96.97	26.92	19.29	-5	2.22	
	Right				200	160				130	5		10		35.00	96.88			-5		

Table A.8. Bond temperature effects on PMMA microchannels and thermal bond strength at 2 MPa bond pressure, 120 sec holding time and 1600 μm top PMMA thickness.

Exp. No.		Bonding Temp.	Plate Seperation Temp.	Holding Time (sec.)	INITIAL					FINAL					PERCENTAGE CHANGE				Effective channel Left	Tensile Bond Strength (Mpa)	
					Channel		Top Thin PMMA Thickness (um)	Thickness of PMMA with channel (um)	Pressure (Mpa)	Channel		Top Thin PMMA Thickness (um)	Depth that top goes into the channel (um)	Thickness of PMMA with channel (um)	Channel		Top Thin PMMA Thickness (um)	Bottom PMMA thickness (um)			
					Width (um)	Depth (um)				Width (um)	Depth (um)				Width (um)	Depth (um)					
16	Left	95	50	480	200	160	1600	1515	2	190	55	1460	25	1450	5.00	65.63	8.75	4.29	30	1.55	1600μm thick top PMMA
	Right				200	155				190	40		25		5.00	74.19			15		
77	Left	100	60	120	195	170	1600	1420	2	160	45	1447	25	1320	17.95	73.53	9.56	7.04	20	1.77	
	Right				195	170				160	40		25		17.95	76.47			15		
2_7	Left	105	60	120	205	165	1600	1400	2	145	20	1380	20	1240	29.27	87.88	13.75	11.43	0	1.98	
	Right				200	160				145	20		20		27.50	87.50			0		
17	Left	95	50	480	195	160	1600	1470	4	180	50	1340	40	1310	7.69	68.75	16.25	10.88	10	1.84	
	Right				195	160				180	45		45		7.69	71.88			0		
78	Left	100	60	120	195	170	1600	1390	4	155	30	1270	30	1100	20.51	82.35	20.63	20.86	0	1.91	
	Right				200	170				160	35		30		20.00	79.41			5		
2_8	Left	105	60	120	200	165	1600	1390	4	135	10	1230	15	1140	32.50	93.94	23.13	17.99	-5	2.20	
	Right				200	160				140	10		15		30.00	93.75			-5		
18	Left	95	50	480	190	155	1600	1470	6	170	45	1225	55	1180	10.53	70.97	23.44	19.73	-10	1.93	
	Right				200	155				185	40		55		7.50	74.19			-15		
79	Left	100	60	120	200	175	1600	1380	6	145	15	1105	25	1020	27.50	91.43	36.25	26.09	-10	2.13	
	Right				195	170				145	15		20		25.64	91.18			-5		
2_9	Left	105	60	120	190	170	1600	1380	6	120	5	1140	20	1080	36.84	97.06	28.75	21.74	-15	2.35	
	Right				200	170				125	5		20		37.50	97.06			-15		

Table A.9. Holding time effects on PMMA microchannels and thermal bond strength at 95 ^{0}C bond temperature, 2 MPa bond pressure and 400 μm top PMMA thickness.

Exp. No.		Bonding Temp.	Plate Seperation Temp.	Holding Time (sec.)	INITIAL					FINAL					PERCENTAGE CHANGE				Effective channel Left	Tensile Bond Strength (Mpa)	
					Channel		Top Thin PMMA Thickness (um)	Thickness of PMMA with channel (um)	Pressure (Mpa)	Channel		Top Thin PMMA Thickness (um)	Depth that top goes into the channel (um)	Thickness of PMMA with channel (um)	Channel		Top Thin PMMA Thickness (um)	Bottom PMMA thickness (um)			
					Width (um)	Depth (um)				Width (um)	Depth (um)				Width (um)	Depth (um)					
55	Left	95	50	240	200	160	560	1450	2	200	145	545	15	1400	0.00	9.38	2.68	3.45	130	0.65	400μm thick Top PMMA
	Right				195	155				195	140		10		0.00	9.68			130		
56	Left	95	50	480	200	160	525	1430	2	195	140	500	15	1370	2.50	12.50	4.76	4.20	125	0.78	
	Right				205	150				200	130		15		2.44	13.33			115		
27	Left	95	50	960	190	150	500	1400	2	180	125	470	20	1305	5.26	16.67	6.00	6.79	105	1.19	
	Right				200	150				185	120		15		7.50	20.00			105		
28	Left	95	50	240	205	150	525	1490	2	205	135	510	10	1420	0.00	10.00	2.86	4.70	125	0.60	
	Right				200	150				200	130		10		0.00	13.33			120		
29	Left	95	50	480	190	165	570	1475	2	185	145	545	10	1370	2.63	12.12	4.39	7.12	135	0.83	
	Right				200	160				190	145		15		5.00	9.38			130		
30	Left	95	50	960	195	160	630	1450	2	185	135	585	20	1350	5.13	15.63	7.14	6.90	115	1.10	
	Right				200	155				180	130		20		10.00	16.13			110		
37	Left	95	50	240	200	160	450	1440	2	200	145	440	10	1395	0.00	9.38	2.22	3.13	135	0.56	
	Right				200	155				200	140		10		0.00	9.68			130		
38	Left	95	50	480	200	160	475	1450	2	195	140	455	10	1360	2.50	12.50	4.21	6.21	130	0.75	
	Right				205	160				195	145		15		4.88	9.38			130		
39	Left	95	50	960	200	155	430	1470	2	185	130	395	20	1350	7.50	16.13	8.14	8.16	110	1.02	
	Right				195	155				180	125		20		7.69	19.35			105		

Table A.10. Holding time effects on PMMA microchannels and thermal bond strength at 95 ^{0}C bond temperature, 2 MPa bond pressure and 1000 μm top PMMA thickness.

Exp. No.		Bonding Temp.	Plate Seperation Temp.	Holding Time (sec.)	INITIAL					FINAL					PERCENTAGE CHANGE				Effective channel Left	Tensile Bond Strength (Mpa)	
					Channel		Top Thin PMMA Thickness (um)	Thickness of PMMA with channel (um)	Pressure (Mpa)	Channel		Top Thin PMMA Thickness (um)	Depth that top goes into the channel (um)	Thickness of PMMA with channel (um)	Channel		Top Thin PMMA Thickness (um)	Bottom PMMA thickness (um)			
					Width (um)	Depth (um)				Width (um)	Depth (um)				Width (um)	Depth (um)					
22	Left	95	50	240	205	160	1040	1420	2	205	115	1010	15	1380	0	28.13	2.88	2.82	100	1.58	1000μm thick Top PMMA
	Right				200	155				200	105		15		0	32.26			90		
23	Left	95	50	480	195	160	1050	1435	2	185	110	990	20	1375	5.128	31.25	5.71	4.18	90	1.89	
	Right				200	150				190	100		15		5	33.33			85		
57	Left	95	50	960	195	150	1060	1440	2	180	100	990	25	1375	7.692	33.33	6.60	4.51	75	1.91	
	Right				200	150				180	100		20		10	33.33			80		
31	Left	95	50	240	200	150	1090	1440	2	200	110	1050	15	1390	0	26.67	3.67	3.47	95	1.53	
	Right				195	150				195	105		15		0	30.00			90		
58	Left	95	50	480	200	165	1105	1410	2	190	115	1045	20	1340	5	30.30	5.43	4.96	95	1.67	
	Right				205	160				195	110		15		4.878	31.25			95		
33	Left	95	50	960	190	160	930	1475	2	175	105	870	20	1390	7.895	34.38	6.45	5.76	85	2.06	
	Right				200	155				185	100		20		7.5	35.48			80		
40	Left	95	50	240	200	160	1040	1410	2	200	115	1000	15	1370	0	28.13	3.85	2.84	100	1.55	
	Right				200	155				200	110		15		0	29.03			95		
41	Left	95	50	480	200	160	1005	1370	2	190	110	940	20	1300	5	31.25	6.47	5.11	90	1.75	
	Right				205	160				195	110		15		4.878	31.25			95		
42	Left	95	50	960	195	155	1020	1455	2	175	100	945	25	1355	10.26	35.48	7.35	6.87	75	1.99	
	Right				195	155				180	100		20		7.692	35.48			80		

Table A.11. Holding time effects on PMMA microchannels and thermal bond strength at 95 ^{0}C bond temperature, 2 MPa bond pressure and 1600 μm top PMMA thickness.

Exp. No.		Bonding Temp.	Plate Seperation Temp.	Holding Time (sec.)	INITIAL					FINAL					PERCENTAGE CHANGE				Effective channel Left	Tensile Bond Strength (Mpa)	
					Channel		Top Thin PMMA Thickness (um)	Thickness of PMMA with	Pressure (Mpa)	Channel		Top Thin PMMA Thickness (um)	Depth that top goes into the	Thickness of PMMA with	Channel		Top Thin PMMA Thickness (um)	Bottom PMMA thickness (um)			
					Width (um)	Depth (um)				Width (um)	Depth (um)				Width (um)	Depth (um)					
34	Left	95	50	240	200	160	1600	1515	2	200	110	1460	25	1450	0.00	31.25	8.75	4.29	85	1.63	1600μm thick Top PMMA
	Right				200	155				200	105		25		0.00	32.26			80		
35	Left	95	50	480	200	160	1600	1470	2	185	105	1440	20	1390	7.50	34.38	10.00	5.44	85	1.81	
	Right				205	160				190	110		15		7.32	31.25			95		
36	Left	95	50	960	195	155	1600	1470	2	175	100	1420	20	1375	10.26	35.48	11.25	6.46	80	2.11	
	Right				195	155				175	100		20		10.26	35.48			80		
43	Left	95	50	240	205	150	1600	1370	2	205	100	1450	15	1310	0.00	33.33	9.38	4.38	85	1.62	
	Right				200	150				200	105		20		0.00	30.00			85		
44	Left	95	50	480	195	165	1600	1420	2	180	105	1435	25	1330	7.69	36.36	10.31	6.34	80	1.89	
	Right				200	160				180	105		25		10.00	34.38			80		
45	Left	95	50	960	195	160	1600	1410	2	170	100	1410	25	1310	12.82	37.50	11.88	7.09	75	2.03	
	Right				205	165				180	100		25		12.20	39.39			75		
59	Left	95	50	240	200	155	1600	1420	2	200	105	1455	15	1350	0.00	32.26	9.06	4.93	90	1.55	
	Right				195	155				195	105		15		0.00	32.26			90		
60	Left	95	50	480	205	165	1600	1430	2	190	105	1430	20	1345	7.32	36.36	10.63	5.94	85	1.75	
	Right				200	160				185	105		25		7.50	34.38			80		
61	Left	95	50	960	190	150	1600	1440	2	170	95	1415	30	1340	10.53	36.67	11.56	6.94	65	1.99	
	Right				200	155				180	100		25		10.00	35.48			75		

Table A.12. Average value of PMMA microchannel degradation and thermal bond strength due to effects of holding time at 95 ^{0}C, 2 MPa and different top PMMA substrate thickness.

AVERAGE				Top PMMA Thickness
Holding Time (sec)	Percentage Decrease		Bond Strength	
	Depth	Width		
240	10.24	0.00	0.60	400 µm
480	11.53	3.32	0.785	
960	17.32	7.18	1.10	
240	29.03	0.00	1.55	1000 µm
480	31.44	4.98	1.77	
960	34.58	8.51	1.98	
240	31.89	0.00	1.6	1600 µm
480	34.52	7.89	1.81	
960	36.67	11.01	2.04	

Table A.13. Top PMMA substrate thickness on PMMA microchannels and thermal bond strength at 95 ^{0}C bond temperature, 2 MPa bond pressure and 480 sec holding time

Exp. No.		Bonding Temp.	Plate Seperation Temp.	Holding Time (sec.)	INITIAL					FINAL					PERCENTAGE CHANGE				Effective channel Left	Tensile Bond Strength (Mpa)	Top PMMA Thickness (µm)
					Channel		Top Thin PMMA Thickness (µm)	Thickness of PMMA with channel (µm)	Pressure (Mpa)	Channel		Top Thin PMMA Thickness (µm)	Depth that top goes into the channel (µm)	Thickness of PMMA with channel (µm)	Channel		Top Thin PMMA Thickness (µm)	Bottom PMMA thickness (µm)			
					Width (µm)	Depth (µm)				Width (µm)	Depth (µm)				Width (µm)	Depth (µm)					
10	Left	95	50	480	200	165	440	1400	2	195	145	430	20	1360	2.50	12.12	2.27	2.86	125	0.75	400
	Right				200	150				195	125		15		2.50	16.67			110		
13	Left	95	50	480	190	150	1045	1280	2	180	95	990	20	1225	5.26	36.67	5.26	4.30	75	1.55	1000
	Right				190	150				185	95		20		2.63	36.67			75		
16	Left	95	50	480	200	160	1600	1515	2	185	55	1460	25	1450	7.50	65.63	8.75	4.29	30	1.61	1600
	Right				200	155				190	40		25		5.00	74.19			15		
38	Left	95	50	480	205	160	475	1450	2	200	140	455	10	1360	2.44	12.50	4.21	6.21	130	0.75	400
	Right				205	160				195	145		15		4.88	9.38			130		
41	Left	95	50	480	200	160	1005	1370	2	190	110	940	20	1300	5.00	31.25	6.47	5.11	90	1.75	1000
	Right				205	160				195	110		15		4.88	31.25			95		
44	Left	95	50	480	195	165	1600	1420	2	180	60	1435	25	1330	7.69	63.64	10.31	6.34	35	1.89	1600
	Right				200	160				180	60		25		10.00	62.50			35		
46	Left	95	50	480	190	155	450	1380	2	185	135	440	15	1350	2.63	12.90	2.22	2.17	120	0.68	400
	Right				200	155				195	140		15		2.50	9.68			125		
49	Left	95	50	480	195	155	1040	1320	2	185	95	990	20	1260	5.13	38.71	4.81	4.55	75	1.68	1000
	Right				200	160				195	95		15		2.50	40.63			80		
52	Left	95	50	480	190	150	1600	1420	2	175	55	1435	25	1365	7.89	63.33	10.31	3.87	30	1.79	1600
	Right				195	150				185	50		25		5.13	66.67			25		
56	Left	95	50	480	195	150	525	1430	2	190	135	500	15	1370	2.56	10.00	4.76	4.20	120	0.78	400
	Right				205	150				200	130		15		2.44	13.33			115		
58	Left	95	50	480	205	165	1105	1410	2	195	115	1045	20	1340	4.88	30.30	5.43	4.96	95	1.67	1000
	Right				205	160				195	110		15		4.88	31.25			95		
60	Left	95	50	480	205	155	1600	1430	2	190	60	1430	20	1345	7.32	61.29	10.63	5.94	40	1.75	1600
	Right				200	160				185	60		25		7.50	62.50			35		

REFERENCES

1) http://www.memsnet.org/mems/what-is.html
2) http://en.wikipedia.org/wiki/mems.
3) http://en.wikipedia.org/wiki/Microfluidics
4) http://www.memsnet.org/mems/applications.html
5) W. Geiger, B. Folkmer, J. Merz, H. Sandmaier and W. Lang, A new silicon rate gyroscope, Sensor and Actuators A: Physical, Volume 73, Issue 1-2, 45-51 (March 1999)
6) Thomas H. Schulte, Ron L. Bardell and Bernhard H. Weigl, Microfluidic technologies in clinical diagnostics, Micronics, Inc., Redmond, WA, USA, Clinica Chimica Acta, Volume 321, Issues 1-2, 1-10 (July 2002).
7) Demetri Psaltis, Stephen R. Quake & Changhuei Yang, Developing optofluidic technology through the fusion of microfluidics and optics, NATURE, Vol 442, (27 July 2006)
8) W. Judy Jack. Biomedical applications of MEMS. University of California, Los Angeles, 68-121 Engineering IV, Box 159410, Los Angeles, CA 90095-1594.
9) S. Bouaidat, B. Winther-Jensenb, S. Flygenring Christensena, and J. Jonsmann. Plasmapolymerized coatings for bio-MEMS applications. Sensors and Actuators A: Physical, 110(1-3).
10) Ernst Thielicke and Ernst Obermeier, Microactuators and their technologies, Technical University of Berlin, Microsensor and Microactuator Technology Center

11) (MAT), TIB 3.1, Gustav-Meyer-Allee 25, 13355, Berlin, Germany, Mechatronics Volume 10, Issues 4-5, 431-455 (1 June 2000).

12) http://faculty.washington.edu/yagerp/microfluidicstutorial/basicconcepts/basicconcepts.htm.

13) http://www.gmu.edu/departments/seor/student_project/syst10100b/team07/benefits.html

14) S. Dewitt, Microreactors for chemical synthesis, Current Opinion in Chemical Biology, 3, 350-356 (1999)

15) G. Sanders and A. Manz, Chip-based Microsystems for genomics and proteomics analysis, Trends in Analytical Chemistry, 19, 364-378 (2000).

16) http://en.wikipedia.org/wiki/pmma.

17) PolyMethylMethAcrylate delivery system for bone morphogenetic protein, United States Patent 4526909

18) http://extra.ivf.se/ngl/documents/chapterc/chapterc1.pdf.

19) D Gomez, I Goenaga, I Lizuain, and M Ozaita. Femtosecond laser ablation for microfluidics. Optical Engineering, 44(5) (May 2005)

20) Anisotropic-electroconductive adhesive film, US Patent issued on March 15, 1988.

21) G. Habenicht, Adhesive Bonding: Fundamentals, Technology and Applications, Springer-Verlag, Heidelberger Platz 3, D-1000 Berlin 33, FRG, 1986, 431.

22) Jack R. Vinson, Adhesive bonding of polymer composites, Polymer Engineering and Science, Volume 29, Issue 19 ,1325 – 1331 (23 Sep 2004).

23) Abdirahman Yussuf, Dr. Igor Sbarski, Dr. Jason Hayes, and Dr. Matthew Solomon. Sealing and bonding techniques for polymer-based microfluidic devices. Industrial Research Institute Swinburne (IRIS) (August 2001).

24) P. Kettner, R.L. Pelzer, T. Glinsner, S. Farrens, and D. Lee. New results on plasma activated bonding of imprinted polymer features for bio MEMS applications. Journal of Physics: Conference Series, 34(1):65-71 (2006).

25) www.ntt-at.com/products_e/mold/im_mold_008.gif

26) Helge Luesebrink, Thomas Glinsner, C. Jakeway Stephan, H. Crabtree John, S. Cameron Neil, Helene Roberge, and Veres Teodor. Transition of MEMS technology to nanofabrication. Journal of Nanoscience and Nanotechnology, 5(6):864-868 (2005).

27) Fong Lei Kin, J. Li Wen, Budraa Nasser, and D. Mai John. Microwave bonding of polymer-based substrates for micro/nanofluidic applications. TRANSDUCERS, Solid-State Sensors, Actuators and Microsystems, 12th International Conference, 2(6), 8.

28) N.K. Budraa, H.W. Jackson, M. Barmatz, W.T. Pike and J.D. Mai, Low pressure and low temperature hermetic wafer bonding using microwave heating, Micro Electro Mechanical Systems, 1999. MEMS '99. Twelfth IEEE International Conference, 490-492 (17-21 Jan 1999)

29) M.A. Roberts, J.S. Rossier, P. Bercier, and H.H. Girault. UV laser machined polymer substrates for the development of micro-diagnostic systems. Laboratory of Physical and Analytical Electrochemistry, 69(11), 19.

30) R. Truckenmller, P. Henzi, D. Herrmann, V. Saile, and W.K. Schomburg. Bonding of polymer microstructures by UV irradiation and subsequent welding at low temperatures. Microsystem Technologies, 10(5), 19.

31) Thomas Velten, Hans Heinrich Ruf, David Barrow, Nikos Aspragathos, Panagiotis Lazarou, Erik Jung, Chantal Khan Malek, Martin Richter, Jrgen Kruckow, and Martin Wackerle. Packaging of bio-MEMS: Strategies, technologies and applications, IEEE Transactions on Advanced Packaging, 28(4) (2005).

32) W. Oh Kwang (Student Member and IEEE) H. Ahn Chong, A new flip-chip bonding technique using micromachined conductive polymer bumps. IEEE Transactions on Advanced Packaging, 22(4) (1999).

33) M. Heckele, W. Bacher, and K.D. Muller. Hot embossing - the molding technique for plastic microstructures. Microsystem Technologies, pages 122-124 (1998).

34) Liwei Lin, Chun-Jung Chiu, Walter Bache, and Mathias Heckele. Microfabrication using silicon mold inserts and hot embossing. Micro Machine and Human Science, 1996, Proceedings of the Seventh International Symposium, 2.

35) http://www.chem.queensu.ca/people/faculty/oleschuk/images/Embossing_Stamp.jpg

36) F Nils Roos, Thomas Luxbacher, Thomas Glinsner, Karl Pfeiffer, Hubert Schulz, and Hella-C. Scheer. Nanoimprint lithography with a commercial 4-in. bond system for hot embossing. The International Society for Optical Engineering, 4343:427-435, (2001).

37) X.C. Shan, Y.C. Liu, H.J. Lu, Z.F. Wang and Y.C. Lam. Studies of polymer deformation and recovery in hot embossing.

38) Hyun Sup Lee, Dong Sung Kim, and Tai Hun Kwon. A novel low temperature bonding technique for plastic substrates using x-ray irradiation. Transducers, Solid-State Sensors, Actuators and Microsystems, 12th International Conference, 1331-1334. (2003)

39) H. Becker and C. Gartner. Polymer microfabrication methods for microfluidic analytical applications. Electrophoresis, 2:12-26 (2000).

40) Laurie Brown, Terry Koerner, J. Hugh Horton, and Richard D. Oleschuk. Fabrication and characterization of poly-methylmethacrylate microfluidic devices bonded using surface modifications and solvents. Lab on a Chip.

41) V Studer, A Pepin, Y Chen, Nanoembossing of thermoplastic polymers for microfluidic applications, Applied Physics Letters, 80, 3614-3616 (2002)

42) V. Studera, A. Ppina, Y. Chen, and A. Ajdarib. Fabrication of microfluidic devices for ac electrokineticfluid pumping. Microelectronic Engineering, 61-62:915{920 (2002).

43) C.H. Ahn, J.W. Choi, G. Beaucage, L. Nevin, J.B. Lee. Disposable Smart Lab on a Chip for Point-of-care clinical diagnostics, Proceedings of the IEEE, 92(1), 154-173 (2004).

44) Jun Mizuno, Sharon Farrens, Hiroyuki Ishida, Viorel Dragoi, Hidetoshi Shinohara, Takafumi Suzuki, Masanori Ishizuka, Thomas Glinsner, and Shuichi Shoji. Cycloolefin polymer direct bonding using low temperature plasma activation bonding MEMS, NANO and Smart Systems, 24-27:346-349 (2005)

45) Jianjun Lai, Xiqu Chen, Xuefang Wang, Xinjian Yi and Sheng Liu. Laser bonding and packaging of plastic microfluidic chips. In Electronic Packaging Technology

(ICEPT), Institute of Microsystems, Huazhong University of Science and Technology, Wuhan 430074, P. R. China, 28.

46) Yi Sun, Yien Chian Kwok, and Nam-Trung Nguyen. Low-pressure, high-temperature thermal bonding of polymeric microfluidic devices and their applications for electrophoretic separation. Journal of Micromechanics and Microengineering, 16:16811688 (2006).

47) Winnie Wing Yin Chow, Kin Fong Lei, Guangyi Shi,Wen Jung Li, and Qiang Huang. Microfluidic channel fabrication by PDMS-interface bonding. Smart Materials and Structures, 15:112S116 (2006).

48) S. Zhao Dong, Roy Binayak, T. McCormick Matthew, G. KhurWerner, and A Brazill Sara. Rapid fabrication of a poly(dimethylsiloxane) microfluidic capillary gel electrophoresis system utilizing high precision machining. Lab on a Chip: Miniaturization for Chemistry, Biology and Bioengineering, 3:93 – 99 (2003).

49) Fiorini S. Gina, D.M. Jeffries Gavin, S.W. Lim David, Kuyper L. Christopher, and T. Chiu Daniel. Fabrication of thermoset polyester microfluidic devices and embossing masters using rapid prototyped polydimethylsiloxane molds. Lab on a Chip: Miniaturization for Chemistry, Biology and Bioengineering, 3:158 – 163 (2003).

50) L. Klintberg, M. Svedberg, F. Nikolajeff, and G. Thornell. Fabrication of a paraffin actuator using hot embossing of polycarbonate. Sensors and Actuators A: Physical, 103(3).

51) Sunil Ranganath Belligundu. Experimental characterization of femtosecond laser micromachining for silicon mold fabrication and hot embossing for polymer micro

replication. Dissertation for Degree of Doctor of Philosophy. University of Texas at Arlington (2005).

52) Akash Deodhar, Panos S. Shiakolas, Sunil Belligundu. An AI based Controller for temperature control for a Hot Embossing System, Proceedings of the 13th Mediterranean Conference on Control and Automation, Limassol, Cyprus, (June 27-29, 2005).

53) http://www.sas.com/technologies/analytics/statistics/stat/index.html

BIOGRAPHICAL STATEMENT

Varun Sood was born in Ambala city, India, in 1983. He received his Bachelor of Engineering in Mechanical Engineering from Y.M.C.A Institute of Engineering, India in 2005. He came to The University of Texas at Arlington in Fall 2005 to pursue his Masters in Mechanical Engineering. He is a graduate research assistant in the MARS and bio-MEMS laboratories and will receive his Masters in Mechanical Engineering in December 2007. His current research interests include microfuidics, bio-MEMS, robotics, control systems and designs.